Mitochondrial adaptations involved in hypoxia and anoxia-tolerance of intertidal fish

Jules Devaux

A thesis submitted in fulfilment of the requirements for the degree of Doctor of Philosophy in Biological Sciences, The University of Auckland, 2019

Abstract

Mitochondria are essential for sustaining complex life. They dominate fuel conversion, redox transfer, electron tunnelling, proton pumping and reduction of O_2 to ultimately store significant energy in the form of ATP, and this complex machinery is believed to have occurred through endosymbiosis with an ancestral nucleated cell approximately 1.45 billion years ago. With the coupling of O_2 consumption and ATP production via oxidative phosphorylation (OxPhos), sufficient O_2 is required to match cellular energy demands. However, when O_2 becomes limited, a succession of physiological changes may alter cell functions, and ultimately the organism's life. Most vertebrates are sensitive to hypoxic insults and oxidative damage caused by rapid reoxygenation. However, some species have evolved within environments frequently exposed to dramatic O_2 fluctuations, and this includes some intertidal species that inhabit rockpools exposed to tidal hypoxic and hyperoxic cycles. This thesis aimed to resolve whether mitochondrial adaptations play a role in the hypoxia-tolerance of intertidal New Zealand triplefin fishes and anoxia-tolerant sharks.

The first study assessed the hypoxia-tolerance of intertidal and subtidal triplefins and the overall mitochondrial O_2 consumption capacity in brain tissue, as the organ is extremely sensitive to O_2 deprivation. Hypoxia-tolerance was found and verified and was accompanied with greater O_2 consumption and OxPhos capacities in the rock pool species relative to the subtidal ones. This suggests that intertidal fish have the capacity to better utilise O_2 for ATP production while presumably better conserving carbohydrate stores, even in both hypoxia and hyperoxia.

As OxPhos flux diminishes with hypoxia, glycolytic flux likely accelerates and this mediates an increase in intracellular lactate level, and associates with an overall intracellular acidosis. The second study hence assessed the effect of acidosis mediated by graded lactic acid titrations, on the mitochondrial function *in situ*. Not only do intertidal species display greater mitochondrial pH buffering capacities, they appear to utilise acidosis to maintain function and maintain mitochondrial membrane potentials and sustain ATP production. In effect this also increases the efficiency of oxygen use given that OxPhos is depressed and this will benefit survival with decreasing oxygen.

While hypoxia is relatively well tolerated by these species, rapid reoxygenation presents another challenge to overcome. The rapid oxidation of succinate that has accumulated in the hypoxic brain mediates excess reactive oxygen species (ROS) that can subsequently cause

oxidative damage. In the third study, the combined effect of anoxia-reoxygenation and graded succinate *in vitro* on respiration and ROS production was measured. Intertidal species produced less ROS and electrons from succinate oxidation, which were better directed to respiration rather than ROS production.

Hypoxia-tolerant species have acquired adaptations in different groups, and it is unknown whether similar or different mechanisms have evolved. The last chapter aimed to explore whether traits of hypoxia-tolerance were also apparent by more ancient species, i.e. elasmobranchs. The epaulette shark and grey carpet shark have evolved for ~150 M years and may retain traits that permitted survival on Earth, which had half the atmospheric O_2 of today. Both species are hypoxia tolerant yet display different physiological and behavioural strategies when hypoxic. In the last chapter, shark brain mitochondria were exposed to elevated succinate and exposed to anoxia-reoxygenation. Mitochondria from these two anoxia tolerant shark species displayed contrasting responses, which likely mirror their respective physiological behaviour on anoxia exposure. Overall, this thesis reveals some traits of the mitochondrial function that likely confer hypoxia-tolerance in intertidal fish.

Acknowledgment

I would like to dedicate this thesis to the wonderful people who have supported me during the last few years of this life-changing opportunity that is a *philosophiae doctor*.

Tony (Hickey), there is no word combination nor frenglish that would describe how grateful I am for having done this PhD under your supervision. Not only you have been a scientific mentor, but a trustful person that always provided support, in the best and toughest times. I had fun doing science and this is a feeling that I feel extremely grateful for.

Thank you Neill (Herbert) for your precious support. I may not have requested much of help during these last years, however I have met a humble and respectful scientist I admire and who I would not hesitate to seek advice from in the future.

Gillian (Renshaw), I cannot put enough emphasis on how grateful I am for taking me under your wing, for gifting me a great study on the Gold Coast and for dedicating so much time mentoring me. Thank you again and I am looking forward to fly back over sometime (anytime actually).

Thank you Chris Hedges, who on top of being one of the humblest scientists I know, became a true friend. Your sarcastic kindness highlighted my days at SBS and I am looking forward to work with you in the future.

I would also like to thank Tristan McArley. Perhaps the only regret is not having met you before. Your thorough way to analyse results in a physiological and behavioural relevance always redirected my science in the right path and I retained a big lesson from you.

Although you were across the other side of the world, thank you my family and friends for your support. Thank you for making me feel like home each trip back to Europe. The distance did not affect our great relationship I cherish every day.

Thank you Līga Eglīte for sharing your love and understanding. The rollercoaster of life made me realise what matters the most and I feel lucky and proud to share this with you.

I'd also like to thanks all the wonderful people who have contributed to this experience (not exhaustively and in no particular order): Stewart Masson, Rachelle Zussman, Jaime Willis, Alicia Hellens, Shanalee James, Kirsten Montgomery, Jiwon Hong, Alice Hadford, Lucy Van

Oosterom, Peter Schlegel, Jin Ng, Stefan Andreef, Joana Taris, Tara Gallagher and the other beautiful people of SBS. I have been touched by your kindness.

It is with emotion that I would also like to thank Nigel Birch for his kindness and his dedication to mentoring, teaching and helping others.

A special thought to Marcel Devaux. When in doubt, I would always remember something you were saying (perhaps negligibly): "*Le travail finit toujours par payer*". Since, I have never been afraid of work, with the hope that dedicating such energy will eventually pay off, and… it always did. I guess this made me push my own limits and I'd like to thank you for that.

Chapter 1. General introduction

1.1. The essential element: (di)oxygen.

Oxygen was originally discovered in 1774 by Antoine Lavoisier, although the compound had previously been described by others as an essential substance for combustion (Cook 1968). Nevertheless, the Frenchman was the first to conduct the adequate experiments to reveal the principle of combustion, documented in his Memoire “Sur la combustion en général” (Lavoisier 1777). Originally named “vital air”, Lavoisier renamed it to “oxygen”. “Oxygen” is derived from the Greek, “οξύς/oxys” (sharp) and “γενή/gen” (generation), meaning “producer of sharp” as Lavoisier originally thought it was constitutive of all acids. It is only a few years later that various chemists proved him wrong, however the term was already too well established to change (Edited by Greenwood 1997).

While the term “oxygen” refers to the chemical element, this term is incorrectly yet commonly used to name its allotrope dioxygen (O_2). Oxygen is by mass the third most abundant element in the Universe. Depending on the conditions of pressure and temperature, O_2 can form a gas, blue paramagnetic liquid (boiling point −182.96 °C), or a solid (with a freezing point −218.79 °C) or compression, which is crystalline and with further compression, becomes red (10 GPa) and then metallic (100 Gpa) (Moore, Stanitski et al. 2009). At standard temperature and pressure, O_2 is an atmospheric gas, is dissolved in water or embedded in carrier molecules such as silicone or haem structures (Emsley 2011). Although Heinrich Danneel and Walther Nernst first noted the electrochemical reductive capacities of O_2 in 1897, this was only utilised in the 1940s to measure blood oxygenation. Bare platinum electrodes were first used, which are toxic when immersed in blood. However, by 1954, Leland Clark constructed a membrane-covered O_2 polarographic electrode, which remains named after Clark and commonly used in the scientific community to this day (Severinghaus and Astrup 1986). At sea-water level and 20°C, the atmosphere contains 299 $mg.L^{-1}$, which converted in SI-derived units corresponds to 0.21 atm /160 mmHg / 21% O_2 / 21.27 kPa. The latter represents the partial pressure of O_2 (PO_2), and is commonly used to refer to the O_2 directly available for life, and PO_2 also mediates diffusion between compartments. Physical factors such as temperature, pressure, hygrometry, salinity and pH affect O_2 content. As such, freshwater and seawater under normoxia only hold around 9.09 $mg.L^{-1}$ and 7.62 $mg.L^{-1}$ dissolved O_2, and oceans may store up to 70% of all O_2 (Fenical 1983).

In nature, O_2 is mainly produced by splitting of water during photosynthesis (Walker 2002), and is then consumed by cellular respiration. This makes O_2 absolutely essential since

with the exception of few metazoans (Danovaro, Dell'Anno et al. 2010), most nucleated eukaryote cells depend on O_2, as it is used to efficiently release sufficient energy to support DNA replication, protein synthesis, ionic balance and many fold other cellular functions (Lane 2002). Indeed O_2 is essential for collagen formation or more specifically hydroxyproline, and this was essential for the evolution of animals (Towe 1970). While O_2 is utilised by other oxidases, it is primarily used by mitochondria for OxPhos.

1.2. The other essential requirement for complex life: the mitochondrion

The mitochondrion was first observed in 1841 (Ernster and Schatz 1981) but the organelle was properly described in 1890 by Richard Altmann, who recognised the granular structures as elementary for metabolism and cellular function (Altmann 1890). Altman originally coined the term “bioblast” (life germ), but the organelle was latter named “mitochondrion” (“μίτος-χονδρίον”, “thread-granule” in Greek) 58 years latter by Carl Benda (Benda 1898). Lynn Margulis proposed that the mitochondrion was most likely once bacterial (Sagan 1967), and had been enveloped into an endosymbiotic relationship within an ancestral and possibly nucleated cell ~1.5 billion years ago (Portier 1918).

It was 32 years after the discovery of adenosine triphosphate (ATP), or life’s energetic currency, by Karl Lohmann in 1929 (Lohmann 1929), that much debate ensued. Sir Peter Mitchell linked O_2 consumption to mitochondrial ATP production via the process of oxidative phosphorylation (OxPhos) (Mitchell 2011).

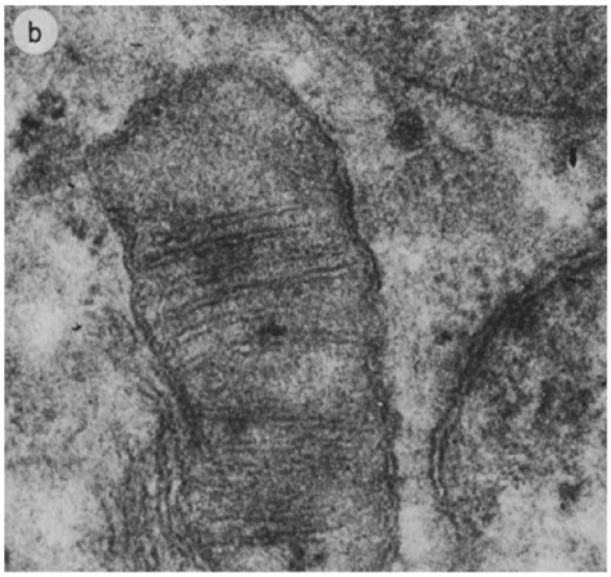

Figure 1. Electron micrograph of kidney mitochondria, x120,000 from Sjöstrand, 1953. (Taken from Enster and Schatz, 1981)

1.2.1. Oxidative phosphorylation

Oxidative phosphorylation within mitochondria fundamentally relies on O_2, and an electron source for the maintenance of a proton gradient (Δp), which constitutes of a chemical gradient (ΔpH) and an electronic potential (ΔΨm). The establishment of Δp separated by an impermeable barrier is a highly conserved feature and shared by every living organism, whether H^+ (Na^+ for some species) is derived from splitting of water, hydrogen-sulphite or carbon sources (Lane 2015). This gradient may even occur in non-living mineral structures that constitute deep-oceanic thermal vents that some propose to have originated life (Martin, Sousa et al. 2014).

In the mitochondrion, hydrogens are stripped from carbon sources (sugar, lipids or proteins) through dehydrogenases and transferred to either nicotinamide adenine dinucleotide (NAD) and flavin adenine dinucleotide (FAD) to become the reduced equivalents NADH + H_2 and $FADH_2$. The reducing power of these molecules motivates the transfer of electrons through the electron transport system (ETS), which is embedded within the inner mitochondrial membranes (Ernster and Schatz 1981). Electrons are transferred through the complexes of the ETS (the most common are Complexes I "CI", II "CII", III "CIII" and cytochrome c oxidase "CCO") via electron carriers ubiquinol/ubiquinone (aka. co-enzyme Q10) and cytochrome c. This electrical potential is dissipated until they reach their final acceptor O_2, which is reduced to form water (Brand and Murphy 1987, Eubel, Heinemeyer et al. 2004). However, during the transfer of electrons, CI and CCO undergo conformational changes, which physically pump protons (4 and 2 H^+ respectively per 2 e^-), while CIII transfers H^+ (4 per 2 e^-) as electrons arrive within ubiquinol and cycle through the Q-cycle. The transfer is directional (vectoral) and protons move from the matrix to the intermembrane space and this mediates the proton gradient (Brand, Brindle et al. 1999). The latter drives the molecular turbine F_0F_1-ATP_{ase} (or ATP synthase, or Complex V) to synthesise ATP from ADP and an inorganic phosphate Pi (Mitchell 2011). For each rotation 3 ATP form, and in mitochondria of animals it appears 8 H^+ mediate a single rotation (yeast require 10 H^+)(Sielaff and Borsch 2013). Notably other less common mitochondrial complexes such as proline oxidase (Hancock, Liu et al. 2016), glyceraldehyde phosphate dehydrogenase (Masson, Hedges et al. 2017) and electron-transferring flavoprotein

dehydrogenase (Zhang, Frerman et al. 2006), are present in some mitochondria and contribute to electron transfer.

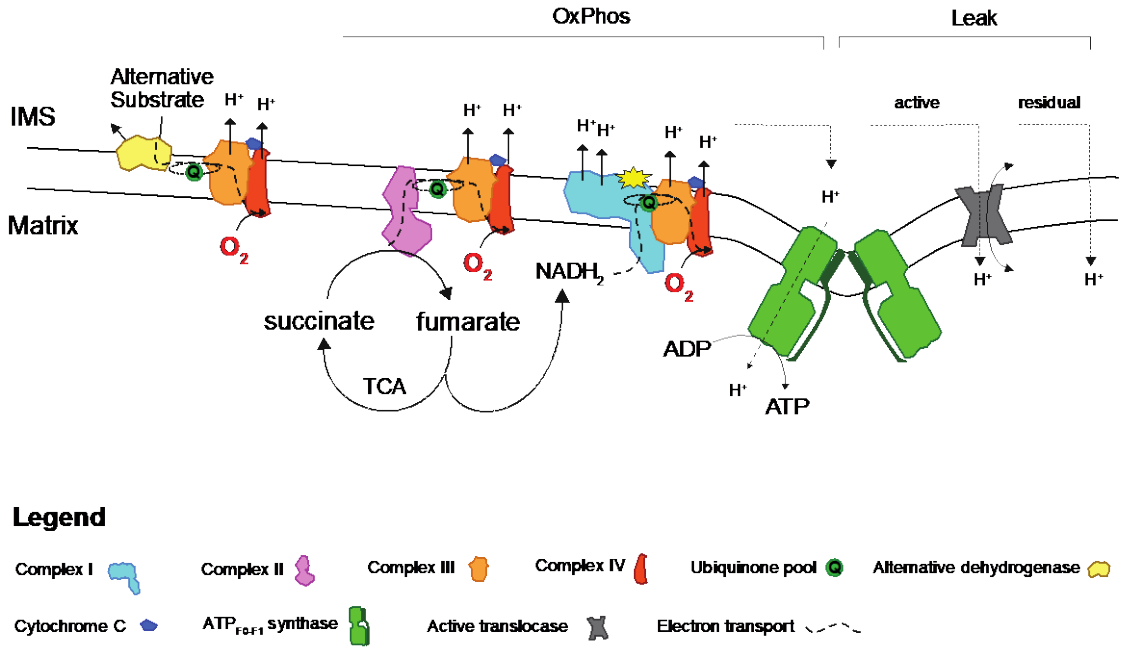

Figure 2. Mitochondrial electron transport system linked to oxidative phosphorylation.

OxPhos occurs across the inner-mitochondrial membrane. Although, some recent studies have presented evidence that H^+ may interact with cardiolipins, which are phospholipid species found in mitochondria, chloroplasts and bacteria, and these may transfer H^+ through part of the membrane bi-layer from the F_0F_1-ATP_{ase} (Khalifat, Fournier et al. 2011). The arrangement of F_0F_1-ATP_{ase} dimers also shape the cristae membrane structure in to folded ridges with elevated negative charge densities within the folds (Davies, Anselmi et al. 2012) and these possibly potentiate H^+ tunnelling towards F_0F_1-ATP_{ase} dimers and the optimise ATP synthesis and decrease the need for larger membrane potentials (Davies, Strauss et al. 2011, Cogliati, Enriquez et al. 2016).

1.2.2. Mitochondrial dynamics

Mitochondria are usually described and presented as beans or round-shaped entities of a bacterial size 0.3-10 µm (Murphy, Lowekamp et al. 2010). This is a result of our general perspective from 2-dimensional electron micrographs. However, with the advancement of imaging resolution and 3D modelling, neuronal mitochondria appear to be arranged into complex networks (Rosselin, Nunes-Hasler et al. 2018), which is lost once sliced for imaging (Peddie and Collinson 2014). Live real-time imaging techniques have allowed observation of dynamic fusion and fission events (Friedman and Nunnari 2014). Regulation of morphology partially dictates the functioning of these organelles. Larger, actively connected mitochondria appear to perform better and produce less oxidant damage than single smaller isolated granules (Anastacio, Kanter et al. 2013). Inter-mitochondrial dynamics are regulated by the fusion proteins mitofusins 1 and 2 (Mfn1 and 2) and optic atrophy 1 (Opa1), whereas fission protein 1 (Fis1), mitochondrial fission factor (Mff) and dynamin-related protein 1 (Drp1) are factors that promote fission (Carter, Chen et al. 2015). Fusion rates are usually in concordance with mitochondrial biogenesis and increases with a healthy lifestyle and exercise in animal models,

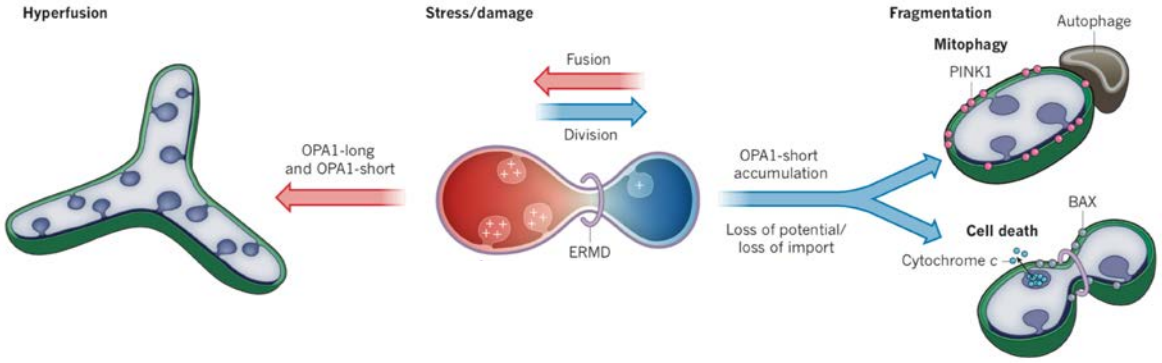

Figure 3. Mitochondrial fusion and fission rates dictate mitochondrial shape and function. Figure adapted from Friedman. J.R. 2014, Nature, 505.

whereas mitochondrial fission leads toward mitophagy, and accelerates with age and several diseases (Carter, Chen et al. 2015). Mitochondria are also actively transported along the cytoskeleton within some cells, including neurones, to specific cellular sites of high ATP demand (Anesti and Scorrano 2006). More recently, it has been discovered that mitochondria are shuttled between cells via tunnelling membrane-bound nanotubes when recruitment or repopulation is needed (Berridge, McConnell et al. 2016). This appears to occur in post-ischemic brain within which, astrocytes appear to export mitochondria-containing vesicles to damaged neurones *in vitro* and *in vivo* (Berridge, Schneider et al. 2016).

1.2.3. Reactive oxygen species production

The first evidence that mitochondria produced reactive oxygen species (ROS) arose in 1966 with the discovery that mitochondrial oxidation lead to the production of hydrogen peroxide H_2O_2 (Jensen 1966). It was later confirmed that the ROS intermediate H_2O_2 came from the dismutation of $O_2^{\bullet-}$ by the superoxide dismutase (SOD) (Weisiger and Fridovich 1973). Therefore, while mitochondria appear to master electron transfer, their controlled binding to O_2 is not completely efficient. Electrons leak from the ETS under certain conditions and due to their extreme reactivity, react rapidly with O_2 to form the anion superoxide $O_2^{\bullet-}$, one of the most "common" reactive oxygen species (ROS) (Boveris 1977). With a half-life of ~1 µs, $O_2^{\bullet-}$ is "moderately" reactive and has oxidising and reducing properties (Halliwell 1977).

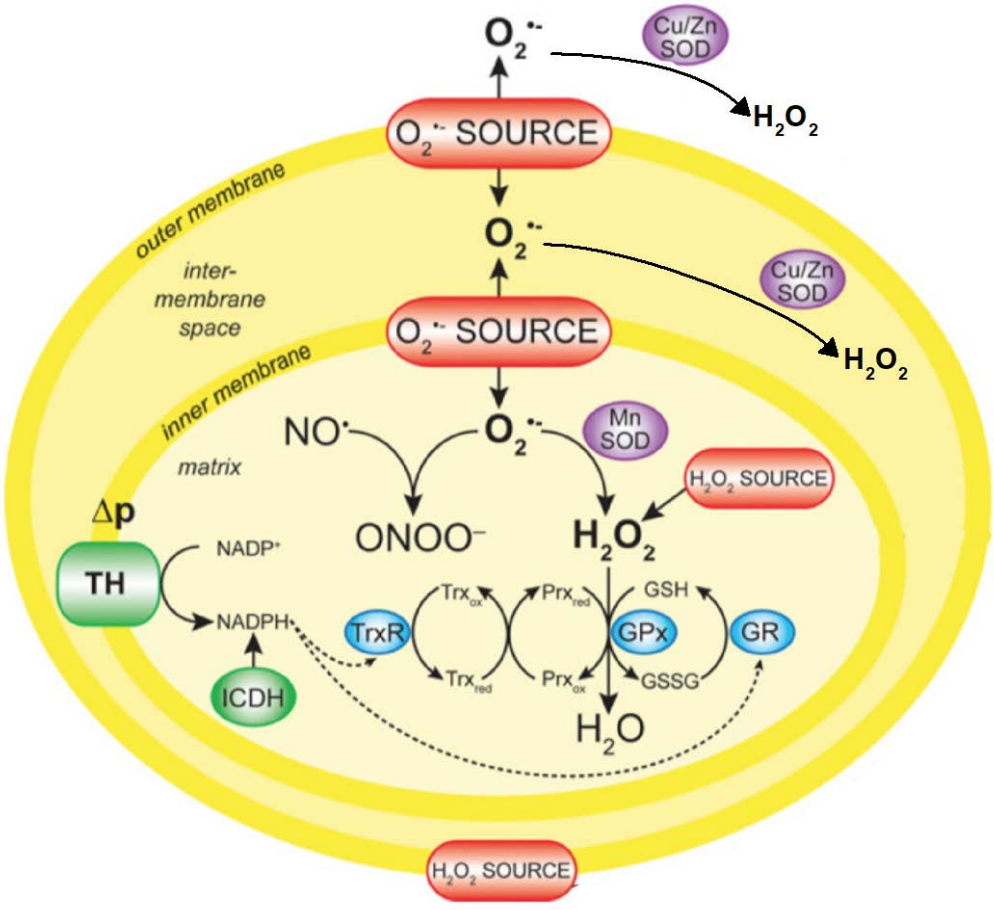

Figure 4. Mitochondrial ROS production and antioxidant systems. The production of $O_2^{\bullet-}$ within the mitochondrial matrix, intermembrane space and outer membrane leads to the formation of H_2O_2 from SOD-catalysed dismutation. Some $O_2^{\bullet-}$ can react directly with nitric oxide ($NO^{\bullet}$) to form peroxynitrite ($ONOO^-$). There are also sources outside mitochondria that produce H_2O_2 directly. Within mitochondria H_2O_2 is degraded by glutathione peroxidases (GPx) or peroxiredoxins (Prx) which depend on glutathione (GSH) and thioredoxin-2 (Trx) for their reduction respectively. Glutathione disulfide (GSSG) is reduced back to GSH by glutathione reductase (GR). Trx is reduced by thioredoxin reductase-2 (TrxR). Both enzymes receive reducing equivalents from the NADPH pool, which is kept reduced by the ⍰p-dependent transhydrogenase (TH), and by isocitrate dehydrogenase (ICDH). Figure adapted from Murphy, 2009, Biochem. J. 417.

With the addition of an electron and two protons, $O_2^{\bullet-}$ can be reduced to H_2O_2, spontaneously or enzymatically via SODs. SOD exists as two intracellular and one extracellular isoforms (Sheng, Abreu et al. 2014). The copper/zinc SOD, encoded by SOD1 gene is primarily distributed within the cytosol while the Manganese SOD, encoded by SOD2, is mainly confined within the mitochondrial matrix (Tan, Pasinelli et al. 2014). SODs have relatively high intracellular activities, and keep the amount of $O_2^{\bullet-}$ in the range of 10-200 pM (Cadenas and Davies 2000). However, these values are to be taken with caution, since the measurement of stable $O_2^{\bullet-}$ levels are challenging (Murphy 2009).

Arguably, H_2O_2 can be considered as an intermediate as the compound is relatively stable compared to other ROS, with a half-life of 1 ms (Mittler and Zilinskas 1991).Once produced, H_2O_2 can then be converted to water by various antioxidant enzyme such as catalase or ascorbate peroxidases (Benov 2001). However, when processed through Fenton or Haber-Weiss reactions, it mediates the production of the hydroxyl radical $^{\bullet}OH$, which is substantially more reactive (Sharma, Jha et al. 2012). In addition, H_2O_2 can easily diffuse across biological membranes, mechanism facilitated with the presence of aquaporin in the plasma membrane (Bienert and Chaumont 2014), and diffuse up to ~40 µm and cause oxidative damage distally (Gáspár 2011).

In mitochondria, electron leakage mainly occurs at the flavoprotein site of CI. This specifically occurs when the Δp is high and the reduced Q-pool is therefore saturated, or when CI capacity is overwhelmed with high $NADH^+$ levels (Murphy 2009). ROS production from CI enhances following anoxia and re-oxygenation, which promotes via a “reverse electron flow” (RET) from CII and the Q-pool to CI (Chouchani, Pell et al. 2014). This phenomenon is detailed in Chapter 3.

Although ROS production appears to be low in physiological conditions, such as when mitochondria are producing ATP, ROS are formed and are involved in the regulation of multiple functions (immune, muscular, reproductive function, etc.) (Rigoulet, Yoboue et al. 2011). However, in excess ROS do have deleterious impacts (Boveris 1977, Murphy 2009). Oxidative damage occurs when labile molecules accept electrons. Not including antioxidant defences, the major targets are the cysteine residues contained at the periphery of various proteins and which oxidation may mediate conformation changes that alter protein structure and function (Miki and Funato 2012). ROS also target lipids of biological membranes, which peroxidation may lead to mitochondrial outer membrane permeabilisation (so called “MOMP”)

and release of apoptotic factors including cytochrome *c* (Orrenius and Zhivotovsky 2005). The third ROS target is DNA, where damage causes alterations and mutations that can change gene and cellular function and can promote ageing and cancers (Jena 2012). Notably, ROS production is most often measured *in vitro* within air saturated media and since ROS are PO_2 dependent (Makrecka-Kuka, Krumschnabel et al. 2015), mitochondrial ROS production may be over-estimated by 5-10 fold in most studies (Murphy 2009).

1.2.4. Apoptosis

Mitochondria do not just "power the cell" in order to transfer energy to sustain life. They paradoxically initiate intrinsic programmed cell death (Tsujimoto 1998). Mitochondria contain a heterogenous class of proteins that promote apoptosis once released intracellularly (Garrido, Galluzzi et al. 2006). One of them is cytochrome-*c* that once in the cytosol, binds to apoptosis-protease activating factor 1 (Apaf-1), which on oligomerization forms the apoptosome (Zou, Li et al. 1999). Most of the cytochrome-*c* is electrostatically bound to anionic phospholipids such as cardiolipin and this ensures its primary function within the mitochondrion, i.e. the shuttling of electrons from CIII to CCO (Kagan, Borisenko et al. 2004). At least 15% of cytochrome-*c* is tightly bound to the inner-mitochondrial membrane. The rest of the

cytochrome-*c* pool is only weakly bound and can be easily released under stress conditions (Garrido, Galluzzi et al. 2006).

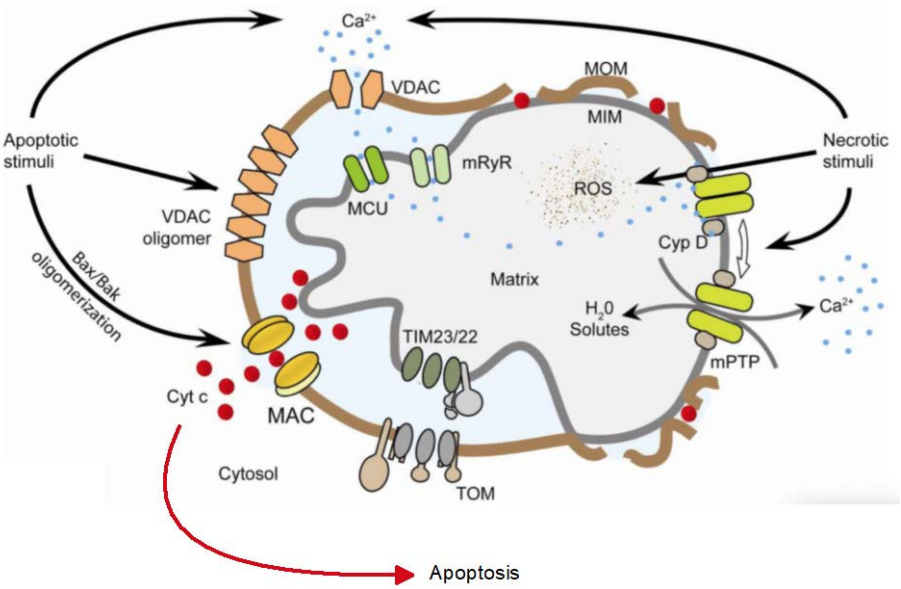

Figure 5. Pro-apoptotic signalling and mitochondrial death pathway. External and internal stimuli motivate the release of cytochrome-*c*, which in turn activates the apoptosome and apoptotic pathway. Figure adapted from (Kinnally, et al., 2011).

Cytochrome-*c* can be released through different processes that ultimately involve the outer mitochondrial membrane permeabilisation (so called "MOMP"). MOMP can be triggered with the binding of Bcl-2 oligomeric proteins, such as Bax and Bak, within the outer mitochondrial membrane (Kinnally, Peixoto et al. 2011). These proteins create "pores" that allow pro-apoptotic compounds caged in the inter-membrane space to freely defuse in the cytoplasm (Kale, Osterlund et al. 2018). However, the structure of the cristae itself may prevent the release of cytochrome-*c* that appear to be mainly contained within cristae pockets. Cristae are dynamic structures whose shape changes under various conditions (Cereghetti and Scorrano 2006). Cristae-shaping proteins such as optic-atrophy 1 protein (OPA1) actively close the structure to form a bottle-like compartment. OPA1 denaturation/alteration has been linked with cytochrome-*c* release and apoptosis (Cogliati, Enriquez et al. 2016, Lee, Smith et al. 2017). More passive hypo-osmotic shock and ischemia-reperfusion may also impair mitochondrial structure and lead to defective function of mitochondrial complexes, which in turn activates apoptosis (Kuznetsov, Schneeberger et al. 2004). As a result, the mitochondrial shape is

actively involved in the regulation of mitochondrial mediated cell death pathways (Cereghetti and Scorrano 2006).

MOMP may also be triggered by the mitochondrial permeability transition pore (mPTP), which is the agglomeration of the voltage-dependent anion channel (VDAC) and recent studies revealed that the ATPase itself would be a major component (Bernardi 2018).

1.2.5. Mitochondrial dysfunction

Diseases from mitochondrial dysfunction range from rare monoallelic mutations to common groups of inherited metabolic disorders including cardiovascular, neuromuscular, neurodegenerative and metabolic diseases (Gorman, Chinnery et al. 2016). Although the effects of single mtDNA or DNA mutations have been relatively well-defined (Greaves and Taylor 2006), the connection between mitochondrial dysfunction and physiological disorders remains less well understood. However, a loss of efficient ATP supply to the cell will clearly be detrimental and if severe promotes necrosis (Sielaff and Borsch 2013).

Mitochondria retain multiple copies of mtDNA encoding 13 proteins for most animals. Yet the other putative~1500 proteins in mitochondria are encoded by the nuclear-DNA and depend on a complex machinery for their import, processing and assembly within the mitochondrion (Brand and Nicholls 2011). The pathophysiology of genetic mutations involving mtDNA, linked or not to nuclear-DNA, is complex since the presence of multiple mtDNA copies within a cell lead to a heteroplasmic mixture of wild-type and mutated genomes, and the effects on the phenotype is dependent on the mutation abundance and importance of the gene (Taylor and Turnbull 2005). The most common mtDNA mutations come from the maternal inherited transmission, although a recent study questions this dogma with occasional evidence of paternal mtDNA in the offspring (Luo, Valencia et al. 2018). The first evidence of pathogenic mtDNA mutation appeared in 1988 (Holt, Harding et al. 1988) and currently more than 250 mtDNA mutations have been identified and impacts 1/3500 people (Taylor and Turnbull 2005), with syndromes such as Leigh's, Pearson's and Kearns-Sayre's syndromes (Tuppen, Blakely et al. 2010).

Mitochondria have multi-scalar regulatory influences on various cellular functions, hence it is no surprise that mitochondrial energy metabolism, dynamic, redox state, ROS production, ion balance and many other functions play important roles in these diseases. For instance within the brain, mitochondrial Ca^{2+} buffering is important as its concentration modifies neuronal

excitability and mitochondrial dysfunction in this context is involved in multiple brain pathologies such as autism, Alzheimer's, Parkinson's, Huntington's and motoneuron diseases (Duchen 2012).

1.3. Hypoxia and the metabolic cascade

"Simply put, hypoxia is a shortage of O_2" (Farrell and Richards 2009). However, this simple definition does not represent the multiple arrays of O_2 shortage that depend on the level and the time of the exposure (Farrell and Richards 2009). Hypoxic levels are therefore challenging to classify and need to be defined within a context. For the purpose of this thesis, I will only focus on cellular hypoxia triggered by a deficiency in O_2 delivery (i.e. not a chronic exposition to hypoxic levels, such as life at high altitude). This can be caused naturally by hypoxic exposure where an animal is an oxy-conformer, and cannot longer sustain O_2 delivery to tissues (Webster and Charlotte 1975), or pathologically with ischemic insult (Lambotte 1977).

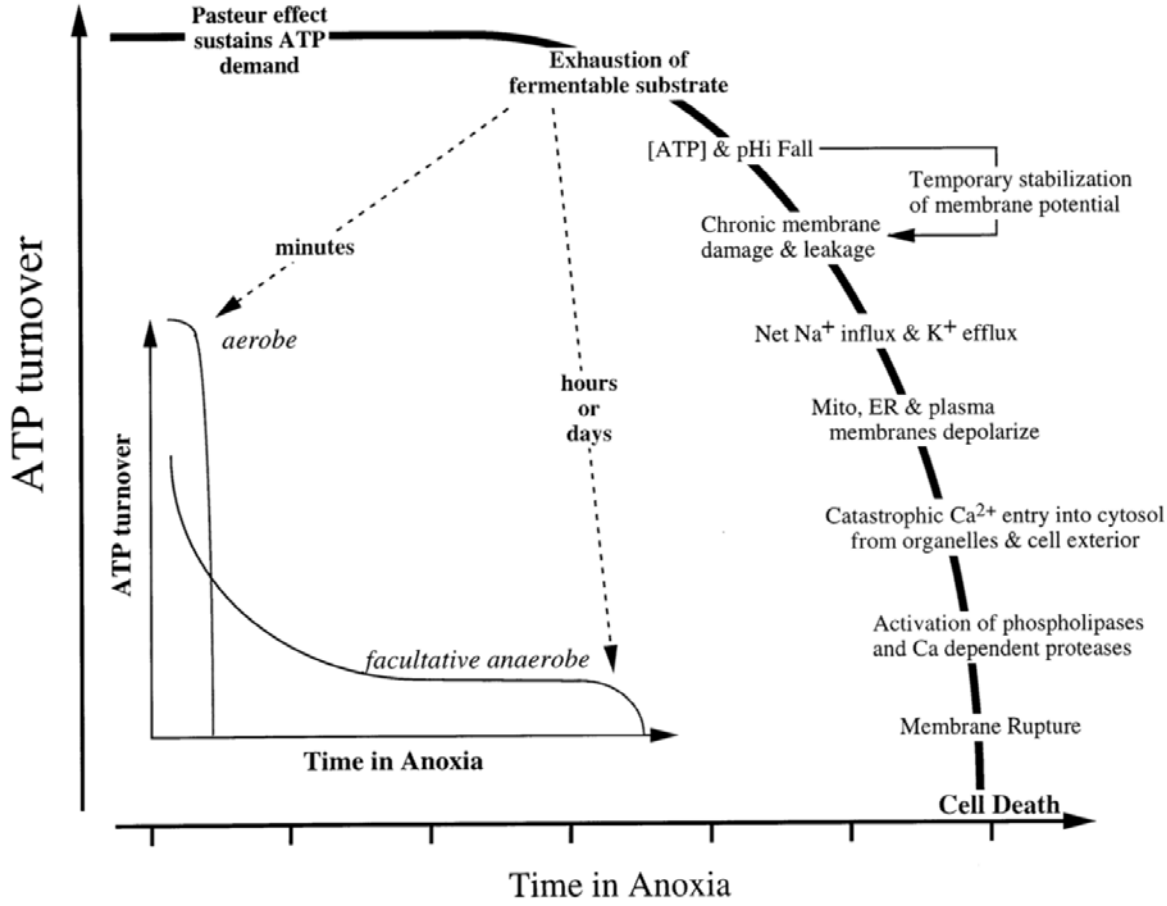

Figure 6. The hypoxic cascade. Figure taken from Boutilier and ST-Pierre, 2000.

1.3.1. Depletion of energy stores

O_2 diffuses from the environment into the blood from alveoli of terrestrial vertebrate lungs, the gills of mature marine vertebrates or passive cutaneous diffusion. O_2 transport and diffusion is generally facilitated by the presence of haemoglobin, which carries 98% of the total blood O_2 and at a concentration that can be regulated by the organism (Kaufman and Dhamoon 2018). In vertebrates, the arterial blood PO_2 ranges from ~5 kPa in fish to ~13.3 kPa in mammals (including humans) and ~18 kPa in birds (Schulte, Kunter et al. 2015). In the capillaries, the haemoglobin affinity to O_2 is no longer sufficient to retain O_2 and it is unloaded to freely diffuse to the proximal cells. Cellular PO_2 is around 2.5 kPa, and may fall below 1 kPa at the mitochondrion (Gnaiger, Lassnig et al. 1998), although this PO_2 estimate may be underestimated (Mik 2013). CCO has a low K_M (i.e. high affinity) for O_2 and therefore changes in PO_2 should have little effect on mitochondrial function (Krab, Kempe et al. 2011).

Since electrons can no longer be transported to O_2 in anoxia, Δp cannot be maintained (Sanderson, Reynolds et al. 2013). With the loss in membrane potential, the $ATP_{F0\text{-}F1}$ appears to reverse, and therefore acts as a proton pump, which may transiently add to the maintenance of Δp. This consumes substantial amounts of ATP and rapidly depletes energy stores (Chinopoulos, Gerencser et al. 2010, Pham, Loiselle et al. 2014, Power, Pearson et al. 2014).

While O_2 delivery to mitochondria diminishes in hypoxia, and electron transfer within the ETS and OxPhos rates fail to be sustained, ATP production from mitochondria decreases (Lambotte 1977). Energy demands for ion balance homeostasis of cells may require increases in anaerobic ATP production. Phosphocreatine within muscle and neuronal tissues can also donate a phosphate to ADP and rapidly buffer local energy imbalance in a thermodynamically favourable manner (Kitzenberg, Colgan et al. 2016). However, while the initiation of this pathway is almost instantaneous, phosphocreatine stores exhaust only a few seconds after recruitment (Bogdanis, Nevill et al. 1996).

Adenylate kinase is another single-enzyme pathway that temporarily buffers ATP levels with the conversion of two ADPs to an ATP and AMP (Zeleznikar, Dzeja et al. 1995). These two enzymes parallel the main anaerobic ATP producing pathway of glycolysis. Glycolysis is ~15 fold less efficient than aerobic metabolism (Zeleznikar, Dzeja et al. 1995, Lutz and Nilsson 1997), and while providing a support for ATP maintenance, enhanced and prolonged glycolytic rates mediate a rapid depletion of carbohydrate stores and the accumulation of waste products

(discussed in chapter 3). For example, ischemic brain of hypoxia-sensitive species can only function for ~15 min on anoxia (Barros 2013).

1.3.2. Metabolic acidosis:

In hypoxic or anoxic conditions, O_2 becomes limiting and OxPhos ATP production is compromised. Under these conditions, vertebrate cells increase anaerobic metabolism activities, and as hypoxia continues, glycolysis may become limited by substrate availability and diminished ATP production mediates rapid depletion of ATP stores (Pamenter 2014). Each ATP hydrolysed mediates the release of one proton H^+ (Wilson 1988) and acts in conjunction with glycolysis in the accumulation of metabolic intermediates and end products (Azarias, Perreten et al. 2011), and metabolic acidosis (Robergs, Ghiasvand et al. 2004). Although contentious, lactate is thought to be oxidised by neurones (Quistorff, Secher et al. 2008, Gallagher, Carpenter et al. 2009, Barros 2013, Riske, Thomas et al. 2017) and also participates to intracellular acidosis (reviewed in Kraut and Madias 2014). In the ischemic brain, up to 60% of glucose can be metabolised to lactate (Teixeira, Santos et al. 2008, Dienel 2012) and its accumulation has been shown to associate with hypercarbia and acidosis (Rehncrona 1985, Katsura, Ekholm et al. 1992).

In most vertebrates, acidosis rapidly occurs and compromises brain function within minutes of anoxia (Katsura, Ekholm et al. 1991), and this promotes irreversible cellular damage (Rehncrona and Kagstrom 1983, Rehncrona 1985, Rehncrona 1985). Intracellular acidosis affects various cellular functions as the protonation of any chemical entities relies in part on surrounding pH (Talley and Alexov 2010). Intracellular acidosis enhances lipid peroxidation (Siesjo, Bendek et al. 1985), protein denaturation (Kraig and Wagner 1987), and alters DNA stabilisation, membrane conductance and muscle contraction (Roos and Boron 1981, Putnam 2012). It can also alter mitochondrial respiration (Hillered, Ernster et al. 1984, Pileggi, Hedges et al. 2018) induce excess ROS release from mitochondria (Selivanov, Zeak et al. 2008), and below pH 6.8 acidosis inhibits the hydrolytic role of the $ATP_{F0\text{-}F1}$ in isolated myelin vesicles (Ravera, Panfoli et al. 2009).

Cells benefit from pH buffering capacities that can protect the intracellular compartment to a certain extent. Most physiological pH buffering is from the bicarbonate system, CO_2/HCO_3^-, or where CO_2 is exhaled from the lungs, excreted in urine under its natural form, or utilised for ammonia clearance (Vaughan-Jones and Spitzer 2002, Krieg, Taghavi et al. 2014). Intracellular $HCO_3^-$is regulated by the Cl^-/ HCO_3^- antiport, which is dependent on Na^+ balance and P_{CO_2}

(Madshus 1988). A second mechanism is the active extrusion of proton or weak acids from the cell, although this only shifts acidosis to an extracellular compartment for excretion (this includes lysosomes that maintain pH as low as 4 U) (Madshus 1988). Finally, peptides carnosine and anserine, which contain histidine-imidazole and many proteins are also major intracellular buffers, which at high intracellular concentrations buffer metabolic acidosis (Lancha Junior, Painelli Vde et al. 2015).

1.4. Hypoxia tolerance in aquatic vertebrates

Hypoxia-tolerance arose from the diversification of habitat occupation by aerial, terrestrial and aquatic organisms that are accustomed to episodic and/or frequent hypoxic or anoxic exposure. Oxygen content in an aquatic environment is dictated by water salinity, temperature, spatial flow (mixing), photosynthesis and respiration rates (Lushchak and Bagnyukova 2006). Since O_2 diffuses only 1/10,000 as fast in water relative to in the atmosphere, hypoxia rapidly occurs when respiration exceeds O_2 production and diffusion rates. Therefore, relative to terrestrial species, marine organisms are constantly exposed to fluctuating O_2 concentrations and present interesting models to explore hypoxia-tolerance.

As the environmental PO_2 decreases, aquatic organism can adapt some behavioural responses to extract more O_2. Escape behaviour and seeking for normoxic areas in the water column may be one of the most obvious means to avoid hypoxia, however some species cannot move in environments such as estuaries, and rock-pools at low tide (Richards 2011). These restricted environments may be particularly variable as overnight resident algae cease to photosynthesise and solely respire, and can become hypoxic and approach anoxia. Some fish have developed different behavioural strategies such as aquatic surface respiration, commonly used by catfish, gobies, sculpins, gourami, sticklebacks or the mummichog. Some teleost species also use air-breathing, which consist in locking an air bubble in the gill allowing the diffusion of O_2 into the blood circulation, which in effect is a simple lung (Chapman, Chapman et al. 2002, Bickler and Buck 2007). Fanning behaviour has also been observed for gobies and clownfish, which create a continuous water flow around eggs (Meunier, White et al. 2013).

Aquatic species that do not display such traits, or cannot access the surface, or have poor dermal gas diffusion appear to have developed physiological adaptations that permit survival in hypoxia. Hypoxia-tolerant species have solved this problem at different scales. In order to meet O_2 demands, an organism may regulate oxygen through increasing O_2 supply (by releasing more red-blood cells, altering haemoglobin affinities and increasing ventilation and blood flow

etc.), or conforming to low O_2 and suppressing metabolism and enduring hypoxia (Chapman and McKenzie 2009). Elevated ventilation rates coupled with a greater blood-O_2 binding (e.g. through erythrocyte cell volume and ATP or GTP regulation, and Hb isoforms) and O_2 delivery (greater cardiac output and diffusion to the tissues), and therefore equilibrate the balance to a certain PO_2 threshold, below which all species become oxy-conformers.

At the organismal level, hypoxia-tolerant species appear to share a similar response of bradycardia (slowed heart rate) at a threshold determined as P_{crit} (critical oxygen tension at which the organism cannot make physiological adjustments that sustain its normoxic metabolic rate) (Gamperl and Driedzic 2009). P_{crit} is a useful indicator for estimating hypoxia tolerance across species (Speers-Roesch, Mandic et al. 2013) that do not undergo metabolic depression (Wood 2018). Species with a low P_{crit} appear to tolerate hypoxic or anoxic events better than species displaying physiological adjustments at higher PO_2. However, there is contention on this point as some hypoxia tolerant species may respond by suppressing metabolism at relatively high PO_2 (Wood 2018). Bradycardia likely saves ATP stores in the heart, but also allows a greater diffusion time for O_2 into the myocardium and other tissues (Speers-Roesch, Sandblom et al. 2010). Stroke volume and cardiac output however, varies among vertebrates and hypoxia-tolerant species. While the hypoxic crucian carp and hibernating squirrel may decrease cerebral blood flow (Larson, Drew et al. 2014), it has been demonstrated that the HT epaulette shark can maintain a constant cerebral blood flow (Renshaw and Dyson 1999) despite depressing ventilation (Routley, Nilsson et al. 2002). Although oxy-conformation is evident at the systemic level these species survive under prolonged hypoxia and have likely developed adaptations at the tissue, cellular and subcellular levels.

The most extreme anoxia-tolerant vertebrate currently known is the freshwater turtle (*Chrysemys picta*) that can survive impressively up to four months of dormancy when trapped in frozen lakes (Jackson, Herbert et al. 1984). To do so, the turtle enters metabolic suppression and drastically supresses ATP consumption rates by 94% relative to the active state (Hochachka, Buck et al. 1996). In normoxic turtle brain, the Na^+ / K^+ ATPase consumes around 19 $\mu mol.g^{-1}.h^{-1}$ ATP to maintain neuronal ion balance but this drops down to ~5 $\mu mol.g^{-1}.h^{-1}$ ATP in the anoxic brain and along with the suppression of other ATP demands, adenylate turnover is relatively well maintained (Hochachka, Buck et al. 1996). The crucian carp (*Carassius carassius*) and its cousin the goldfish (*Carassius auratus*), also enter metabolic suppression and can sustain months or hours, respectively (Johansson, Nilsson et al. 1995, Bickler and Buck 2007). While these species benefit from cold temperatures, which slows

enzymatic activity and metabolism in general, metabolic suppression also occurs in some species that live at higher temperatures, approaching those of mammals (Nilsson and Renshaw 2004). The epaulette shark (*Hemiscillium ocellatum*) lives on the reef platforms of Northern Australia and Southern Indo-Pacific, which frequently hold hypoxic and anoxic water at nocturnal low tides (Nilsson and Renshaw 2004). More details of the epaulette and a close anoxia-tolerant relative shark, the grey carpet shark (*Chiloscyllium punctatum*) are presented in Chapter 5.

To maintain a certain ATP production level, anoxia-tolerant species appear to share high glycogen stores that sustain glycolysis for extensive periods of hypoxia or anoxia (Bickler and Buck 2007). Preconditioning to hypoxia also appears to increase glycogen storage and degradation (Cox, Sandblom et al. 2011, Galli, Lau et al. 2013, Mandic, Speers-Roesch et al. 2013, Larson, Drew et al. 2014). Problematically, sustained anaerobic pathways leads to the accumulation of lactate, which may have deleterious effects (as discussed above). To our knowledge, there have only been a few evolutionary solutions for dealing with excess lactate and associated "acidosis". The freshwater turtle (*Chrysemys picta*) displays a remarkable mechanism, where during prolonged anoxia in the cold, lactate and calcium reach high levels in blood. At these concentrations, both compounds spontaneously form the complex calcium-lactate. Lactate is taken up and bound to calcium by the freshwater turtle shell and skeleton, and this decreases free levels of these compounds and permits continued glycolysis (Jackson 2004). On reoxygenation the energy of released lactate can be re-harnessed (Sun, Li et al. 2017).

The crucian carp (*Carassius carassius*) and the goldfish (*Carassius auratus*) also avoid lactate accumulation through its decarboxylation to ethanol. Brain lactate is exported to red hypaxial swimming muscles where it is oxidised to pyruvate, imported into mitochondria and converted into ethanol due to a mutation in pyruvate dehydrogenase. Ethanol can then be released at an energetic loss through the gills into the surrounding water (Lutz and Nilsson 1997, Mandic, Lau et al. 2008). With some of the highest glycogen stores, *Carassius* can sustain weeks of anoxia and avoids extreme cellular acidosis.

Although the hypoxia and anoxia-tolerance of the species described above are undisputedly impressive, the lack of truly comparable sensitive species does not allow for resolution as to whether hypoxia-tolerance emerged from a common ancestor or from independently evolved adaptation. The best way to reveal physiological adaptations in an

evolutionary contexts relies on the comparison of phylogenetically closely related species through the comparative method (Pagel 1997). In aquatic vertebrates, only the sculpin (superfamily *Cottoidea*) is to our knowledge the model that has been most extensively studied using a comparative physiology approach, with more than 15 species displaying various degrees of hypoxia-tolerance (Richards 2011). Sculpins are small benthic fish belonging to the Scorpaeniformes order and are therefore likely to be predisposed to have low metabolic rates. Sculpins occupy the nearshore environment with species inhabiting the subtidal zone, which varies in oxygenation, and species inhabiting the intertidal zone are also subject to the ebb and flow of tides and exposed to drastic PO_2 fluctuations (Richards 2011). As predicted, behavioural and physiological traits correlate with hypoxia-tolerance. Intertidal sculpin species display a lower critical oxygen tension (P_{crit}), which correlates with delayed loss of equilibrium (LOE) (Mandic, Speers-Roesch et al. 2013). The gill surface areas of most of the intertidal species are greater relative to subtidal species, along with higher O_2 carrying capacities, which allowed the fish to extract more oxygen (Mandic, Sloman et al. 2009). Mitochondria also appear to play an important role in the hypoxia-tolerance of sculpin species as the organelle displayed a greater O_2 affinity, which was partially explained by CCO isoforms having greater O_2 binding properties (Lau, Mandic et al. 2017).

1.5. New Zealand triplefin fish as unique model to test hypoxia

New Zealand triplefin fish (Family Tripterygiidae) are a small carnivorous benthic fish characterized by three dorsal fins and varying body scales patterns. They have no swim bladder, and adults are generally small, i.e. approximately 4-16 cm although some species may reach 30 cm long (Fricke 1994). Tripterygiidae consists of 30 genera and around 130 species distributed worldwide, with much of this diversity endemic to New Zealand, with 14 genera, including 26 genetically closely related nominal species (Feary, Wellenreuther et al. 2009). New Zealand triplefin species ("triplefins" for now on) appear to have radiated from a common ancestor 12-25 million years ago yet are broadly distributed all around New Zealand (Hickey, Lavery et al. 2009). Most triplefins occupy coastal rocky-reefs, with one species, *Bellapiscis medius*, exclusively inhabiting intertidal rock-pools and three species living in deep-abyssal waters down to 500 m. Triplefins display high site fidelity (Feary 2006), which consistency

with habitat partitioning, makes these species great models to study adaptations related to their respective ecophysiologies.

Adult rocky-reef triplefins feed on small crustaceans and invertebrates they engulf whole. While they tend to move in short hops (except for *Forsterygion maryannae* a paedomorphic semi-pelagic species), but can burst swim to a safer area when chased. They appear to mostly sit on the substratum, spreading their pectoral fins and ventral rays for support. Doing so, they can hold position in surge, facing into the flow (Feary 2006). Triplefins breed in autumn and usually spawn after winter, after which they may live up to two to three years (Clements 2006). Protected under depressions, boulders or in rock cracks, males maintain nests that can contain thousands of eggs of around 1 – 1.5 mm that the male fans until they have hatched (Clements 2006).

This thesis focuses on the interspecific differences in how New Zealand triplefin fish, and hypoxia tolerant shark brain mitochondria manage, or behave with fluctuating PO_2 and acidification. Brain was chosen as this is a tissue has a high sensitivity to low PO_2.

Figure 7. Triplefin fish species used as model for this thesis. The exclusive rockpool *Bellapiscis medius* (top left), the estuarine *Forsterygiion capito* (top right), the common triplefin, found intertidally and subtidally, *F. lapillum* (second row), the subtidal *F. malcomi* (bottom left) and *F. varium* (bottom rights).

1.6. Research goals

The aim of this thesis was to determine if there were brain mitochondrial adaptations in intertidal species such as New Zealand triplefin fish, and epaulette sharks, which have evolved to avoid hypoxia, and/or reoxygenation. New Zealand triplefin fish species with various degrees of hypoxia-tolerance were contrasted to resolve evolutionary adaptations. While anoxia-tolerance has been verified in two bamboo shark species, we also tested the mitochondrial response to hypoxia in these elasmobranch lineages, which group has survived through mass extinction events (including that of the dinosaurs), and explore more recently evolved teleost groups such as the triplefin fish. Mitochondrial function was tested in brain tissue, as the brain is highly aerobic and sensitive to O_2 fluctuations. The thesis is arranged as a series of stand-alone studies that have been published or are currently under review in and for international journals.

In Chapter 2, the objective was to verify hypoxia-tolerance in intertidal triplefin fish species relative to subtidal species. Tests were undertaken of whether mitochondrial respiration and CCO capacity would correlate with markers of hypoxia-tolerance as observed in sculpins.

Chapter 3 addresses whether lactate-mediated acidosis was better tolerated by hypoxia-tolerant triplefins, and questions whether extra-mitochondrial protons would support ATP production, independently of OxPhos. This was also done in a novel approach of inducing progressive acidosis. This chapter has been published as “Acidosis maintains the function of brain mitochondria in hypoxia-tolerant Triplefin fish: a strategy to survive acute hypoxic exposure?” in *Frontiers of Physiology*, Dec 2018.

In Chapter 4, ROS production was assessed post an acute episode of anoxia-reoxygentaion *in vitro* and with graded succinate. In this context, I aimed to answer whether electrons were better managed in hypoxia-tolerant triplefins. For the first time, this was undertaken from a saturated PO_2 to anoxia and with consideration of sequential titration of mitochondrial substrates.

Chapter 5 reflected experiments performed in chapter 4, however using a different hypoxia-tolerant model. The effect of graded succinate and acute hypoxia-reoxygenation was tested in two anoxia-tolerant sharks. This was to compare mitochondrial traits in species that have evolved 60 million years ago (Gates, Gorscak et al. 2019), as opposed to the ~2-4 million year old group of New Zealand triplefins (Fricke 1994). The chapter is currently published in

the *Journal of Experimental Biology* (JEB) as “Mitochondrial plasticity in the cerebellum of two anoxia-tolerant sharks: Contrasting responses to anoxia/reoxygenation”.

In Chapter 6, I outline the main findings of my thesis and discuss potential linkages between traits of mitochondrial function, and suggest future avenues of study.

Chapter 2. : Hypoxia-tolerance and mitochondrial adaptations in the brain of intertidal and subtidal New Zealand triplefin fish

2.1. Introduction

Adaptations to hypoxia occur at all biological levels, from behavioural adjustments to transcriptomic alterations (A.L. Val 1998). The primary drive centres on oxygen transport from the environment through the blood, down to its main consumer at the subcellular level, i.e. mitochondria. The mitochondrion oxidises carbon sources and reduces O_2 to water in order to conserve chemical energy in the form of ATP (Ernster and Schatz 1981, Mitchell 2011). Adaptation of mitochondrial structure and function appears to be a key player in hypoxia-tolerance (reviewed in Pamenter 2014), although these adaptations are not universally shared by all hypoxia and anoxia tolerant species (Bickler and Buck 2007, Gorr, Wichmann et al. 2010, Galli and Richards 2014).

Some species have developed physiological adaptations to face extreme environments such as those with dramatic O_2 fluctuations, and represent great natural models (Garland, Bennett et al. 2005). However, in an evolutionary context, most organisms studied to unravel traits of hypoxia-tolerance have been lacking from truly comparable hypoxia-sensitive controls. The best way to reveal physiological adaptations relies on the comparison of phylogenetically closely related species (Pagel 1997). The marine fishes known as sculpins provides a strong model of hypoxia-tolerance in vertebrates, with more than 15 species having graded levels of hypoxia-tolerance depending on the prevalence of environmental hypoxia in each species native habitat (Mandic, Todgham et al. 2009). Mitochondrial affinity to oxygen also correlated with the hypoxia-tolerance of these fishes and this underlies the importance of the organelle in hypoxia-tolerance (Lau, Mandic et al. 2017).

The New-Zealand triplefin fish (Family *Tripterygiidae*) group consists of 26 endemic species occupying stable normoxic habitats, with three species having evolved to inhabit intertidal rockpools that can become hypoxic at low tide (Hickey and Clements 2005, Hilton, Wellenreuther et al. 2008, Hilton 2010, McArley, Hickey et al. 2018). While not linked to hypoxia, there is some evidence of selective pressure on mitochondrial genes within rockpool species relative to subtidal species (Hickey, Lavery et al. 2009), and this suggests that mitochondrial function may vary among triplefin species. With this other evolutionary model

of hypoxia-tolerance, the aim of this study was to determine whether adaptations of the mitochondrial function may have contributed to hypoxia-tolerance in intertidal triplefins.

First, we assessed the hypoxia-tolerance of the four triplefin species. Rested fish were placed in respirometry chambers and measurements of standard metabolic rates from normoxia to sever hypoxia (2 kPa) were performed in order to determine P_{crit}., the O_2 tension at which an organism no longer maintains standard metabolic rate. We also assessed the loss of equilibrium (LOE) to seek for correlation between both parameters. We predicted that intertidal species would display lower P_{crit} and delayed LOE relative to the subtidal species. We then measured O_2 consumption *in vitro*, in brain homogenate and permeabilised brain, and assessed the mitochondrial affinity to O_2 (mP_{50}) and O_2 catalytic efficiencies ($K_{cat,app}$). While homogenate preparation accounts for endogenous substrates and relative tissue O_2 diffusion, that likely better represent respiration occurring in brain *in vivo*, permeabilised brain allows the assessment of maximal mitochondrial respiration *in situ*. Both preparations conjointly informed on O_2 consumption at various mitochondrial states and O_2 consumption profiles assessed here from 20.5 kPa to anoxia. In addition, we also measured CCO activity and inhibition-curve mediated by sodium-aside to determine whereas the O_2 consuming enzyme would be a major determinant of hypoxia-tolerance in triplefin fish species.

2.2. Material and Methods

2.2.1. Experimental animals and housing

The animals used in this study were adult specimens collected from sites on the northeast coast of the Auckland region. The rock pool specialist *Bellapiscis medius* (*BM*) was caught from high intertidal pools using hand nets, while the occasionally intertidal and shallow subtidal species *Forsterygion lapillum (FL)* was caught using minnow traps from nearshore subtidal sites (<1m). The deeper dwelling exclusively subtidal specimens *F. varium* (*FV*) and *F. malcomi* (*FM*) were caught with hand nets by divers at a depth of 10-15m. The experiments carried out in this study were performed at two research facilities. The fish used in the loss of equilibrium trials and mitochondrial assays were housed in a recirculated seawater facility at the University of Auckland's School of Biological Sciences. These fish were held in 30 L tanks provided with a constant flow of recirculated seawater (20 ± 1°C, air saturated, 200 μm filtered, 35 ppt salinity). The fish used for whole animal respirometry were housed at the Leigh Marine Laboratory in 30 L flow-through seawater tanks (20 ± 0.5°C, air saturated, 200 μm filtered, 35 ppt salinity). All fish were acclimated to laboratory conditions for at least 2 weeks prior to the

start of experiments and were fed *ad libitum* on a mixture of shrimp, mussel and fish. Food was withheld for a period of 48 h prior to the start of experiments. All capture, housing and experimental procedures were performed under the approval of the University of Auckland ethic Committee (Approval 001551).

2.2.2. Whole animal respirometry and determination of critical oxygen tension

The P_{crit} of each species (N=10 per species) was determined at 20°C using automated intermittent stop-flow respirometry (Steffensen 1989) to measure mass-specific O_2 consumption ($\dot{M}O_2$; mg O2 g $^{-1}$ h $^{-1}$). The design of the respirometers, general respirometry methods and procedure for $\dot{M}O_2$ calculation are described in detail in McArley et al., (2018). P_{crit} was defined as the oxygen tension where $\dot{M}O_2$ under a progressive hypoxia exposure could no longer be maintained above standard metabolic rate (SMR; $\dot{M}O_2$ in a rested post-absorptive unfed animal) (Claireaux and Chabot 2016). The protocol for P_{crit} determination began with an overnight period (~16 h) of respirometry where $\dot{M}O_2$ was assessed repeatedly over 7-8 min cycles in undisturbed fish under normoxia. SMR was defined as the mean of the lowest 10% of $\dot{M}O_2$ measurements made during the overnight period (Khan, Pether et al. 2014, Norin, Malte et al. 2014, McArley, Hickey et al. 2017), which likely corresponded to periods when fish were completely inactive as these species are benthic and tend to perch in a stationary position on the bottom of the respirometers. $\dot{M}O_2$ measurements were then made at decreasing O_2 tensions (~15.3, 11.6, 7.4, 6.3, 5.2, 4.2, 3.3, 2.3 and 1.6 kPa) and the required water O_2 levels were achieved by bubbling nitrogen into the seawater reservoir supplying respirometers. Three 7-8 min $\dot{M}O_2$ measurements were made at 15.3, 11.6, 7.4, 6.3, 5.2 and 4.2 kPa, and one 7-8 min measurement at 3.3, 2.3 and 1.6 kPa. The entire progressive decline in O_2 tension was completed in ~3 h and the time length of exposure to each O_2 tension was the same for each species. To estimate P_{crit}, SMR and $\dot{M}O_2$ during progressive hypoxic exposure were first mass corrected (see below), then plotted against water O_2 tension. A linear regression (forced through zero) was then established on $\dot{M}O_2$ values that fell below SMR and P_{crit} was calculated by dividing SMR by the slope of this regression line (i.e. the point where $\dot{M}O_2$ under progressive hypoxia could no longer be maintained above SMR; see Fig. 1A) (Schurmann and Steffensen 1997, Behrens and Steffensen 2007, Cook, Iftikar et al. 2013, Cumming and Herbert 2016).

To account for body mass differences between species the $\dot{M}O_2$ values were standardised to the mean body mass of all fish (3.5 g) used for whole animal respirometry. Body mass

correction of $\dot{M}O_2$ values was carried out using the standard formula outlined in (Schurmann and Steffensen 1997) and a mass scaling exponent of 0.8 (Clarke and Johnston 1999).

2.2.3. Loss of equilibrium

Three 48h starved individuals of each species were placed in 40L tanks (total of three) and let to recover overnight. Sea water PO_2 was monitored using NeoFox-GT sensors (Ocean Optics©, Inc). Hypoxia was induced with N_2, bubbled to progressively decrease the PO_2 until 1.5 kPa, which was reached in ~30 min and manually stabilised until all fish were processed. A clear plastic film was placed over the tank, in contact with water to withdraw access for potential aerial respiration.

While for the *Forsterygiion* fishes (*FL*, *FV* and *FM*), the loss of equilibrium (LOE) was determined when the fish was no longer balanced in the water column after swim burst, *BM* and some *FL* LOE was determined after the fish was "tipped over" and would not spontaneously regain equilibrium.

While determined by two different methods, the PO_2 and the time of LOE was uniformly distributed using both methods in *FL*, and this comforts the relevance in LOE determination using our hypoxic induction profile (displayed **Fig. 1B**). Time and the PO_2 at which fish lost equilibrium were considered for LOE measurements, which was expressed as $s.pKa^{-1}$.

2.2.4. Tissue and mitochondrial respirometry

All fish were euthanized by section of the spinal cord at the skull. In experiments using homogenates, the brain was dissected, and excess blood was removed prior to weighing and introduction in tissue respirometry chambers within a maximum of 30 sec. In experiments using permeabilised samples, immediately after removal, brains were placed in ice-cold biopsy buffer containing (in mM hereon, unless stated) 2.77 CaK_2 EGTA, K_2 7.23 EGTA, 5.77 Na_2 ATP, 6.56 $MgCl_2.6H_2O$, 20 taurine, 15 Na_2-phosphocreatine, 20 imidazole, 0.5 DTT, 50 KMES, 50 sucrose, pH 7.22 at 20°C (Gnaiger, Kuznetsov et al. 2000). Cellular permeabilisation was undertaken by the addition of 50 $\mu g.ml^{-1}$ freshly prepared saponin and left for 30 min of gentle agitation in cell culture plastic plates held on ice. The permeabilised tissue was then removed and washed three times for 10 min in ice-cold respiration medium (containing 0.5 EGTA, 3 $MgCl_2.6H_2O$, 60 K-lactobionate, 20 taurine, 10 KH_2PO_4, 2.5 HEPES, 30 MES, 160 sucrose, 1 $g.l^{-1}$ BSA, pH 7.22 at 20°C) prior to its addition in respirometry

chambers. Fish were weighed and measured after dissection and the brain proportion was calculated relative to body mass.

Respiration was measured with Oroboros™ O2ks (Innsbruck, Austria). The O_2 electrode was calibrated from 0-20.46 kPa PO_2 (0-100% air saturation, 262 µM dissolved O_2 equivalent at 20ºC and 101 kPa) prior to respirometry assays. Brains (around ~5 mg homogenate or permeabilised) were introduced in the respirometry chambers containing 2 ml respiration medium calibrated prior to experiment at 100% O_2. After signal stabilisation and the measurement of the routine state in brain homogenates, saturated mitochondrial substrates (pyruvate, malate, glutamate and succinate) and ADP were added to allow for maximum oxidative phosphorylation (OxPhos). The medium was then re-aerated fully and brains were left to deplete O_2 until anoxia was held for ~5 min and after which re-oxygenation was performed. In chambers containing permeabilised brain, oligomycin (5 µM) was added to measure respiration attributed to proton leak (Leak), followed by carbonyl cyanide m-chlorophenyl hydrazone (0.5 µM titration steps until signal stabilisation) to measure the maximum O_2 consumption capacity of the electron transport system when uncoupled from OxPhos. In all assays, cyanide (1 mM) was added to measure non-mitochondrial O_2 consumption, which was then subtracted from raw respiration data.

2.2.5. Determination of mitochondrial affinity to O_2

Respirometry data was recorded with DatLab software with the minimum smoothing to maximise resolution, especially at low PO_2. Correction for time response of the electrode was also accounted (Gnaiger 2008). Above 2.05 kPa, a moving average of 20 seconds was calculated in Excel to lower the signal to noise ratio. The mitochondrial affinity to O_2 (mP_{50}) was then determined as the PO_2 at which the respiration rate is half of maximum OxPhos rate. The O_2 turnover rate ($K_{cat,app}$) was calculated as mP_{50} / OxPhos.

2.2.6. CCO capacity and catalytic efficiency

CCO capacity was assessed using two different methods. In permeabilised brain at OxPhos, sodium azide was titrated to gradually inhibit CCO, resulting in a progressive decrease in respiration rate, until full CCO inhibition (final concentration of 12 mM). Inhibition dose response curves (Hill curves) were fitted with the least-squares method using GraphPad© Prism. Secondly, maximum CCO oxidation rates in permeabilised brain were assessed by excess electron feeding with *N*,*N*,*N*',*N*'-tetramethyl-p-phenylenediamine (TMPD, 0.5 mM) and additional ascorbate (2 mM) to minor TMPD auto-oxidation. Background chemical auto-

oxidation was measured with additional KCN (2 mM) and subtracted to CCO consumption rates, which were then normalised by the electron transport system (ETS) capacity determined in the uncoupled state described above.

2.2.7. Statistical analysis

Statistical analysis was performed with GraphPad© Prism 7. One-way ANOVA or two-Way ANOVA followed by Turkey's *post-hoc* tests were used accordingly to test for interactions and differences between species and/or parameters, with a P value chosen at 0.05. Mitochondrial respiration from 20.5 kPa to anoxia was fitted to a three-parameters dose-response curve using the least-squares method and curves for each species were compared using the extra-sum of squares F-test to test for shared parameters. Linear regression was used to test for correlation between P_{crit}-LOE and OxPhos-mP_{50}.

2.3. Results

2.3.1. Brain mass

Overall, the intertidal species were smaller than the subtidal species (**Table 1**). Notably, the brain proportion of the two rockpool species *BM* and *FL* was ~1.65 times greater than *FV* and more than two times greater than *FM* (P<0.05).

Table 1. Anatomical features of the four New Zealand triplefin fish species. Data presented as mean of 14 individuals ± s.e.m. Statistical difference tested with one-way ANOVA chosen at P < 0.05 and presented as b, l, v and m for difference to *B. medius*, *F. lapillum*, *F. varium* and *F. malcomi*, respectively.

	Body length (mm)	Body mass (g)	Brain/Body mass ($mg.g^{-1}$)
B. medius	54.36 ± 4.81^{lm}	2.54 ± 0.29^{vm}	7.3 ± 0.04^{vm}
F. lapillum	68.57 ± 1.41^{bm}	2.32 ± 0.07^{vm}	7.2 ± 0.02^{vm}
F. varium	65.00 ± 2.80^{m}	4.01 ± 0.21^{blm}	4.4 ± 0.01^{blm}
F. malcomi	80.64 ± 2.83^{blv}	6.84 ± 0.25^{blv}	3.4 ± 0.01^{blv}

2.3.2. Hypoxia tolerance of triplefin fish species

SMR under normoxia was similar among species with the exception of *FV* having a slightly higher resting $\dot{M}O_2$ than *BM* (P<0.05; **Fig. 1A**). There were significant differences among species in P_{crit} (P<0.05). The intertidal specialist *BM* had a lower P_{crit} than all other

species and the occasional intertidal occupant *FL* had a lower P_{crit} than the exclusively subtidal species *FV* and *FM*. There was no difference in P_{crit} between *FV* and *FM*.

The two subtidal species could not reach PO_2 the two rock-pool species were able to tolerate and lost equilibrium at ~2.8±0.2 and 1.8±0.1 kPa for *FM* and *FV*, respectively (**Fig. 1.B**). While some *FL* would lose balance around 2 kPa, the most tolerant *FL* maintained equilibrium for ~1.25h at 1.2 kPa. *BM* tolerated 1.2 kPa with an average time of 1.5h before LOE. To account for both time and PO_2, we expressed LOE as $s.kPa^{-1}$ and revealed that *BM* was the most tolerant species to hypoxia (**Fig. 1.C**). A linear correlation between P_{crit} and LOE was verified with R^2 of 0.92.

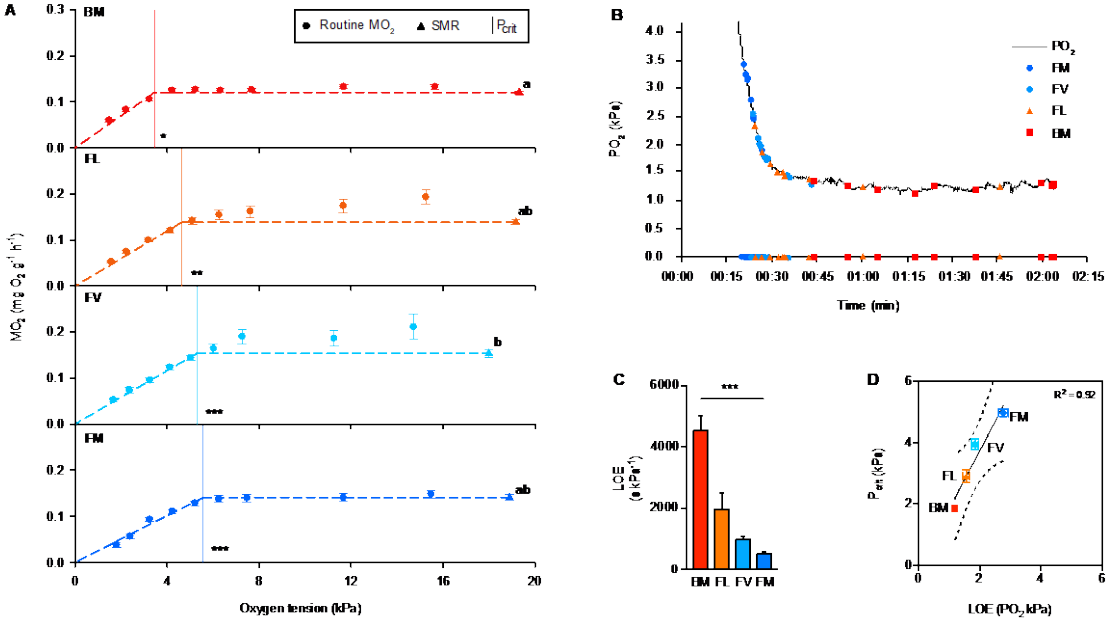

Figure 8. Metabolic rates and tolerance to hypoxia in triplefin fish species. (A) Standard metabolic rates (SMR) of the rock-pool exclusive *Bellapiscis medius* (BM), the intertidal *Forsterygiion lapillum* (FL), subtidal *F. varium* (FV) and *F. malcomi* (FM) were measured in respirometry chamber after at least 16h rest. The O_2 tension was then decreased until 2 kPa and metabolic rate (MO_2) measured, to determine the O_2 tension at which metabolism is no longer maintained (P_{crit}, represented by the coloured line crossing the x axis). Data presented as mean of 10 ± s.e.m. (B) PO_2 profile to determine the loss of equilibrium ("LOE") of 9 individuals of each species. (C) To account for the PO_2 and the time at which fish lost equilibrium, LOE was expressed as $s.kPa^{-1}$. (D) Linear correlation between P_{crit} and LOE was verified for the four triplefins species and presented with 95% confidence. Fish species are denoted as BM: *Bellapiscis medius*, FL: *Forsterygion lapillum*, FV: *F. varium*, FM: *F. malcomi*. Data presented as mean of n = 9 individuals ± s.e.m. in (B) and (C). Difference between species tested with one-way ANOVA chosen at P<0.05, 0.01 and 0.001 presented as *, ** and ***, respectively.

2.3.3. *Oxygen kinetics in the brain*

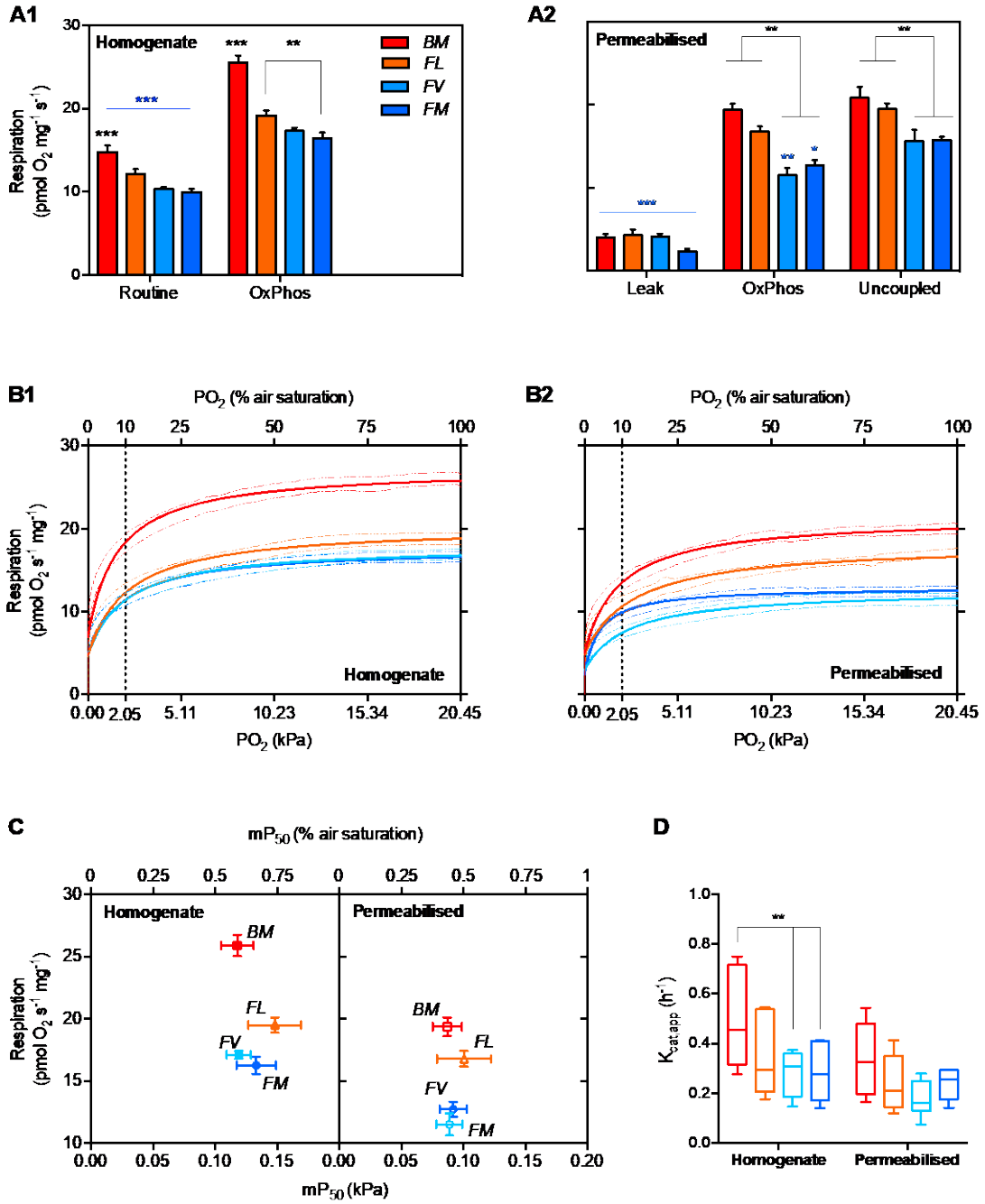

Figure 9. Oxygen kinetics at the cellular level. (A) The mitochondrial respiration was measured in brain homogenates (A1) with no added substrates (i.e. only endogenous substrates present; "Routine") and in the presence of saturated mitochondrial substrates (OxPhos). In permeabilised brain (A2) were measured the basal respiration attributed to proton leak (Leak), OxPhos and maximum respiration when uncoupled from OxPhos. (B) In air saturated medium and saturated respiratory substrates, oxygen consumption was measured in brain homogenate (B1) and permeabilised brain (B2), let to deplete O_2 until anoxia. The line at 2.05 kPa (10% air saturation) correspond to the level bellow which the O_2 tension is likely encountered intracellularly. (C) The correlation between affinity to O_2 (mP_{50}) and the maximum oxidative respiration rates (OxPhos) is not a characteristic of hypoxia tolerance in New Zealand triplefin fishes. Parameters were extracted from the respiration curves in (A). Species indicated as "*BM*": *B. medius*, "*FL*": *F. lapillum*, "*FV*": *F. varium* and "*FM*": *F. varium*. (D) Brain homogenates of the most hypoxia tolerant species has a higher oxygen turnover rate ($K_{cat,app}$) than the two subtidal species. Data are mean of 8 and 7 (respectively homogenate and permeabilised) ± s.e.m. Statistical difference in black between species and in blue between states chosen at $P < .05$, .01 and .001 represented as *, ** and *** respectively.

Overall, the respiration was higher in the brain of *BM* relative to the subtidal species *FV* and *FM*, regardless of preparation or mitochondrial state ($P<0.01$; **Fig. 2A**). In brain homogenate, Routine respiration was ~31% lower than OxPhos respiration ($P<0.01$; **Fig. 2A**). In permeabilised brain without added substrates, Leak respiration rates were less than a third of OxPhos rates ($P<0.01$; **Fig. 2A**), which were however ~20% lower than in brain homogenates ($P<0.05$). In permeabilised brain, only *FV* and *FM* benefited of a reserve capacity, revealed by lower OxPhos rates relative to uncoupled respiration ($P<0.05$).

To cover O_2 levels the brain likely encounters *in vivo*, we then sought to assess O_2 consumption kinetics *in vitro* in real-time on brain homogenate and permeabilised brain at OxPhos state (i.e. without substrate limitation). In brain homogenates, respiration was the highest in *BM* ($P<0.001$), which retained almost two times higher O_2 flux at $PO_2 < 2.05$ kPa (**Fig. 2B**). Respiration in *FL* was significantly higher at $PO_2 > 2.05$ kPa ($P<0.05$), however was similar to the two subtidal species at $PO_2 < 2.05$ kPa. Similarly, in permeabilised brain, respiration was more than 75% higher in the two subtidal species ($P>0.001$; **Fig. 2B**), however rates were ~30% lower in all species but *FL* relative to respiration rates in homogenates (unshared fitted curves, $P<0.0001$).

No difference in mP_{50} was found between the fish species with no correlation between maximum OxPhos respiration (**Fig. 2C**). However, $K_{cat,app}$ was higher in the rock-pool *BM* relative to the subtidal species in brain homogenates ($P<0.01$), but not in permeabilised brain despite an apparent trend (**Fig. 2D**).

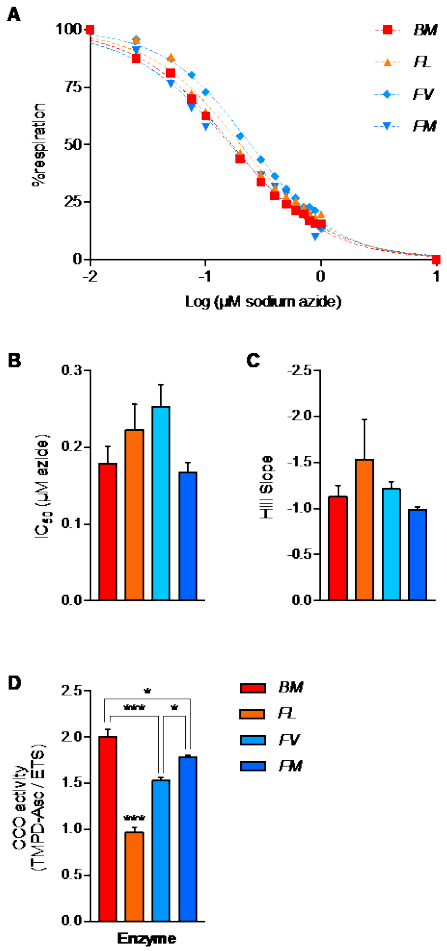

Figure 10. Cytochrome c oxidase properties in brains of triplefin fishes. (A) Graded inhibition of brain cytochrome c oxidase was performed with the titration of sodium azide *in situ*. (B) Half inhibition (IC_{50}) and (C) cooperativity (Hill slope) extracted from (A), with no apparent difference between the species of fish. (D) The maximum activity of the enzyme *in situ* was assessed with TMPD-ascorbate with correction for auto-oxidation and expressed as relative to the mitochondrial electron transport system capacity (ETS). Data presented as mean of 6 individuals ± s.e.m. Intertidal fish species are "*BM*": *B. medius* and "*FL*": *F. lapillum*, and subtidal species are "*FV*": *F. varium* and "*FM*": *F. varium.*

2.3.4. Cytochrome C oxidase

Comparison of curve-fits revealed unshared inhibition dose responses to sodium azide between the CCO of each species of fish ($F_{6,375}$=7.16; P<0.001; **Fig. 3A**), despite similar IC_{50} (**Fig. 3B**) and Hill slope (**Fig. 3C**). While in the *Forsterygiion* genus, the most hypoxia-tolerant *FL* had the lowest CCO activity (P<0.001; **Fig. 3D**), it was the highest in the hypoxia-tolerant species *B. medius* (P<0.05).

2.4. Discussion

In this study, we aimed to resolve whether differences in hypoxia-tolerance among intertidal and subtidal triplefin fish could be explained by differences in brain mitochondrial function. We showed that while elevated oxygen affinity and O_2 respiration at the mitochondrial level correlate with hypoxia-tolerance, it was independent of CCO kinetics.

2.4.1. Intertidal triplefins have superior hypoxia-tolerance

While generally utilised to compare hypoxia-tolerance between species, P_{crit} has recently come under criticism as a reliable marker of hypoxia-tolerance, particularly when used in the

absence of other measures such as LOE (Wood 2018). However, in phylogenetically close marine species that do not enter metabolic depression, P_{crit} appears to be a reliable estimator of hypoxia-tolerance (Rogers, Urbina et al. 2016). This has been verified comparing hypoxia-tolerant in 11 sculpin species, where linear correlation was verified between LOE and P_{crit} (Mandic, Speers-Roesch et al. 2013). Here, we also demonstrate a linear correlation between LOE and P_{crit}, of 26 LOE + 3 kPa. This indicates that both parameters may be good indicators of hypoxia-tolerant in benthic fishes that do not enter metabolic depression.

2.4.2. Oxygen utilization is greater in hypoxia-tolerant brain mitochondria

We then sought to assess the mitochondrial function in brain tissue, as such other aerobically active organs, it is vulnerable to damage from anoxic insults (Cervós-Navarro and Diemer 1991). Notably, the proportion of brain to body mass in intertidal triplefins was around two times greater relative to the two subtidal species (**Table 1).** Rock-pool species appear to have a fine-scale localised nesting area (Feary 2006). Perhaps the greater brain density could be attributed to greater memorisation for local mapping. The brain is primarily composed of glial cells, among which astrocytes represent ~17% (Panov, Orynbayeva et al. 2014). Astrocytes can supply a hypoxic brain with high glycogen stores, which can sustain energy demand of a resting brain for about 15 minutes anaerobically (Barros 2013). With bigger brains, rock-pool species may benefit from volumetrically greater glycogen stores and this likely help to sustain energy levels fuelled for long hypoxic periods. Higher glycogen content also appear to be a common trait of other anoxia-tolerant species such as the freshwater turtle (*Chrysemys picta*) and *Carassius* species (Bickler and Buck 2007).

Brain of hypoxia-tolerant and hypoxia-sensitive triplefins had similar affinities to O_2, as revealed by similar mP_{50} of around 0.10 kPa (**Fig. 2C**). We note that the least hypoxia-tolerant sculpin displayed mP_{50} of around 0.08 kPa (Lau, Mandic et al. 2017), suggesting a greater capacity to extract O_2 in sculpin species relative to triplefin fish. Although mitochondria function at much higher PO_2 *in vivo* (4 kPa) (Mik, Johannes et al. 2008, Mik 2013) and such difference may not be perceivable physiologically. We also note that there was no apparent correlation between mP_{50} and P_{crit} in the present study. This differs from sculpin species within which linear correlation was observed (Lau, Mandic et al. 2017). However, in both homogenate and permeabilised brain, basal O_2 consumption (Routine or Leak, respectively) and OxPhos were greater in the intertidal hypoxia-tolerant species (**Fig. 2.C**). Along with greater efficiencies to consume O_2, given by greater $K_{cat,app}$ (**Fig. 2.D**), this suggests greater aerobic

ATP production rate efficiencies in hypoxia-tolerant species relative to hypoxia-sensitive species.

This greater ability to consume O_2 at the mitochondrial level may be surprising, especially in hypoxic environments when O_2 would need to be preserved to sustain longer. However, we note that fish are exposed to only few hours hypoxia in their environment and may not be exposed to prolonged anoxia (McArley, Hickey et al. 2018). The capacity to further use aerobic metabolism in an O_2 poor environment, ultimately benefits to drastically preserve substrate stores and maintain ATP levels. OxPhos is ~15x more efficient than glycolysis when converting glucose catalysis to ATP production (Mitchell 2011). Hence, an organism able to better extract and utilise O_2 will have a consequent advantage over an organism with similar ATP demand, but fuelled by anaerobic metabolism.

2.4.3. Cytochrome c oxidase is not associated with hypoxia-tolerance

A greater mitochondrial O_2 utilisation may reside from multiple adjustments. This includes a greater capacity to import and oxidise mitochondrial substrates, a greater electron carriage capacity from the different components to the ETS associated or not with greater O_2 consumption via enhanced CCO activity. While no clear correlation between CCO and hypoxia-tolerance was apparent, we note that the CCO capacity was higher than ETS capacity, which suggests that CCO is not limiting and that ETS regulation likely play a more important role in the hypoxia-tolerance of New Zealand triplefins. Notably, dose-inhibition curves were unshared between the species (**Fig. 3.A**). Along with differences in species-specific CCO capacities, this presumably implies differences in isoforms, although this was not tested.

2.5. Conclusion

Hypoxia-tolerance was verified with lower P_{crit}, linearly correlated with a delayed LOE in intertidal species that could sustain up to 2h in 20°C sea water at 1.40 kPa. Brain mitochondria in hypoxia-tolerant species displayed higher respiration rates than brain of hypoxia-sensitive triplefins, even at PO_2 mitochondria function *in vivo*. Although CCO, enzyme at the end of the O_2 cascade, was not correlated with hypoxia-tolerance, it did not appear to limit O_2 consumption in phosphorylating mitochondria. Despite similar mitochondrial affinity to O_2 between hypoxia-tolerant and hypoxia-sensitive triplefins, the capacity to utilise more O_2 in hypoxic environments suggests that ATP production may partially be sustained with a greater ability to preserve carbohydrate stores in hypoxia-tolerant species, and this may explain how intertidal triplefins cope longer in hypoxia.

Chapter 3. : Acidosis maintains the function of brain mitochondria in hypoxia-tolerant Triplefin fish: a strategy to survive acute hypoxic exposure?

Published in *Frontiers in Physiology*: DEVAUX, J. B. L., HEDGES, C. P., BIRCH, N., HERBERT, N., RENSHAW, G. M. C. & HICKEY, A. J. R. 2019. Acidosis Maintains the Function of Brain Mitochondria in Hypoxia-Tolerant Triplefin Fish: A Strategy to Survive Acute Hypoxic Exposure? *Frontiers in Physiology,* 9.

3.1. The other essential element: the mitochondrion

In hypoxic or anoxic conditions, O_2 becomes limiting and ATP production via mitochondrial OxPhos is compromised. To support ATP requirements, vertebrate cells increase anaerobic metabolism activities, which is ~15 folds less efficient than the OxPhos. If hypoxia is sustained, glycolysis may become substrate limited, and diminishing ATP production mediates rapid depletion of ATP stores (Pamenter 2014). ATP hydrolysis mediates proton (H^+) release (Wilson 1988) alongside the accumulation of metabolic end-products (Azarias, Perreten et al. 2011), which contributes to metabolic acidosis (Robergs, Ghiasvand et al. 2004). Although lactate is possibly oxidised by neurones (Quistorff, Secher et al. 2008, Gallagher, Carpenter et al. 2009, Barros 2013, Riske, Thomas et al. 2017) this requires oxygen, and lactate accumulation contributes to intracellular acidosis (reviewed in Kraut and Madias 2014). In the ischemic brain, up to 60% of glucose can be metabolised to lactate (Teixeira, Santos et al. 2008, Dienel 2012), which accumulation has been shown to associate with hypercarbia and acidosis (Rehncrona 1985, Katsura, Ekholm et al. 1992).

Acidosis alters mitochondria respiration in ischemic mammalian brain (Hillered, Ernster et al. 1984), enhances brain lipid peroxidation *in vitro* (Siesjo, Bendek et al. 1985) and denatures proteins (Kraig and Wagner 1987). Low pH (< 6.8) also inhibits the hydrolytic role of F0F1-ATP synthase in isolated myelin vesicles (Ravera, Panfoli et al. 2009), and acidosis generally promotes irreversible cellular damage (Rehncrona and Kagstrom 1983, Rehncrona 1985, Rehncrona 1985). In most vertebrates, acidosis occurs rapidly and compromises brain function within minutes of anoxia (Katsura, Ekholm et al. 1991). Hypoxia tolerant species (HTS) however, routinely survive hypoxic or anoxic environments for several hours up to months, which make these animals useful model systems to explore adaptations against hypoxic damage.

Adult vertebrates such as the carp (*Carassius carassius*), its cousin goldfish (*C. auratus*) and the freshwater turtle (*Chrysemys picta*) have strategies that decrease lactate-mediated acidosis (Jackson 2004, Vornanen, Stecyk et al. 2009). Among mammalian hibernators, the artic ground squirrel (*Spermophilus parryii*) suffers little damage from ischemia while torpid at body temperatures as low as -3 ^oC (Barnes 1989, Ma, Zhu et al. 2005). Independently of hibernation cycle, normothermic brain slices of the ground squirrel tolerate O_2, ATP and glucose deprivation (Bhowmick, Moore et al. 2017). However, determining how such physiological adaptations to hypoxia evolve is harder to explore. Comparative approaches

using multiple phylogenetically related species can provide insights (Pagel 1997) in particular if species range in their tolerances to hypoxia.

The New Zealand triplefin fish group (Family *Tripterygiidae*) consists of 26 endemic species, most of which occupy stable normoxic habitats and are considered to be hypoxia-sensitive species (HSS). However, three HTS species are apparent, and these have evolved to inhabit the intertidal zone that can become hypoxic at low tide (Hickey and Clements 2005, Hilton, Wellenreuther et al. 2008, Hilton 2010, Richards 2011). In our previous work, the hypoxia-tolerance of intertidal triplefins, such as *Bellapiscis medius* show significantly greater tolerance to hypoxia with a lower critical O_2 pressure (P_{crit}), while subtidal species such as *Forsterygiion varium* had significantly higher P_{crit} (Hilton, Clements et al. 2010). Moreover, the intertidal triplefin species have elevated anaerobic enzymes and pH buffering capacities in skeletal muscle (Hickey and Clements 2003), which likely extend energy production and prevent from acidic damage. In addition, there appears to have been selective pressures on the mitochondria genomes of rock-pool species relative to subtidal species (Hickey, Lavery et al. 2009), suggesting aerobic metabolic pathways may have been influenced by the stress of life in the intertidal zone.

The close genetic background within this group (Hickey and Clements 2005) make these fish a natural model to understand adaptations, such as those to survive hypoxic environments. Therefore, we selected four triplefin species with various degrees of hypoxia tolerance. *B. medius* was our exclusive HTS, as this species occupies high rock pools. The more generalist species *F. lapillum* and *F. capito* yet have a marginally lower tolerance to hypoxia and served as intermediates between the HTS and the HSS *F. varium* occupying stable subtidal waters do not typically encounter hypoxia. We hypothesised that intertidal triplefins will show mitochondria adaptations commensurate with physiological stressors associated with hypoxia. As mitochondria respiration (JO_2) regulates the mitochondria membrane potential ($\Delta\Psi m$) and maintains a pH gradient (Mitchell 2011), we tested the influence of lactate mediated acidosis on brain mitochondria of triplefin fish, and predicted that mitochondria of HTS would maintain function at lower pH compared to HSS.

3.2. Material and Methods

3.2.1. Animal sampling and housing.

Adult specimens of four triplefin species (5-10 cm) were collected from different sites around the greater Auckland region using hand nets and/or minnow traps. Adult *B. medius* were caught from high rock-pools at low tide, *F. lapillum* and *F. capito* from rock-pools and off piers, and *F. varium* at 5-10m depth. Individuals were maintained in 30 L tanks (20 fish per tank) in recirculating aerated seawater and were fed with a standard mixture of shrimps and green-lipped mussels every two days for a two weeks acclimation period prior to experiments procedure at 20 ± 1°C. All capture, housing and experimental procedures were performed with under the approval from the University of Auckland Ethic Committee (Approval R001551).

3.2.2. Brain preparation and tissue permeabilization.

Fish were euthanized by section of the spinal cord at the skull. The brain was immediately removed and placed in a modified ice-cold biopsy buffer containing (in mM from hereon unless stated) 2.77 CaK_2EGTA, 7.23 K_2EGTA, 5.77 Na_2ATP, 6.56 $MgCl_2.6H_2O$, 20 taurine, 15 Na_2-phosphocreatine, 20 imidazole, 0.5 DTT, 50 KMES, 50 sucrose, pH 7.1 at 30°C (Gnaiger, Kuznetsov et al. 2000). Cellular permeabilization was undertaken by the addition of 50 µg ml^{-1} freshly prepared saponin and 30 min of gentle agitation within cell culture plastic plates held on ice. The permeabilized tissue was then removed and washed three times for 10 min ice-cold modified MiR05 respiration medium (Kuznetsov, Brandacher et al. 2000) containing 0.5 EGTA, 3 $MgCl_2.6H_2O$, 60 K-lactobionate, 20 taurine, 10 KH_2PO_4, 2.5 HEPES, 30 MES, 160 sucrose, 1g.l^{-1} BSA, pH 7.1 at 30°C. Brain tissues were then split longitudinally into two halves, blotted dry on filter paper, and weighed before loading into respirometers.

3.2.3. Mitochondrial isolation from minimal fish brain tissues.

A miniaturised mitochondria isolation was required to assess the mitochondria swelling. Triplefin brain masses varied from only ~8-30 mg of tissue, hence the whole triplefin brain was required for mitochondria isolation. The brain was first removed from the skull and gently homogenised in 1 ml cold MiR05 by expulsion and suction through a modified 1 ml syringe with decreasing gauge needles (16 – 25 gauge). Mitochondrial integrities were better preserved with this method compared to other standard homogenisation methods and the small sample was also better retained (personal observation). The homogenate (600 µl) was centrifuged at 300 *g* for 5 min at 4°C, the supernatant, which contained suspended mitochondria was collected and spun at 11,000 *g* for 10 min. The supernatant and the white lipid ring surrounding the

brown mitochondria rich pellet was discarded prior to the addition of 500 µl cold MiR05. The last step was repeated twice and isolated mitochondria were then re-suspended in 50 µl ice-cold MiR05 and were held on ice for one hour to permit recovery before respirometry assays. Post to respirometry assay, the medium containing the mitochondria was removed from the chambers and stored at -80°C for the ulterior determination of protein concentration. Prior to the protein assay, samples were slowly defrosted at 4°C and the protein concentration was determined with the Pierce™ BCA Protein Assay Kit as specified by the manufacturer, against a BSA standard and modified MiR05 control.

3.2.4. Acidification protocol optimisation.

To explore the influence of pH on mitochondria function we chose to titrate lactic acid into a modified buffer to induce acidosis. Although acidosis results from ATP hydrolysis, other glycolytic and TCA intermediates and CO_2 (Roos and Boron 1981), and whether lactate ionises to an acid *in vivo* is contentious (Robergs, Ghiasvand et al. 2004), unbuffered lactate (ULac) provides an organic acid without inorganic ions (such as Cl^- if HCl were to be used (Selivanov, Zeak et al. 2008)). Given the high buffering capacity of typical respiration media (MiR05) (Gnaiger, Kuznetsov et al. 2000), we decreased the pH buffering to mimic the pH changes expected in hypoxic brain, which may decrease to an extracellular pH of 6.3 in ischemic brain of non-hyperglycemic vertebrate brain (Katsura, Ekholm et al. 1991, Katsura, Asplund et al. 1992, Kraut and Madias 2014) and of ~6 *in vivo*, at least in hyperglycemic mammals (Katsura, Ekholm et al. 1991, Katsura, Asplund et al. 1992). Assuming parallel changes in pH, these changes should equate to intracellular pH ~5.6-5.5. Therefore, we decreased the HEPES concentration to 2.5 mM and used 30 mM MES to buffer at low pH. With this buffer system, ULac/or buffered lactate ("BLac", pH ~7 adjusted with KOH) was titrated to cover physiological concentrations (Jokivarsi, Grohn et al. 2007, Witt, Larsen et al. 2017), and the pH changes mediated by ULac covered those that occur within vertebrate ischemic brain with a decrease 0.048 pH units per mM ULac. The media (or extra-*mt* pH) was recorded simultaneously with respiration and mitochondria membrane potential ($\Delta\Psi m$) using a solid state ISFET electrode (IQ Scientific Instruments) connected to the pX port of the O2k and calibrated using a three-point calibration (pH 4, 7 & 10) prior to experiments and allowed a ± 0.001 pH U sensitivity. Measurements were performed on permeabilized brain and isolated *mt*, and pH buffering capacities were calculated relative to no-sample controls. As lactate is oxidised by LDH to produce $NADH^+$ and pyruvate, which is further oxidised by mitochondria for oxidative phosphorylation (OxPhos) (Halestrap 1975), it likely alters JO_2, $\Delta\Psi m$ and pH in

the presence of other respiratory substrates. Therefore, the influence of pH changes mediated by ULac was made relative to BLac controls. A representative trace of the protocol is displayed in **Fig. 11**.

3.2.5. Respirometry.

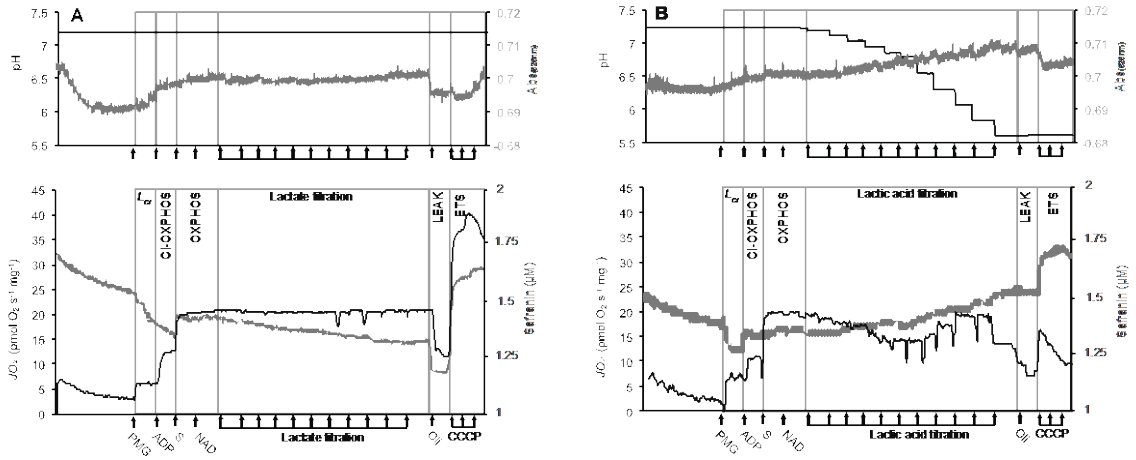

Figure 11. Representative traces of the respirometry protocol. Experiments were conducted with Oroboros™ O2ks on isolated *mt* and permeabilized brain from triplefin fish. The medium pH (top panels, black traces), Vol_{mt} (top panels, grey traces), *mt* respiration rates ("JO_2", lower panel, black traces) and *mt* membrane potential (ΔΨm, lower panels, grey traces) are presented in two different graphs. However, a maximum of three parameters (JO_2, medium pH and ΔΨm assessed on permeabilized brain; or JO_2, medium pH and Vol_{mt} assessed on isolated *mt*) was assessed in a single experiment. Permeabilized brain or isolated *mt* from triplefin fish brain were introduced in the O2k chamber and left to recover and signals to stabilize for 20 min. The LEAK state supported by CI (L_{CI}) was mediated by the addition of CI-linked substrates (PMG for pyruvate, malate and glutamate) at saturating concentrations. The addition of ADP then activates CI-mediated OXPHOS and the addition of saturated succinate (S) allowed the measurement of full OXPHOS capacities with the contribution of both CI and CII. Then, NAD^+ (75 µM) was added to stimulate extra-*mt* lactate oxidation into pyruvate. Buffered lactate (control samples) or unbuffered lactic acid was then titrated to 30 mM (A and B, respectively). To test for *mt* coupling, the $ATP_{F0\text{-}F1}$ inhibitor oligomycin (Oli) was added to determine the LEAK state (affected or not by pH) followed by the uncoupler CCCP, titrated to define the maximum ETS capacity. The ΔΨm was calculated from the fluorescence signal recorded from a calibrated-safranin concentration (up to 2 µM). An increase in safranin concentration corresponds to a decrease in ΔΨm. Vol_{mt} was estimated with the absorbance at 525 nm. All experiments were performed at 20ºC with sufficient O_2 (between 100-260 µM dissolved O_2).

Between 5-12 mg of tissue was placed in respirometer chambers (Oroboros Instrument, Innsbruck, Austria) containing 2 ml (or 3.4 ml when extra-*mt* pH measured to accommodate the electrode) oxygen saturated modified-MiR05 (O_2 concentration = 290 µM at 20°C and 101.5 kPa barometric pressure). Two substrate uncoupler inhibitor titration protocols were performed. The first assay informed on the lactate-mediated respiration and consisted in the sequential addition of NAD^+ (75 µM) and BLac (30 mM, pH 7.25) to initiate a leak state measurement (LEAK), followed by the addition of ADP (700 µM) to initiate OxPhos. The second assay was designed to assess the effect of pH on mitochondria at OxPhos state and consisted of the subsequent addition of the $NADH_2$-generating substrates pyruvate (10 mM) malate (5 mM) and glutamate (10 mM) to initiate LEAK. OxPhos supported by CI was then commenced by the addition of ADP (700 µM). The subsequent addition of 10 mM succinate

activated parallel inputs from CI and CII to OxPhos. NAD^+ (75 µM) was added to the media to avoid cytosolic limitations (i.e. LDH and malate aspartate shuttle, discussed in Kane 2014). BLac or ULac was then titrated to a 30 mM final concentration. Then, the F0F1-ATP synthase inhibitor oligomycin (2.5µl) was added to place mitochondria into artificial LEAK state. Subsequently, respiration was uncoupled from OxPhos using three injections of the protonophore carbonyl cyanide m-chlorophenyl hydrazone (CCCP, 0.5 µM each) to determine the maximal ETS capacity. O_2 concentration was maintained above 100 µM to avoid diffusion limitation. The protocol was applied on both isolated mitochondria and permeabilised brain, however only respiration and ΔΨm data from permeabilised brains are presented in the main manuscript (please refer to supplementary figures for isolated mitochondria respiration data). The differences due to changes in pH within the same permeabilized brain in term of JO_2, ΔΨm and mitochondria matrix volume (Vol_{mt}) were determined by referencing experiments with ULac relative to those with BLac.

3.2.6. Mitochondrial volume (Vol_{mt}) dynamics.

Mitochondria are dynamic organelles and shrink or swell when exposed to variable conditions (Cereghetti and Scorrano 2006, Casteilla, Devin et al. 2011, Friedman and Nunnari 2014). Changes in mitochondria volume (shrinkage or swelling) of isolated mitochondria were measured by following changes in absorption at 525 nm, which changes proportionally to the volume of the mitochondria matrix (Beavis, Brannan et al. 1985, Garlid and Beavis 1985, Das, Parker et al. 2003). Fluorescence sensors (green LED, 525 nm I_{50} ± 25 nm) were used without an emission filter, to follow the light absorption within the O2k. The voltages were recorded simultaneously with JO_2, ΔΨm and pH and light absorbance was calculated with:

$$A_\lambda = -\log_{10} \frac{(I-D)}{(R-D)} / W \quad (1)$$

Where A_λ corresponds to the total absorbance, *I* to the sample intensity, *D* to the dark intensity, *R* to the reference intensity and *W* to the amount of protein in mg. Changes in absorbance ΔA_λ were normalised by A_λ in the OxPhos state to account for the effect of pH on phosphorylating mitochondria only and where mitochondria shrinkage and swelling occurs when $\Delta A_\lambda < 1$ and $\Delta A_\lambda > 1$ respectively.

3.2.7. ΔΨm measurement and calculation.

Safranin-O was used to estimate ΔΨm, simultaneously with JO_2 and pH measurements on permeabilized brain and isolated *mt*. Safranin is a cationic dye that undergoes a fluorescent

quench upon its movement from the intermembrane space (IMS) into anionic sites within the mitochondria matrix (Akerman and Wikstrom 1976, Zanotti and Azzone 1980). A near-linear correlation between the safranin spectral shift and mitochondrial energised state permits estimates of ΔΨm. As recommended, $[Safr]_{final}$ of 2 µM was chosen for this study (Krumschnabel, Eigentler et al. 2014) and the fluorescence signal (Ex/Em 465/587nm) was calibrated using a four-step titration (0.5-1-1.5-2 µM) into the O2k chamber prior to experiments. Although the signal in control experiments (no sample) was unchanged by the addition of different substrates-inhibitors, nor by changes in pH, quenching occurred over time (3 nM min^{-1}) and was accounted for in ΔΨm calculations. ΔΨm was calculated from the recorded concentration of safranin "[Safr]" as per previous work (Pham, Loiselle et al. 2014), where:

$$\Delta\psi m = 2.3026 \times \frac{RT}{zF} \times Log10\left(\frac{[Safr]out}{[Safr]in}\right) \quad (2)$$

Where *R* is the gas constant, *T* is the temperature in Kelvin, *z* the valence state of the ion (+1) and *F* the Faraday constant. While the safranin concentration outside the mitochondria "$[Safr]_{out}$" corresponds to the calibrated fluorescent signal directly obtained from DatLab7, the safranin concentration in the mitochondria matrix "$[Safr]_{in}$" is dependent on the Vol_{mt}, back-calculated from OxPhos state, which was assumed to be at -120 mV (Huttemann, Lee et al. 2008, Perry, Norman et al. 2011). As mitochondria shape is dynamic (Fujii, Nodasaka et al. 2004, Casteilla, Devin et al. 2011), the Vol_{mt} was readjusted at each state following the estimation and the integration of the mitochondria swelling or shrinkage (ΔA_λ):

$$Vol_{mt}\ (\mu l\ mg^{-1}) = \frac{Safr \times 10^{-\frac{120}{Cst}}}{[Safr]out \times W}\ 10^6 \times \Delta A_\lambda \quad (3)$$

Where *Cst* corresponds to $2.303 \times \frac{RT}{zF}$ (58.17 mV) under our conditions, *Safr* the amount of safranin in mitochondria in µmol, $[Safr]_{out}$ the recorded safranin concentration in µM, *W* the amount of tissue in mg and ΔA_λ the change in Vol_{mt} (described below).

3.2.8. Estimation of mitochondrial work to maintain Δ Ψm with additional external charges.

We further estimated the energy required by mitochondria to maintain ΔΨm as this summarises the combined effects of JO_2, ΔΨm and acidosis. The total energy of a closed system can be determined by:

$$J = C\ .V \quad (4)$$

Where *J* is the derived unit of energy transferred to an amount of work in Joules, *C* is electric charge in Coulombs and *V* is the electric potential in Volts. A Joule is the work required to move an electric charge of 1C against an electric potential of 1V. In this present study, we treat mitochondria as a closed system and the respiration rate a measure of the work performed by complexes to transfer H^+ across the MIM for each O_2 reduced against ΔΨm. Proton pumping varies from 12 H^+ to 20 H^+ per O_2 consumed with full support from CII or CI (respectively). Therefore, the relative contribution of CI to OxPhos was calculated and total proton pumping per O_2 determined:

$$nH^+ = 12 + 8 * \frac{\mathrm{OxPhos}_{(\mathrm{pyruvate+malate+glutamate})}}{\mathrm{OxPhos}_{(\mathrm{pyruvate+malate+glutamate+succinate})}} \quad (5)$$

The flux of proton was then calculated:

$$J(nH^+) = JO_2 * nH^+ \quad (6)$$

The equation (*4*) was transposed:

$$J_{mt} = e * J(nH^+) * \Delta\Psi\mathrm{m} \quad (7)$$

Where *e* equals the elementary charge constant corresponding for H^+ to 96.525 kC mol^{-1}, ΔΨm the mitochondria membrane potential expressed in mV and $J(nH^+)$ the rate of protons passed through the MIM in pmol H^+ s^{-1} mg^{-1}. While other ions contribute to ΔΨm *in vivo*, only K^+ and Cl^- ions in our media impact ΔΨm, and these remain constant relative to the changes in H^+.

To better relate mitochondrial work to equation 4, we thought to calculate the amount of charge (in Coulomb, "C_{add}") mediated by the decrease in pH (i.e. additional protons), where:

$$C_{add} = 10^{-pH} * V_{chamber} * N_A * C_H \quad (8)$$

Where pH is the recorded pH in the chamber, $V_{chamber}$ is the volume of the respirometry chamber (2 ml), N_A is the Avogadro constant ($6.02.10^{23}$) and C_H the charge carried by a proton ($1.602.10^{-19}$).

At stable ΔΨm, charges moved from the mitochondria matrix to the inter-membrane space equates those moved back to the matrix. To better represent the effect C_{add} at a given pH onto charges flux within *mt*, J_{mt} was normalised by C_{add} at corresponding pH.

3.2.9. ATP production

ATP production was assessed based on previous work (Chinopoulos, Vajda et al. 2009, Pham, Loiselle et al. 2014, Masson, Hedges et al. 2017) in permeabilised brain of the most HTS *B. medius* and the HSS *F. varium*. Due to the variable properties of the fluorescent dye Magnesium Green™ (ThermoFisher Scientific, USA) to acidosis, we performed an experiment to assess ATP production at pH 7.25 and pH 6.65, which appears to be the pH at which mitochondria function is preserved in HTS but altered in the HSS (**Fig. 14**). In separated experiments, O2k chambers were filled with modified MiR05 and mitochondrial substrates (pyruvate, malate, glutamate and succinate) at concentrations described above. This was supplemented with 10 mM BLac or ULac to set the medium pH at 7.25 or 6.65 respectively. Magnesium Green™ (5µM) was then added and $MgCl_2$ was titrated to calibrate the Mg^{2+}_{free} in the chamber. The equivalent of one permeabilised brain hemisphere was then added to the chamber and let to recover for around 15 min. Then, ADP was titrated (3 x 0.5 µM) to calibrate the Mg^{2+}_{free} signal to [ADP]. After 15 min, antimycin A (2.5 µM) was added to block proton pumping by the ETS. Once JO_2 signal was stable (> 20min), oligomycin (10 nM) was added to block mitochondrial ATP synthesis and measure ATP hydrolysis. Data was exported into Excel and the rate of ATP was calculated as

$$JATP = \frac{[ADP]_t - [ADP]_{t-1}}{t - t_{-1}} * Cst \quad (9)$$

Where $[ADP]_t$ corresponds to the concentration of ADP at the end of a mitochondria state and $[ADP]_{t-1}$ the ADP concentration at the start of the mitochondria state and t and t-1 the time at which corresponding [ADP] where taken. Cst corresponds to the relative difference between K_{DADP} and K_{DATP} extracted from (Chinopoulos, Vajda et al. 2009). Then ATP consumption rate determined after the addition of oligomycin (JATP < 0), was subtracted to the other state to determine the net ATP production rate (JATP > 0) in pmol s^{-1} mg^{-1}. The PO ratio was calculated as

$$PO = \frac{JATP}{\frac{JO_2}{2}} \quad (10)$$

3.2.10. Data and statistical analysis.

Respirometry and simultaneous spectrometry data were extracted from DatLab 7.0 software. All data were copied and processed in Excel © 2016. GraphPad Prism v7 was used

to perform two way-ANOVA to test for the effect of pH between species and the mitochondria parameters (JO_2, $\Delta\Psi m$, Vol_{mt} and ATP) within mitochondria states. Two-way ANOVA repeated-measures were performed to analyse the effect of BLac, ULac and associated pH titrations on the mitochondria parameters between the species of fish. Post hoc tests using Turkey's correction were used for pairwise comparisons and a P value of 0.05 was chosen to represent statistical difference.

3.3. Results

3.3.1. Mitochondrial pH buffering capacities.

Permeabilized brain of *B. medius* had a 4.5-6% (~0.05 pH-unit mg^{-1}) greater buffering capacities than the HSS *F. varium* (P = 0.006; **Table 2**). Brain tissue pH buffering capacities of *F. lapillum* were similar to those of the more HTS *B. medius*, while mitochondria of *F. capito* had similar buffering to *F. varium*. In isolated mitochondria however, only the *F. varium* differed, with a lower pH buffering capacity (P < 0.04), indicating most, but not all, of the buffering results from non-*mt* components. Estimated contributions of mitochondria to brain buffering capacities approach ~20% in HTS and 10% in HSS brain.

Table 2. pH buffering capacities, mitochondrial volume and efficiency of permeabilized tissue and isolated *mt* from triplefin brain. Buffering capacities were calculated relative to controls (no sample) in permeabilised brain and isolated *mt* at OXPHOS state exposed to graded acidosis, mediated by acid lactic titration (0-30 mM, 7.24-5.73 pH equivalent). Results expressed as mean (n = 5) ± s.e.m. The *mt* volume (Vol_{mt}) was back-calculated from the membrane potential signal as per described in the material and method section, with the assumption that in phosphorylating *mt*, the membrane potential equates -120 mV. Data expressed as mean of n=7 ± s.e.m. Respiratory control ratio (RCR) in both permeabilised and isolated *mt* and relates to coupling efficiencies. Data expressed as mean of 7 ± s.e.m. Significant difference at P < 0.05 from designated species between *B. medius*, *F. lapillum*, *F. capito* or *F. varium* indicated as *m*, *l*, *c* and *v*, respectively. The difference between sample preparation states was chosen at P < 0.05 and indicated as # (all tested with two-way ANOVA with Turkey correction).

	pH buffering		RCR		Vol_{mt} ($\mu l\ mg_{permeabilised\ brain}^{-1}$)
	Permeabilised (pH-unit mg_{brain}^{-1})	Isolated *mt* # (pH-unit $mg_{protein}^{-1}$)	Permeabilised	Isolated *mt*	OXPHOS (at -120 mV)
B. medius	0.940 ± 0.007 *cv*	0.193 ± 0.059 *v*	2.66 ± 0.25	6.64 ± 1.64 #	2.06 ± 0.24 *v*
F. lapillum	0.929 ± 0.011 *v*	0.169 ± 0.072 *v*	3.38 ± 0.51	3.17 ± 1.29	2.09 ± 0.25 *v*
F. capito	0.892 ± 0.005 *m*	0.177 ± 0.028 *v*	2.42 ± 0.10	1.79 ± 0.10	2.14 ± 0.18 *v*
F. varium	0.889 ± 0.008 *m*	0.089 ± 0.062 *mlc*	1.94 ± 0.15	6.74 ± 0.73 #	1.53 ± 0.21 *mlc*

3.3.2. Overall mitochondrial oxygen flux and pH effects on the mitochondrial function.

In phosphorylating mitochondria (presence of sufficient mitochondria substrates and ADP), buffered lactate addition did not alter OxPhos JO_2 in any species ($F_{10,60}$ = 0.381, P = 0.95; **Fig. 12.A**). However, in the absence of other mitochondria substrates, lactate mediated

JO_2 in the HTS mitochondria >22% more than in *F. varium* mitochondria ($P < 0.03$; **Fig. 12.B**) and *F. lapillum* JO_2 was also 30% greater than *B. medius* ($P < 0.01$).

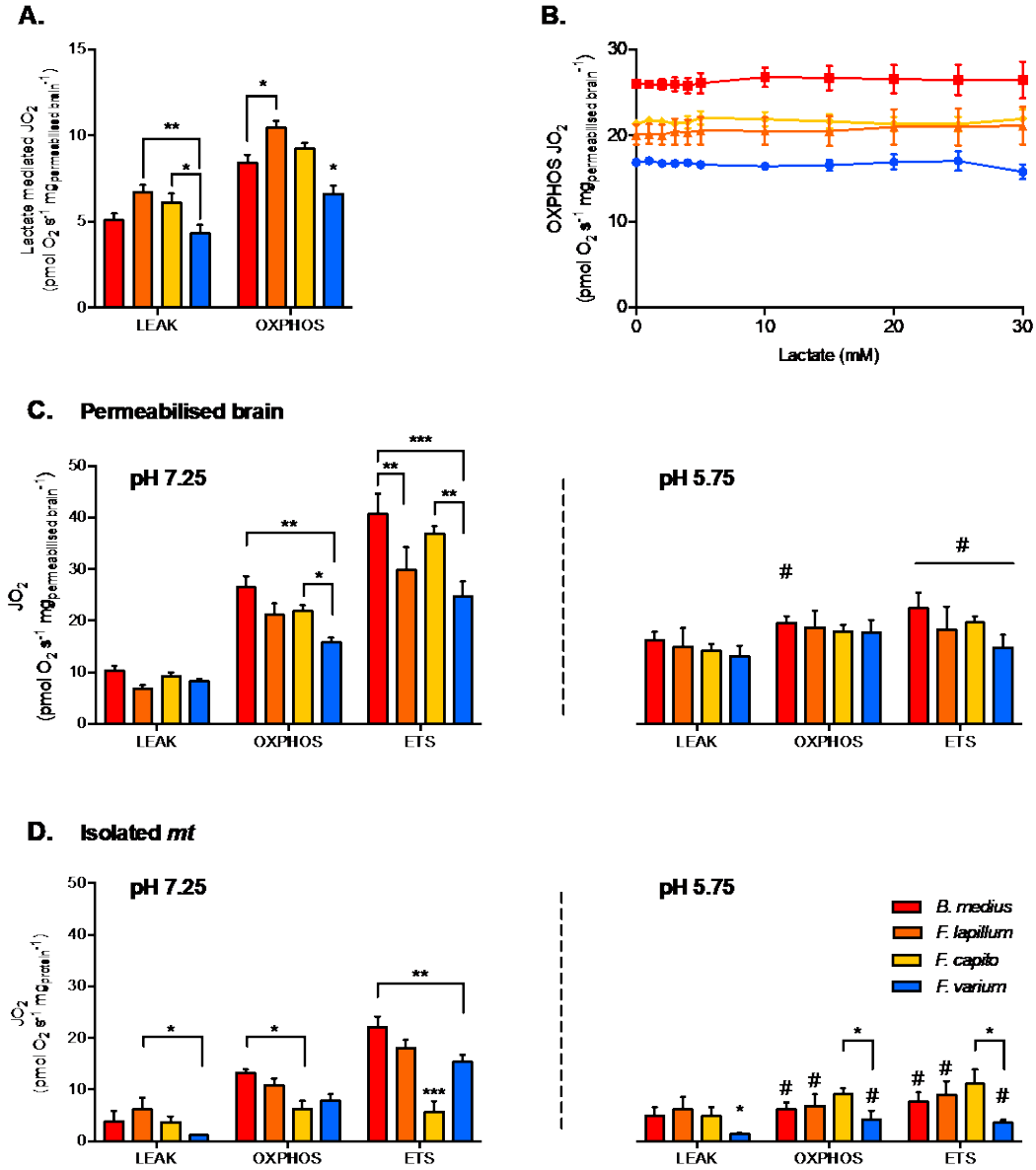

Figure 12. Mitochondrial respiration rates and the effect of lactate and pH on mitochondrial states. (A) The capacity of lactate (30 mM) to fuel LEAK and OXPHOS respirations in the absence of other mitochondrial substrates. (B) Titration of buffered lactate (pH 7.25) on mitochondria in OXPHOS state, in the presence of saturating CI and CII substrates (pyruvate, malate, glutamate and succinate), ADP and NAD+. In permeabilized brain (C) and isolated mitochondria (D), the respiration attributed to OXPHOS was determined with 30 mM buffered lactate. The portion of respiration attributed to proton leak (LEAK) was measured with the further addition of oligomycin and the maximum capacity of the electron transport system (ETS) was measured as the maximum respiration uncoupled from OXPHOS, reached with the titration of the uncoupler CCCP. Experiments were conducted at physiological pH (left panel) and acidic conditions (pH 5.75, right panel) mediated with 30 mM lactic acid instead of buffered lactate. Hypoxia tolerant species are presented in warm colours while the hypoxia sensitive species is presented in blue. Results presented as mean ± s.e.m of n = 7 individuals in (A) and (C) and n = 5 in (B). Significance difference between species at $P < 0.05$; 0.01 or 0.001 indicated as *, **, *** respectively and between pHs (within a mitochondrial state) chosen at $P < 0.05$ and indicated as # (two-way ANOVA and post-hoc test with Turkey correction).

The JO_2 differed among species for permeabilized brain and isolated mitochondria held at a physiological pH (species effect $F_{3,48} = 15.8$ and $F_{3,72} = 10.5$ respectively, $P < 0.01$; **Fig. 12**). While the LEAK JO_2 in permeabilized brain was similar among species (**Fig. 12.C**), OxPhos

and ETS JO_2 were greater in *B. medius* and *F. capito* relative to *F. varium* ($P < 0.05$). No difference was observed between *F. lapillum* and *F. capito*, which JO_2 at both OxPhos and ETS states, sat between JO_2 of the two other species. All species had greater ETS fluxes than OxPhos fluxes ($P < 0.02$) indicating some limitation of the OxPhos system relative to the ETS, and this was further observed in isolated mitochondria (**Fig. 12.D**).

In the presence of 30 mM ULac, which mediated a decrease of pH to 5.75, JO_2 was similar between species and across all states in permeabilized brain ($P = 0.26$; **Fig. 12.C**). However, while LEAK was increased by ~50% with ULac relative to BLac ($F_{1,6} = 47.4$, $P < 0.001$), ETS was significantly decreased by ~50% ($F_{1,6} = 139$, $P < 0.001$). In OxPhos, there was interaction between species and pH ($F_{3,18} = 4.35$, $P = 0.02$), mediated by a significant decrease in JO_2 in *B. medius* ($P = 0.02$) only. In isolated mitochondria (**Fig. 12.D**), acidosis did not affect *F. capito*, but decreased OxPhos and ETS by >50% in all other species ($P < 0.05$). OxPhos was 50% lower and ETS was 65% lower in *F. capito* than in *F. varium* mitochondria ($P = 0.05$ and 0.009, respectively).

We then assessed the effect of graded acidosis on OxPhos, which overall, mediated a contrasted response between the HTS and the HSS (main effect of species $F_{3,18} = 4.42$, $P = 0.02$; **Fig. 13**). First, JO_2 was gradually decreased in HTS until around pH 6.4 to ~18% relative to $OxPhos_{initial}$ (at pH 7.25, **Fig. 13.A**). Below pH 6.4, the response was more variable in the *Forsterygiion* genus, whereas JO_2 was more stable in *B. medius*. In *F. varium* however, JO_2 increased by 12% and was more variable below pH 6.9. JO_2 was significantly different between *B. medius* and *F. varium* below pH 7 ($P < 0.01$).

3.3.3. Membrane potential and changes in mitochondrial volume Vol_{mt}.

The Vol_{mt} in HTS was 30% higher than *F. varium* in OxPhos ($P < 0.04$, **Table. 2**). Below pH 6.9, acidosis mediated swelling in HTS *mt*, and decreased Vol_{mt} in *F. varium* mitochondria (interaction between species and pH of $F_{30,120} = 3.59$, $P < 0.001$; **Fig. 13.B**). While the Vol_{mt} increased to around 50% in *F. capito* and *F. lapillum*, it decreased by 12% in *F. varium*, relative to Vol_{mt} at pH 7.25 ($P < 0.04$). Differences between *B. medius* and *F. varium* were significant below pH 6.6 ($P < 0.03$).

Using estimates of Vol_{mt} dynamics with pH changes, we incorporated Vol_{mt} into the Nernst equation to better derive the $\Delta\Psi m$ relative to pH (**Fig. 16**). Two-way ANOVA revealed an interaction between $\Delta\Psi m$, species and pH ($F_{30,180} = 3.71$, $P < 0.001$, **Fig. 13C**). While the main

effect of pH was significant for all species ($F_{3,18}$ = 9.39, P = 0.001), only ΔΨm at pH 5.75 (around -100 mV) differed from its original value at pH 7.25 (-120 mV) in the HTS. In contrast, ΔΨm in *F. varium* mitochondria gradually decreased down to around -50 mV at pH 5.75 and was significantly lower than ΔΨm *in B. medius* mitochondria (P < 0.05 from pH 7). For comparison, a ΔΨm of -110 mV was reached at pH 7 in *F. varium* and 6.12-6 in the HTS.

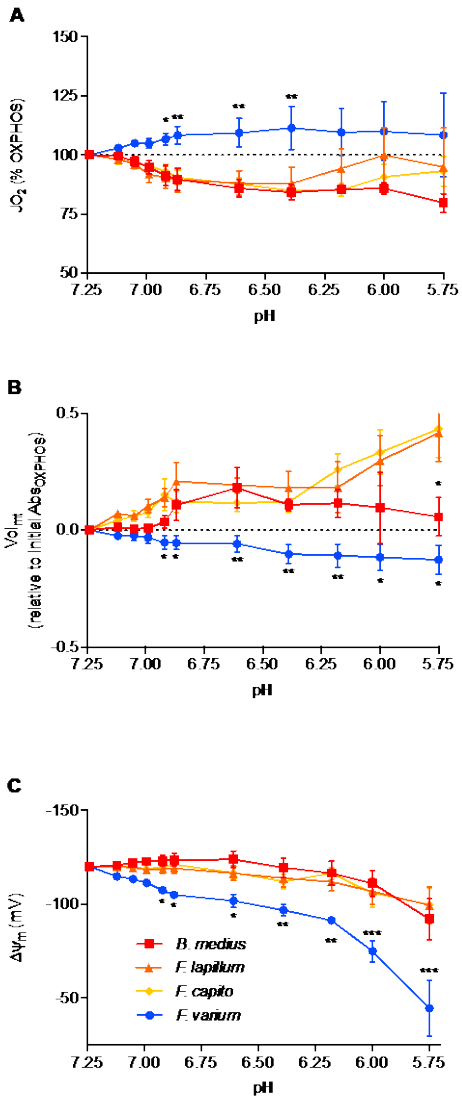

Figure 13. The effect of pH on the mitochondrial function. Respiration rate (JO_2, **A**), membrane potential (ΔΨm, **B**) and mitochondrial volume (Vol_{mt}, **C**) were measured at in the presence of saturating mitochondrial (*mt*) substrates and ADP in chambers of oximeters at 20°C (see the material and method section for more details). Buffered lactate (controls, constant pH) or unbuffered lactic acid (to decrease the medium pH) was then titrated in parallel respirometry chambers up to 30 mM and the lactate acid results were subtracted from the lactate results to account for the specific effects of pH on the mitochondrial parameters. ΔΨm was calculated from the fluorescence of safranin-O and with the consideration of the change in Vol_{mt}, calculated with the change in absorbance at 525 nm. Overall, acidosis mediated a contrasted response between the hypoxia sensitive species (blue) and the hypoxia-tolerant species (warm colours), with an inhibition of JO_2 and greater maintenance of ΔΨm induced with mitochondrial swelling in HTS. Results presented as mean (n = 7) ± s.e.m. For clarity, only the difference between *F. varium* and the other species is displayed as *, ** and *** for P < 0.05; 0.01 or 0.001 (main effect of pH and species tested with two-way ANOVA repeated measures).

3.3.4. Energy attributed to sustaining Δ Ψm.

Combined JO_2, ΔΨm and extra-*mt* pH data allowed an estimate of the work by mitochondria to develop ΔΨm in OxPhos state in regard to additional positive charges mediated by addition of acid ("C_{add}", additional H^+) (**Fig. 14**). Brain mitochondria from *F. varium* showed graded increase in work with C_{add}, up to ~50 µJ s^{-1} mg^{-1} at 100 µC charges (pH 6.6 equivalent, **Fig. 14.A**). In contrast, the remaining species showed a graded decrease in work

down to -50 µJ s^{-1} mg^{-1} at ~25 µC (pH 7). We then normalized the mitochondria work by C_{add}, which represents the use of C_{add} against or used to develop ΔΨm (**Fig. 14.B**). While internal work was maximized in *F. varium* with the first decrease in pH (from 7.25 to 7.12), C_{add} were fully used by *B. medius* to develop ΔΨm (P = 0.02). Between pH 7.12 – 6.4, internal work was further decreased in *B. medius* (P < 0.04), although increased for *F. varium* (P < 0.04). C_{add} was appeared to be utilised by *F. lapillum* and *F. capito* mitochondria between pH 7.05-6.6 and pH 6.9-6.6, respectively (P < 0.05). Progressively, mitochondria work (positive in *F. varium* and negative in HTS) returned to near zero values at approximately pH 6.

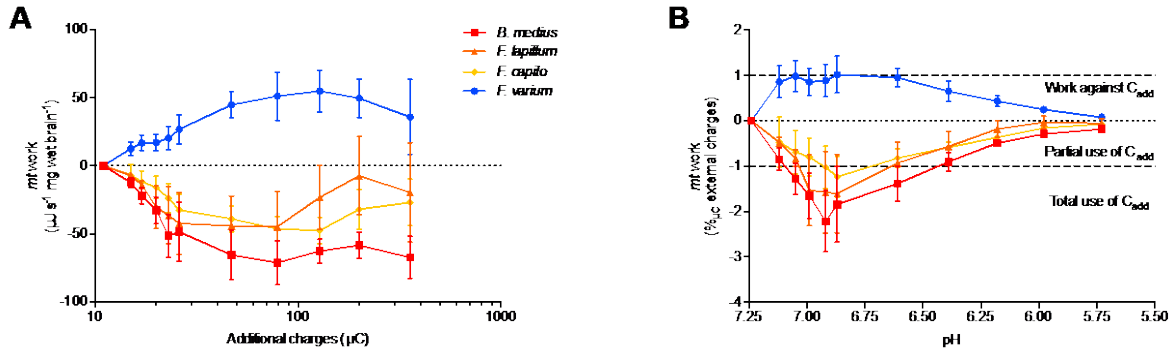

Figure 14. Mitochondrial work exposed to external charges loads mediated by acidification. Work is defined here by the protons/charges transferred against the mitochondrial membrane potential (ΔΨm). At OXPHOS state, the mitochondrial respiration rate was used as proxy for the proton pumping, calculated with the relative contribution of the mitochondrial complexes to respiration (between 12 and 20 H^+ pumped per O_2 consumed). ΔΨm was accurately calculated accounting for mitochondrial volume dynamics and the extra-*mt* charges were calculated from the measurement of medium pH, adjusted with lactic acid titration on permeabilized brain from triplefin fishes. A: Mitochondrial work was then calculated and expressed as the mass specific energy (µJ s^{-1} mg^{-1}) used to transfer protons and plotted against the additional charges (µC) mediated by acidosis (additional H^+). B: The relative work exercised by *mt* was then normalized against additional positive charges (C_{add}) and plotted against the medium pH. Positive values indicate the use of internal energy derived from the ETS to develop the ΔΨm against C_{add}, whereas negative values represent the portion of C_{add} that contributes to ΔΨm maintenance. While the hypoxia sensitive *F. varium* exerts positive work against acidosis, the other species seem to take advantage of external charges to maintain ΔΨm. Results of n = 7 individuals per species, expressed as mean ± s.e.m.

3.3.5. ATP production

Two-way ANOVA revealed an interaction between species and acidosis ($F_{1,10}$ = 9.01; P = 0.01; **Fig. 15.B**) as well as a difference between the two species ($F_{1,10}$ = 7.8; P = 0.02). While ATP production is supressed with acidosis in *F. varium*, it is increased by ~3.6 fold in *B. medius*. With a simultaneous decrease in JO_2 (**Fig. 15.A**), this significantly increases the P:O ratio in *B. medius* from 1.14 ± 0.36 at pH 7.25 to 4.95 ± 1.67 at pH 6.65 (P = 0.032; **Fig. 15.C**).

For *F. varium*,at pH 6.65 the JO_2 trended higher (P = 0.06), while the P:O ratio decreased from 1.56 ± 0.65 to -0.59 ± 0.43 (P < 0.05).

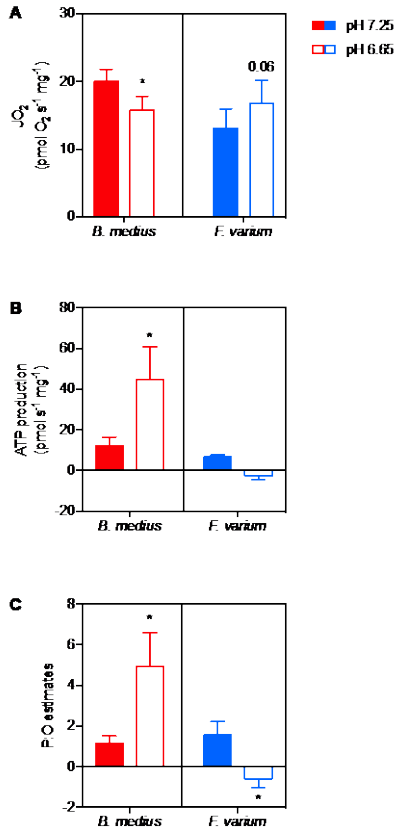

Figure 15. Acidosis enhances ATP production in brain mitochondria of the intertidal species. Permeabilised brain hemispheres were placed in respiratory chamber with mitochondrial substrates (described in the method) and 10 mM buffered lactate or unbuffered lactic acid to set the respiratory medium pH at 7.25 or 6.65, respectively. Mitochondrial respiration ("JO_2", A) was measured simultaneously with ATP production (B) using the fluorescent probe Mg-Green™. ATP consumption was measured with the addition of saturated antimycin A and oligomycin to block ATP production. P:O ratios were then calculated as ATP produced per oxygen element consumed (C). Data presented as scattered plot of 6 individuals and mean ± s.e.m. Statistical difference presented as * for P < 0.05, tested with two-way ANOVA followed by Turkey's *post-hoc* test.

3.4. Discussion

In the present study, we assessed the mitochondria function across a range of pH down to those experienced by hypoxic brain (Katsura, Ekholm et al. 1991, Katsura, Asplund et al. 1992, Kraut and Madias 2014, Witt, Larsen et al. 2017). It is the first study to explore these effects through pH titration and on a range of species with different tolerance to hypoxia, and it revealed significant differences among species that are consistent with species distribution. This differs from studies that test mitochondria function with a large variation of pH, as here we titrated unbuffered lactic acid sequentially to modulate pH in order to mimic *in vivo* lactate accumulation and associated pH changes. This includes the progressive nature of pH changes and the duration of changes. Here, we were able to follow mitochondria respiration, $\Delta\Psi m$ and pH or JO_2, Vol_{mt} and pH simultaneously. However, as lactate may modulate the mitochondria function and is a possible substrate of neurons (Philp, Macdonald et al. 2005, Chen, Mahieu et al. 2016, Caruso, Koch et al. 2017), we divided tissues from single brains to provide a control

and reference for comparisons between buffered and unbuffered samples. We show that while intertidal HTS suppress JO_2 they preserve $\Delta\Psi m$ and ATP production as pH declines. However, the $\Delta\Psi m$ decreased with the suppression of ATP synthesis despite JO_2 increases in the subtidal species *F. varium*. We contend that with decreasing pH the HTS mitochondria may harness the H^+ accumulation to maintain $\Delta\Psi m$ and ATP synthesis rates.

3.4.1. Lactate management of triplefin brain mt.

In the brain, the lactate anion is a putative substrate for aerobic metabolism (Reviewed in Barros 2013, Kane 2014). While lactate had little influence on JO_2 for any species in the presence of other mitochondria substrates (**Fig. 12.A**), lactate and NAD^+ could sustain OxPhos at higher rates in the HTS than in *F. varium* (**Fig. 12.B**). This indicates a greater capacity for lactate oxidation in HTS, which is likely advantageous post-hypoxia (Dienel 2012).

3.4.2. pH buffering capacities in the brain of triplefin fish.

Under acidosis, cells rely on bicarbonate and non-bicarbonate buffering capacities (Roos and Boron 1981), and despite the low apparent pH buffering capacity of mitochondria (Poburko, Santo-Domingo et al. 2011), mitochondria may play a role in the pH regulation when required. We measured the overall buffering capacities of permeabilized brain and isolated *mt*. In both preparations, HSS brains displayed a lower buffering capacity than HTS (**Table 2**). Although permeabilized tissue buffering differed only marginally (~5%) across species, isolated mitochondria buffering differed by ~2-fold between *B. medius* and *F. varium*. The mitochondria pH buffering contributes to approximately 17% of the cell pH buffering capacity, and while this suggests that some cytosolic components may remain following the permeabilisation process, which may significantly buffer pH changes within cells, mitochondria also contributes to some pH buffering and protects the mitochondria as well and this varies in accordance with hypoxia tolerance.

Comparison of Vol_{mt} also revealed that mitochondria from HTS exposed to acidosis swelled by 45% of their initial volume at pH 7.25 (**Fig. 13**). This dilutes matrix solutes, which includes enzymes, substrates and ions including H^+. A 1.4-fold swelling of the matrix (observed in *F. lapillum*) should mediate an alkalisation of approximatively 0.15 pH units, preventing excess acidification of the mitochondria matrix and would likely assists mitochondria pH buffering. In a recent study, acidosis (pH 6.5) mediated mitochondria elongation and cristae remodelling (Khacho, Tarabay et al. 2014). While neither pH buffering nor Vol_{mt} were discussed, these observations accord with an increase in Vol_{mt} measured in our

study. We note that this is one of the few studies to incorporate estimates of Vol_{mt} into estimates of ΔΨm and it has significant effect. One limitation is that the changes in Vol_{mt} were measured on isolated mitochondria and applied for the calculation of ΔΨm in permeabilised tissue. *Mt* exhibit a structural network within cells that is disrupted during the isolation process (Picard, Taivassalo et al. 2011). The response of isolated mitochondria may therefore differ from the response within the cells. Although the mitochondria integrity was similar (RCRs) across preparations (**Table 2**).

3.4.3. Acidosis mediates contrasted responses in the brain mitochondria of hypoxia-sensitive and hypoxia-tolerant species.

Notably in mammalian models, intracellular acidosis has generally been shown to impact mitochondria function with some loss of ΔΨm (Tiefenthaler, Amberger et al. 2001, Bento, Fagian et al. 2007) and a partial decrease in JO_2 (Hillered, Ernster et al. 1984), putatively through CII inhibition (Lemarie, Huc et al. 2011). We observed a significant elevation of JO_2 coincided with a decrease in ΔΨm in *F. varium* (**Fig. 13**). This indicates a loss of OxPhos efficiency as pH decreases, thereby decreasing ATP synthesis alongside an elevated O_2 turnover. Moreover, with a substantial drop in ΔΨm, i.e. below -110 mV the $ATP_{F0\text{-}F1}$ can reverse and act as a hydrolase, thereby elevating ATP consumption (Chinopoulos, Gerencser et al. 2010).

In contrast, mitochondria of the remaining HTS decreased JO_2 which would appear to be deleterious for OxPhos (Hillered, Ernster et al. 1984). However, with these species maintained ΔΨm to moderately low pH (**Fig. 13**). The lesser O_2 utilization for ΔΨm maintenance suggests that there is either a decrease in proton leak and/or the $[H^+]$ increase in the media (or cytosol) diffuses into the intermembrane space, may contribute to maintaining the ΔΨm. Notably the permeability of the mitochondria outer membrane is high (Cooper 2000).

3.4.4. Mitochondria of hypoxia tolerant species may harness the extra-mt protons to maintain function.

The ΔΨm represents the repartition of charge, between the mitochondria matrix and the intermembrane space and drives, in part, ATP production (Mitchell 1961). ΔΨm dissipates with H+ transfer into the matrix through three “negative fluxes”; 1) Constitutive leak (not regulated) results from the basal proton diffusion across the inner mitochondria membrane; (Jastroch, Divakaruni et al. 2010, Divakaruni and Brand 2011); 2) Inducible leak (regulated), resulting from the proton exchange through proteins (UCPs, ANT, NXHs) (Bernardi 1999,

Halestrap 2009) that can be modulated by ROS, fatty acids and GDP (Stuart, Brindle et al. 1999, Jastroch, Divakaruni et al. 2010, Masson, Hedges et al. 2017); and 3) the proton flux used to produce ATP by the F0-F1ATP synthase (Mitchell 2011). These all act in opposition to the proton flux transferred by the ETS (Mitchell 2011), or if some of the F0-F1ATP synthases have reversed (Chinopoulos, Gerencser et al. 2010). Work by the ETS (i.e. the positive transfer of H^+) can be estimated by O_2 consumption rates and balances these negative fluxes to sustain the ΔΨm. With physiological intracellular pH, the proton gradient (and therefore ΔΨm) that drives ATP production is maintained by the work performed by the ETS.

In 1966, André Jagendorf manipulated the extra-thylakoid pH of chloroplast vesicles to drive ATP synthesis in the dark (Jagendorf and Uribe 1966), confirming Mitchell's chemiosmotic hypothesis (Mitchell 1961) and indicating that ATP synthesis can be mediated with the manipulation of pH changes not generated by the ETS. Here, we sought to assess whereas pH modulation would partially assist ΔΨm and ATP synthesis and if this would influence the work performed by the ETS (illustrated in **Fig. 17.A**).

Modulation of the cytosolic pH (i.e. medium pH in permeabilised tissue) mediated an increase of the work performed by the ETS in mitochondria of HSS brains (**Fig. 14**), associated with a decrease in ΔΨm (**Fig. 13.C**) and ATP synthesis (**Fig.1 5.B**). With the dogma that acidosis as detrimental to cellular functions, a deleterious effect of acidosis was somewhat expected. However, in brain mitochondria of HTS, ΔΨm was maintained despite a decrease in ETS work and ATP production was further increased. This was associated with an elevation of P:O ratios that exceeded 2.7. This indicates that extra-*mt* H^+ may participate in the proton motive force in phosphorylating mitochondria (illustrated in **Fig. 17.B**). Such findings are in concordance with a recent study, which showed that in mammalian cortical neurones, mild acidosis (pH 6.5) mediates mitochondria remodelling and helps to sustain ATP production regardless of O_2 levels (Khacho, Tarabay et al. 2014).

3.5. Conclusion

With the switch to glycolysis and overall increase in ATP hydrolysis, acidosis mediated by hypoxia generally impairs mitochondria function of most vertebrates. In this study, we demonstrate that brain mitochondria of hypoxia-tolerant intertidal fish species buffer H^+ better than the subtidal species *F. varium.* In their natural habitat, as O_2 dwindles during nocturnal low-tides, intertidal triplefins may turn the problem of acidosis into a solution, and means to sustain ATP synthesis. As opposed to the subtidal *F. varium*, intertidal hypoxia tolerant

triplefins appear to take advantage of extra-*mt* protons that helps for maintenance of ΔΨm and ATP production. Acidosis also partially depresses proton pumping by the ETS and resulted in a significant increase in P:O ratio. The increase in mitochondria volume also appears to help with ΔΨm maintenance since this dilutes matrix compounds, including protons. We note that a similar process was recently proposed to occur in mammalian cortical neurones (Khacho, Tarabay et al. 2014). The partial suppression of JO_2 may also slow O_2 depletion in a hypoxic environment. While the mechanisms underlying the difference between the responses in HSS and HTS are yet to be resolved, these species provide natural strategies that have evolved to support mitochondria function in the acidifying brain.

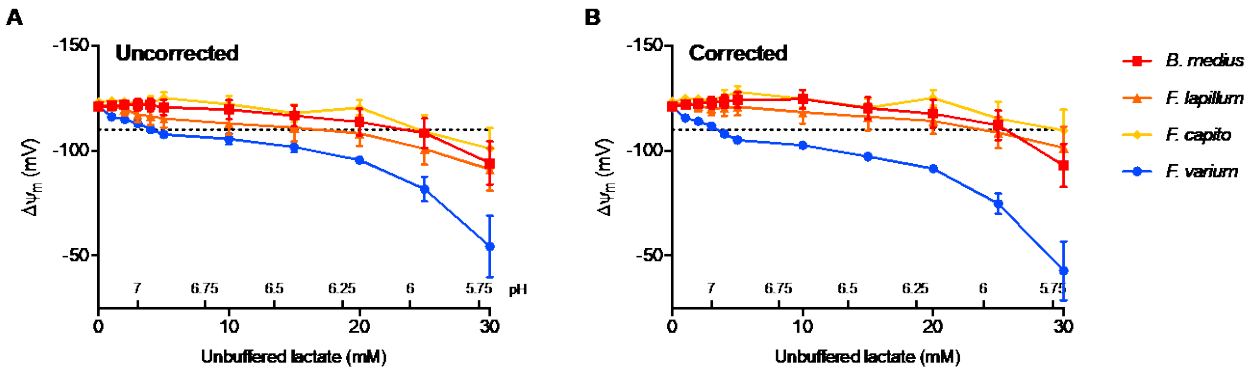

Figure 16. Effect of unbuffered lactate on the mitochondrial membrane potential (ΔΨm), without (A) or with (B) the integration of changes in *mt* volume. Estimates of *mt* volume (Vol_{mt}) is necessary to calculate ΔΨm when using cationic dyes. However, Vol_{mt} is dynamic and alters ion repartition and therefore ΔΨm. Here, we simultaneously followed Vol_{mt} and incorporated the relative change to ΔΨm calculations (see material and method section for more details on the calculation). Results presented as mean (n=7) ± s.e.m.

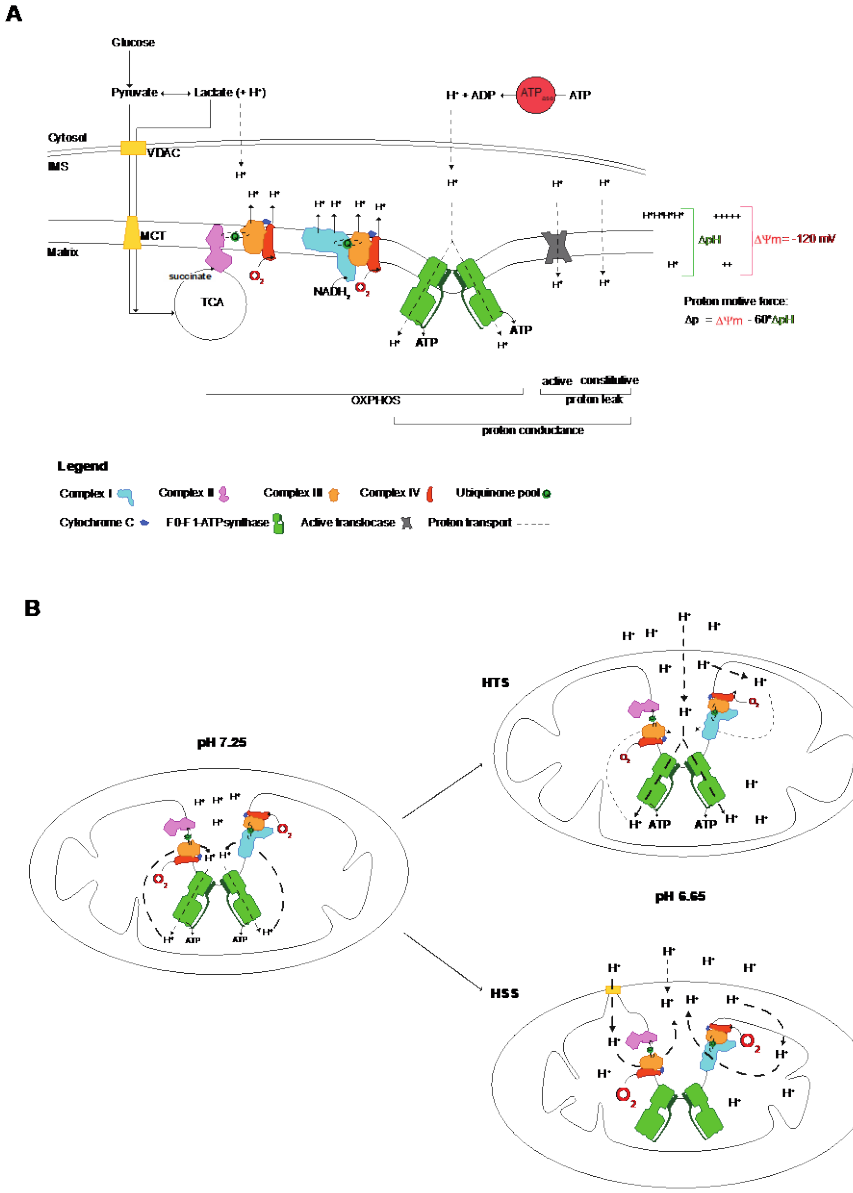

Figure 17. Simplified representation of how acidosis may help to maintain the mitochondrial function. (A) ATP production relies on the proton motive force Δp, which in part consists of a proton gradient. In physiological conditions, O_2 consumption reflects "work" performed by the ETS, which is seen here as proton pumping. At a given Δp, proton pumping equally opposed the combined negative proton fluxes (inward), which includes proton leak (constitutive and active) and "efficient" flux through the F0-F1-ATP synthase. As O_2 becomes limiting, proton pumping decelerates, decreasing Δp and ATP synthesis. However, as ATP hydrolysis rates surpass synthesis rates, protons accumulating in the cytosol may freely diffuse to the IMS (Cooper 2000) and these extra-*mt* protons may contribute to Δp, independently ETS "work". (B) In this study, triplefin fish brain mitochondria fish were exposed to gradual acidosis, mediated by the titration of lactic acid. Relative to control (pH 7.25), mitochondria in the subtidal HSS shrank with decreased pH and increased O_2 consumption rates, but ΔΨm and ATP production decreased. In contrast, intertidal HTS mitochondria swelled and maintained ΔΨm with increased ATP production rates while O_2 consumption rates were decreased.

Abbreviations: differential pH "ΔpH"; electron transport system "ETS"; hypoxia sensitive species "HSS"; hypoxia tolerant species "HTS"; inter-membrane space "IMS"; mitochondrial membrane potential "ΔΨm"; monocarboxylate transporter "MCT"; oxidative phosphorylation "OXPHOS"; proton motive force "Δp"; tricarboxylic acid cycle "TCA"; voltage dependent anion channel "VDAC".

Chapter 4. : Reactive oxygen species generation in the brain of hypoxia-tolerant New Zealand triplefin fish

Under Review: DEVAUX, J. B. L., HEDGES, C. P., BIRCH, N., HERBERT, N., RENSHAW, G. M. C. & HICKEY, A. J. R. 2019. “Reactive oxygen species generation in the brain of hypoxia-tolerant New Zealand triplefin fish”.

4.1. Introduction

By definition oxygen is essential to sustain life for aerobic organisms (Brahimi-Horn and Pouyssegur 2007), as it is used to release and convert energy into ATP via the process of oxidative phosphorylation (OxPhos) (Mitchell 2011). While over 90% of the O_2 consumed by an organism is utilised for ATP production by mitochondria, under rare conditions up to 2% of the electrons may leak from the mitochondrial electron transport system (ETS) and rapidly react with the surrounding O_2 to form reactive O_2 species (ROS) (Solaini, Baracca et al. 2010). ROS may react directly with lipids, proteins, nucleic acids, and nitric oxide and these can compromise tissue functions if antioxidant responses and repair processes are overwhelmed, or are limiting (Dickinson and Chang 2011). While ROS formation depends on the probability of electron leakage, accentuated if the mitochondrial membrane potential is elevated and the electron transport system is overly reduced, it is also dependent on the O_2 concentration and pressure (Scandurra and Gnaiger 2010, Makrecka-Kuka, Krumschnabel et al. 2015). Therefore, while O_2 is essential for OxPhos, paradoxically it is toxic in excess and when the ETS is excessively reduced.

While electron leakage from mitochondria may occur at numerous sites, it appears to mainly occur at the FMN site of complex I (CI), and complex III (CIII), which are respectively, the upstream and downstream sites interacting with the Co-Q pool (Turrens, Alexandre et al. 1985, Murphy 2009). More recently, complex II ("CII"; or succinate dehydrogenase, SDH) has been shown to be involved in a "reverse electron transfer" (RET) on reperfusion (Chouchani, Pell et al. 2014). With ischemia the ETS slows and succinate elevates due to a decrease in O_2 required for its oxidation. Succinate elevates several folds higher than all other tricarboxylic acid cycle (TCA) intermediates in all tissues through reversal of succinate dehydrogenase. On reperfusion succinate is rapidly oxidised at CII, and the limited coenzyme Q pools become overly reduced (QH_2). Instead of flowing to CIII, QH_2 appears to flow to CI and mediates electron leakage, resulting in the production of superoxide, $O_2^{\cdot -}$ (Chouchani, Pell et al. 2014). Typically, succinate-mediated ROS production is explored experimentally in the presence of rotenone, class A CI inhibitor (Degli Esposti 1998). The specific effects of rotenone remain unclear since it increases or decreases ROS production dependent on mitochondrial respiration state (Zorov, Juhaszova et al. 2014). A representation of the processes described above are summarised in Figure 18.

While much attention has been placed on the role of succinate and mitochondrial ROS release in clinical contexts (Pell, Chouchani et al. 2016), the implications of ROS production within

organs of animals frequently exposed to ”natural ischemia-reoxygenation”, or at least hypoxia-reoxygenation, warrants investigation as these animals may have circumvented issues or buffered mitochondria from oxidative stressors (Pfleger, He et al. 2015, Pell, Chouchani et al. 2016, Tretter, Patocs et al. 2016, Valls-Lacalle, Barba et al. 2016, Wijermars, Schaapherder et al. 2016, Andrienko, Pasdois et al. 2017). Relative to terrestrial species, fish are more prone to varying O_2 levels and associated oxidative stress (Lushchak and Bagnyukova 2006). In the intertidal zone, stagnant rock-pool water can reach near anoxic levels at night, but they can also rise to 300% O_2 saturation on sunny summer days when photosynthesis is active (Richards 2011, McArley, Hickey et al. 2018). Therefore, intertidal fish are frequently exposed to both hypoxia and hyperoxia in their natural environment. While there are only a few studies that have explored mitochondrial ROS production in fish tissues exposed to hypoxia (Hickey, Renshaw et al. 2012, Du, Mahalingam et al. 2016, Zeng, Wang et al. 2016, Pelster, Wood et al. 2018), we have found only one study exploring hyperoxic oxidative stress in fish, the Atlantic cod (*Gadus morhua*), which was exposed to O_2 at 200% air saturation (Karlsson, Heier et al. 2011), and this is a demersal species. We note that elevated PO_2 also elevates mitochondrial ROS formation (Makrecka-Kuka, Krumschnabel et al. 2015), and that in these experiments, ROS production was assessed at an initial PO_2 that is significantly higher than that occurring at the cellular level under normoxia.

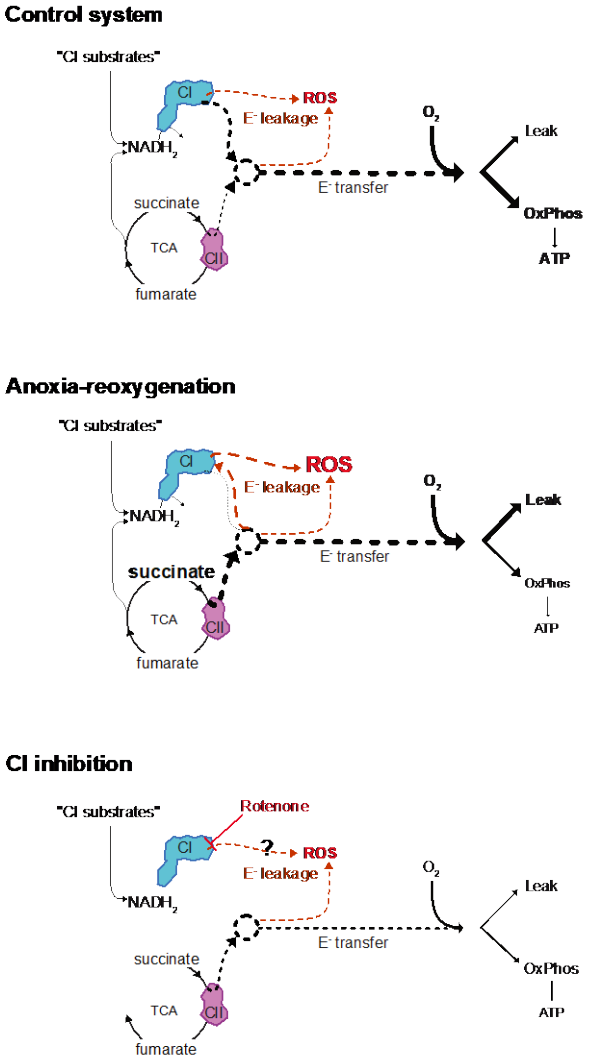

Figure 18. Mitochondrial electron transport system and electron transfer. With sufficient substrate and O_2, mitochondrial substrates are metabolised to reduced equivalents, which are oxidised by either complex I ("CI") or complex II ("CII"). As a result, electrons are stripped and directed though the electron transport system to O_2. The free energy released from this transfer is then coupled to oxidative phosphorylation "OxPhos" and ATP production, or dissipated as proton leak, or "Leak". Electrons may leak from the electron transfer system and mediate the production of reactive oxygen species "ROS". Post an anoxic event, accumulated succinate is highly reduced by CII and saturates the electron transfer at its site. This likely mediates a back-transfer of electrons to CI that increases electron leakage and ROS production. ROS likely mediate damage to membranes, which may increase Leak. Excess ROS production may be prevented using CI inhibitor such as rotenone that blocks electron transfer at the Q-site of CI. Rotenone hence supposedly decreases electron leakage and associated ROS production, however it blocks the electron transfer from CI to the electron transfer system, which significantly decreases OxPhos and ATP production. We note that without competition for the Q-pool, CII may have a greater contribution to the electron transfer system.

Here, we aimed to determine the ROS production at a broad PO_2 range in hypoxia-tolerant and sensitive species (HTS and HSS respectively) of fish, and whether succinate and anoxia-reoxygenation (AR) modulate the ROS formation. Intertidal New Zealand triplefin fish (*Tripterygiidae* family) frequently experience episodes of hypoxia-reoxygenation in their ecological niches (McArley, Hickey et al. 2018). They also experience hyperoxia with PO_2 levels exceeding 200% air saturation in rock-pool during sunny summer days (McArley, Hickey et al. 2018) , and this likely increases intracellular PO_2 and the likelihood of ROS formation (Karlsson, Heier et al. 2011). The close phylogenetic background of the 26 endemic species (Hickey and Clements 2005) make these fish a great model to understand adaptations, such as those to survive hypoxic and hyperoxic environments (Hickey, Lavery et al. 2009).

Here we use brain, a tissue that is highly dependent on aerobic metabolism, to compare mitochondrial respiration and ROS production of three intertidal HTS to a subtidal hypoxia-

sensitive species. We test how ROS production changes with gradual accumulation/titration of succinate, a substrate that accumulates in hypoxia in vertebrates (Chouchani, Pell et al. 2014), and we tested the effects of anoxia-reoxygenation *in vitro* and ROS production in the contexts of O_2 concentration, from a relative hyperoxia to anoxia.

4.2. Material and methods

4.2.1. Animal sampling and housing

Four triplefin fish species with various degrees of hypoxia tolerance were chosen for this study. The exclusively intertidal *Bellapiscis medius* was the most hypoxia-tolerant species and was caught in exposed rock-pools at low tide. Two "intermediate" species *Forsterygion lapillum* and *F. capito*, occupy intertidal waters and can be found in low rock-pools and sub-tidally (> 5 m) and were caught in exposed rock-pools at low tide and off estuarine piers. The most hypoxia sensitive *F. varium* occupies subtidal waters and was caught while scuba diving. Adult specimens were housed in flow through aerated sea water (20ºC) and fed with mixture of shrimp and green lipped mussels for at least two weeks. Animal capture, handling and experimental procedures were approved by the University of Auckland Ethics Committee (R001551).

4.2.2. Brain sampling and permeabilisation process

Fish were euthanized by sectioning the spinal cord and the whole brain was quickly dissected and placed in ice-cold preservation media (in mM: 2.77 CaK_2EGTA, 7.23 K_2EGTA, 5.77 Na_2ATP, 6.56 $MgCl_2.6H_2O$, 20 taurine, 15 Na_2 phosphocreatine, 20 imidazole, 0.5 DTT, 50 KMES, and 30 Sucrose, pH 7.24 at 20°C). Cellular permeabilisation was undertaken with the addition of 50 µg ml^{-1} freshly prepared saponin and gentle shaken for 30 min at 4ºC. The brain sections were then transferred into three subsequent ice-cold respiration medium baths (0.5 EGTA, 3 $MgCl_2.6H_2O$, 60 K-lactobionate, 20 taurine, 10 KH_2PO_4, 2.5 HEPES, 30 MES, 160 sucrose, 1g.l^{-1} BSA, pH 7.24 at 20°C) and mixed gently at 4ºC for 10 min. Sections of brain were then blotted dry and weighed prior to use for respiration assays.

4.2.3. Respirometry and ROS assays

Oroboros™ oxygraphs (Innsbruck, Austria) were used for the simultaneous measurement of the mitochondrial respiration and ROS production (Hickey, Renshaw et al. 2012). Oxygen sensors were calibrated prior to each experimental procedure to account for the instrumental and chemical background flux (including time-response of the electrode near anoxia). Around 5 mg of freshly permeabilised triplefin brain was introduced into the

respirometry chambers containing respiration medium at 20ºC (261.9 µM O_2 = 20.5 kPa PO_2 at 101.5 kPa barometric pressure). Assays consisted of the sequential addition of substrates, inhibitors and uncoupler to inform on the mitochondrial respiration, ROS production and therefore electron leakage at (i) decreasing PO_2, (ii) post anoxia-reoxygenation in the chamber, (iii) that mediated by either complex I or II (CI and CII, respectively) in the absence or presence of rotenone, and (iv) that mediated by graded succinate. Assays are detailed in **Table 3**. Experiments were designed so the applied condition and control were run on samples from the same individual. O_2 fluxes attributed to oxidative phosphorylation (OxPhos) were measured in the presence of saturated pyruvate (10 mM), malate (5 mM), glutamate (10 mM), succinate (10 mM) and ADP (1 mM). Samples were left to deplete O_2 until anoxia was reached, held for 20 min and then reoxygenated (up to ~ 240 µM O_2 = 18.8 kPa PO_2). Control groups were run in a parallel chamber and held with sufficient O_2 for the same length of time. Respiration that was not attributable to OxPhos, i.e. proton leak (Leak) was measured with the addition of the ATP_{F0-F1} synthase inhibitor oligomycin (2.5 µM) and the adenylate translocase inhibitor carboxy-atractyloside (0.75 mM). Potassium cyanide (1 mM) was then added to account for residual O_2 consumption (yet insignificant).

Table 3. Respirometry assays employed to assess the effect of anoxia-reoxygenation, graded succinate and complex contribution on the mitochondrial respiration and ROS production in permeabilised brain of New Zealand triplefin fish species. For each assay (1, 2 and 3), freshly permeabilised brain was partitioned equally between control and experimental chambers containing fully aerated respiration medium thermostated at 20ºC. Mitochondrial respiration and ROS production were measured simultaneously using Oroboros™ O2k. P: pyruvate; G: glutamate; ADP: adenosine diphosphate; CCCP: carbonyl cyanide m-chlorophenyl hydrazone; KCN: potassium cyanide.

	Assay 1 (Fig. 2&3)		Assay 2 (Fig. 4)			Assay 3 (Fig. 5)	
State	Control	Experimental			+ Rotenone	Control	Experimental
Leak	PMG + succinate	PMG + succinate	PMG	Succinate	Succinate	PMG	PMG
OxPhos	ADP	ADP	ADP	ADP	ADP	ADP	ADP
		20min anoxia	Succinate	PMG	PMG		20min anoxia
		Reoxygenation					Reoxygenation
						Succinate titration	Succinate titration
Leak	Oligomycin c-atractyloside	Oligomycin c-atractyloside				Oligomycin c-atractyloside	Oligomycin c-atractyloside
Uncoupled	CCCP	CCCP				CCCP	CCCP
Resting O_2 consumption	KCN	KCN	KCN	KCN	KCN	KCN	KCN

The maximum contribution of CI and CII to respiration, ROS production and electron leakage was assessed in multiple settings. Firstly, with saturating CI substrates (pyruvate, malate and glutamate) + ADP. The additive effect of CII ("+CII") was then measured following the addition of saturating succinate. Net CII contribution to OxPhos was then assessed in separated

assays with saturating succinate + ADP, with or without the CI inhibitor rotenone (0.5 µM), and additional CI ("+CI") was then mediated by the addition of the CI substrates stated above. The contributions of accumulating succinate to ROS production was also measured in different settings. Succinate was first titrated in the absence of additional CI substrates and ADP (to mimic ischaemic depletion of adenylates). Respiration and ROS production were then also measured in the presence of saturating CI substrates and ADP. In this setting, succinate was titrated (0-10 mM) in samples exposed to an episode of anoxia reoxygenation (AR), while controls were held with sufficient O_2 (such as described above) to simulate and explore the effects of anoxia-reoxygenation.

4.2.4. Data and statistical analysis

As ROS production is dependent on the O_2 availability (Scandurra and Gnaiger 2010, Makrecka-Kuka, Krumschnabel et al. 2015), the dependence of ROS for O_2 at Leak and OxPhos states was calculated for each sample. Linear correlations between the ROS production and PO_2 were apparent with no difference detected among species ($P > 0.53$) and there was also no effect of AR ($P > 0.40$). There was however a stronger effect in Leak state (ROS = 0.02±0.006 PO_2 + 2.71±0.98) relative to the OxPhos state (ROS = 0.012±0.005 PO_2 + 1.38±0.75; $F_{1,5} = 60$; $P < 0.001$). Therefore, the dependence of PO_2 was then used to correct the ROS data in defined states (i.e. Leak or OxPhos) for a specific PO_2 (**Fig. 20B, 21B** & **22B**). ROS production can also be expressed as the portion of electrons not directed to O_2 reduction, i.e. a loss of efficiency to convert the electrical gradient to proton pumping. We therefore calculated the relative portion of electron leakage by normalising the ROS production by the respiration rate (as ROS / respiration).

For succinate titration assays, agonist dose response (three parameters) curves were fitted (least squares method) and maximum respiration mediated by succinate and mitochondrial affinity to succinate ($aK_{M,S}$) were extracted and compared (extra sum-of-squares F test) using GraphPad Prism. The catalytic efficiency ($K_{cat,S}$; in s^{-1} mg^{-1}) was calculated as maximum respiration divided by $aK_{M,S}$.

Respiration rates and ROS production were recorded from the calibrated signal in DatLab v7.1 and processed in Excel. GraphPad Prism 7 was used for curve fitting and statistical analysis. Three-way ANOVA was first employed to assess the interaction effect of AR, succinate and species. Since no clear interaction was found, two-way ANOVA repeated measures was employed followed by Turkey's post-hoc tests were applied to assess (i) the effect of PO_2 and (ii) graded succinate on the mitochondrial respiration, and test for differences among species

in ROS production, and electron leakage. Two-way ANOVAs followed by Turkey's post-hoc tests were performed to test for the effect of AR and test for the complex contribution on the ROS production and electron leakage between species. Non-linear models fitted with the least squared method were compared to find the best fit, and extracted parameters were compared between species using the extra-sum-of-squares F test. Significance differences were determined at $P < 0.05$. All data are presented as mean ± s.e.m of 6 individuals.

4.3. Results

4.3.1. The effect of the oxygen tension on the mitochondrial function.

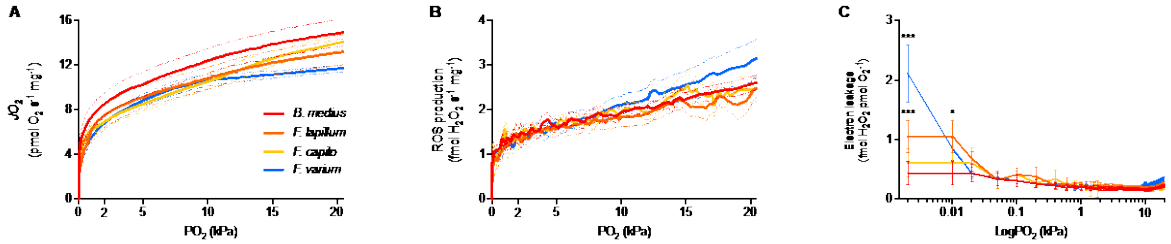

Figure 19. The dependence of the oxygen consumption, reactive oxygen species production and electron leakage to decreasing oxygen tension (PO_2). In permeabilised brain of four triplefin fish species with various degree of hypoxia tolerance, mitochondrial respiration (A), ROS production (B) and electron leakage (C) were assessed at decreasing PO_2 to anoxia. Data are presented as mean ± s.e.m. of 6 individuals of the rockpool species *B. medius* (red), the intertidal species *F. lapillum* (orange) and *F. capito* (yellow) and the subtidal species. *F. varium* (blue). In (C), PO_2 was logged to appreciate the increase in electron leakage near anoxia. Data presented as mean ± s.e.m. (plain and dashed line, respectively). The difference between species was chosen at $P < 0.05$ or 0.001 and indicated in black as * or *** (respectively), tested with two-way ANOVA repeated measures followed by Turkey's *post-hoc* test.

To determine whether the PO_2 at which permeabilised brain were held *in vitro* affects O_2 flux, ROS production and the electron leakage, three parameters were measured in samples as they depleted O_2. At air saturation, the three intertidal species had greater respiration rates than the subtidal species *F. varium* (**Fig. 19A**, $P < 0.001$). As O_2 was depleted below 12 kPa, O_2 flux of the two "mid-tidal" species matched those of *F. varium*, with *B. medius* sustaining higher O_2 flux at lower PO_2 (< 2.05 kPa).

The ROS dependence on O_2 from 20.5-2.1 kPa PO_2 fitted a linear regression (**Fig. 19B**, $F_{1,543} = 0.196$, $P < 0.05$). In this range, the ROS production was greater in *F. varium* than the three HTS (unshared slope and intercept; $F_{6,22} = 32.82$, $P < 0.0001$). However, at a PO_2 mitochondria most likely function *in vivo* under normoxia (i.e. $PO_2 < 2.05$ kPa), the ROS dependence on PO_2 fitted a three-parameter dose-response ($P < 0.005$), and did not differ among species ($P = 0.48$). The portion of electrons directed to ROS production (i.e. ROS / respiration) was similar similarly and stable among species until 5% air saturation (**Fig. 19C**). However, on approaching anoxia ($PO_2 < 0.02$ kPa), electron leakage in *F. varium* increased ~5-fold and was higher than for the other intertidal species ($P < 0.001$).

4.3.2. Anoxia-reoxygenation impacts mitochondrial function regardless of hypoxia-tolerance

The subtidal species *F. varium* had the lowest OxPhos flux at PO_2 above 15.4 kPa, below which no difference in respiration was apparent among species (**Fig. 20A**). Following AR, OxPhos respiration decreased for the HTS and matched this in *F. varium* such that they were similar among species. No differences among species were observed for Leak state flux (**Fig. 20B**).

In Leak and OxPhos states, ROS production was assessed at various PO_2 in control groups and groups exposed to AR. We therefore could account for the influence of altered PO_2 on ROS production (**Fig 23**), and ROS production was higher from mitochondria in the Leak state than mitochondria in the OxPhos state (**Fig. 20B**; $F_{1,5} = 60$; $P < 0.001$). In control-non-AR samples, ROS production in OxPhos state was ~2 times higher in *F. varium* than the other species, however no significant differences were apparent among species in the Leak state. Exposure to AR *in vitro* did not affect ROS production in the OxPhos state, however ROS production decreased in the Leak state for all species relative to prior to AR (main effect of $F_{3,15} = 1.2$, $P = 0.02$).

Electron leakage was similar among species in the presence of sufficient elevated O_2 (i.e. PO_2 > 2.04 kPa; **Fig. 19C** & **Fig. 20C**). However, electron leakage significantly increased approaching anoxia in *F. varium* only, and was significantly greater than the other species at 0.01% PO_2 (**Fig 19C**). Following AR, electron leakage decreased in *F. lapillum* only ($P < 0.001$) and was lower than the other species ($P < 0.05$; **Fig. 20C**).

Table 1. The mitochondrial affinity for succinate is lower in the hypoxia-tolerant species. Succinate was titrated on permeabilised brain of the four triplefin fish species in the absence of other substrates (Leak), in the presence of mitochondrial substrates (OxPhos) and brain exposed to an event of anoxia-reoxygenation (OxPhos post-AR). Agonist vs. response (three parameters) curves were fitted (least squares method) and maximum respiration mediated by succinate and succinate affinity ($aK_{M,S}$) were extracted and compared (extra sum-of-squares F test) using GraphPad Prism. The catalytic efficiency ($K_{cat,S}$) was calculated as maximum respiration divided by $aK_{M,S}$. One-way ANOVAs were used to test for statistical differences, chosen at $P < 0.05$ and displayed as "*" for the difference between species and as "#" for the difference between states.

	Maximum respiration (pmol O_2 .s^{-1} .mg^{-1})			$aK_{M,S}$ (mM succinate)			$K_{cat,S}$ (s^{-1} mg^{-1})		
Species	Leak	OxPhos	OxPhos post-AR	Leak	OxPhos	OxPhos post-AR	Leak	OxPhos	OxPhos post-AR
B. medius	1.7 ± 0.3#	8.9 ± 3.2	6.4 ± 1.0	2.0 ± 0.9#	13.5 ± 7.7	3.4 ± 1.4#	1.2 ± 0.1	1.0 ± 0.2	2.2 ± 0.7#
F. lapillum	1.9 ± 0.1#	5.0 ± 1.5	7.5 ± 0.9	1.4 ± 0.3#	5.8 ± 4.0	4.4 ± 1.4	1.7 ± 0.8	1.2 ± 0.5	2.0 ± 0.5#
F. capito	1.8 ± 0.2#	10.0 ± 3.5	8.0 ± 0.9	1.6 ± 0.4#	11.6 ± 6.8	3.4 ± 1.0#	1.2 ± 0.3	1.5 ± 0.5	3.0 ± 0.8#
F. varium	2.0 ± 0.1	2.8 ± 0.6*	2.9 ± 0.4*	1.3 ± 0.2	1.1 ± 1.1*	0.5 ± 0.3*	1.3 ± 0.2	4.1 ± 1.4*	10.3 ± 4.0*#

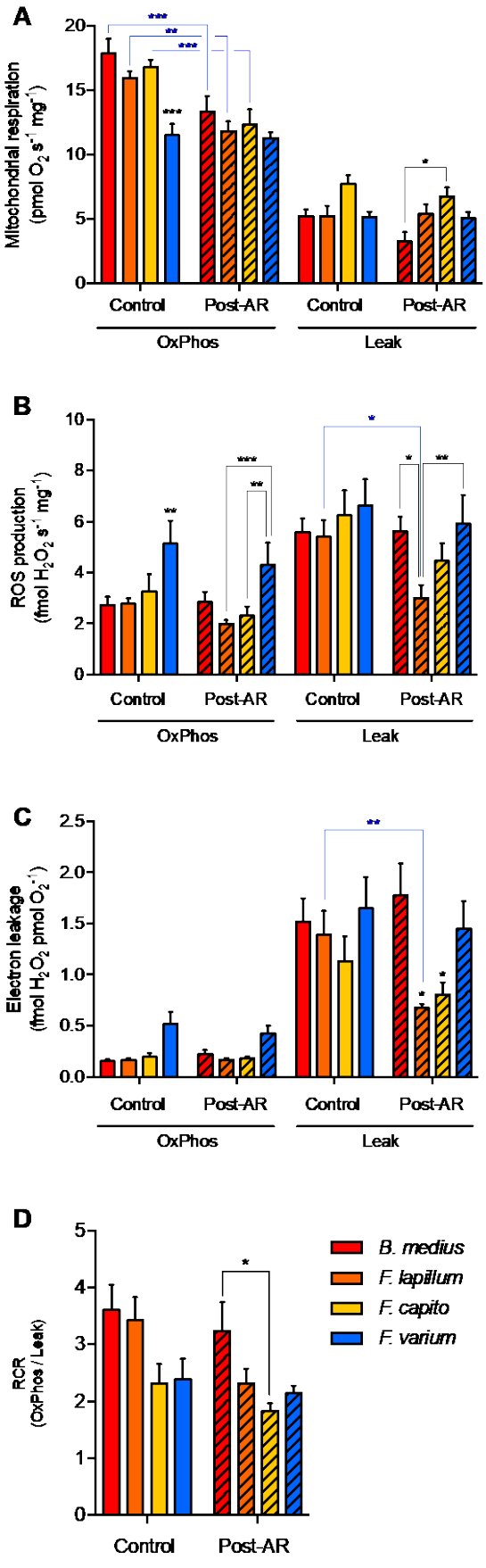

Figure 20. Exposure to anoxia-reoxygenation (AR) *in vitro* does not affect the ROS production. The effect of AR on the mitochondrial respiration (A), the ROS production (B) and the electron leakage (C) were assessed on permeabilised brain of the rock-pool species *B. medius* (red), the intertidal species *F. lapillum* (orange) and *F. capito* (yellow) and the subtidal species *F. varium* (blue). Samples were induced in OxPhos state with saturated mitochondrial substrates (pyruvate, malate, glutamate and succinate) and ADP and let to deplete the O_2 until anoxia, held for 20min and followed by rapid reoxygenation ("post-AR"). Control groups were held with sufficient O_2 (> 60% air saturation). Once respiration recovered and OxPhos rates post-AR measured, Leak state was induced by inhibition of the ATP_{F0-F1} with olygomycin. (D) Respiratory control ration (RCR) were then calculated (as OxPhos / Leak) to appreciate the coupling of respiration to OxPhos. Data are presented as mean ± of 6 individuals ± s.e.m. Statistical difference tested with two-way ANOVA repeated measures followed by Turkey's *post-hoc* test and presented in black for the difference between species, and blue for the effect of AR, as *, ** and *** for $P < 0.05$, 0.001 and 0.0001, respectively.

4.3.3. Mitochondrial complexes contribution to ROS production and to electron leakage

We assessed the contribution of either CI or CII linked pathways and their respective additive effects ("+CI" and "+CII") to respiration, ROS production and to electron leakage (**Fig. 21**). With CI substrates and ADP (**Fig. 21** left panels), *F. varium* had the lowest respiration and the highest ROS production ($P < 0.04$). While the addition of saturating succinate (+CII) mediated an increase in respiration in all species ($P < 0.001$), it did not affect the ROS production, which remained highest in *F. varium*.

Experiments commencing with saturating succinate and ADP (**Fig. 21** central panels) respiration was similar across species. However, ROS production was highest in *F. lapillum* and *F. capito* relative to *B. medius* and *F. varium* ($P < 0.01$). The subsequent addition of CI substrates ("+CI") mediated a significant

increase in respiration in all species ($P < 0.001$), and enhanced electron leakage in *F. varium* only ($P < 0.001$). ROS production remained the highest in *F. lapillum* and was the lowest in *B. medius* ($P = 0.01$).

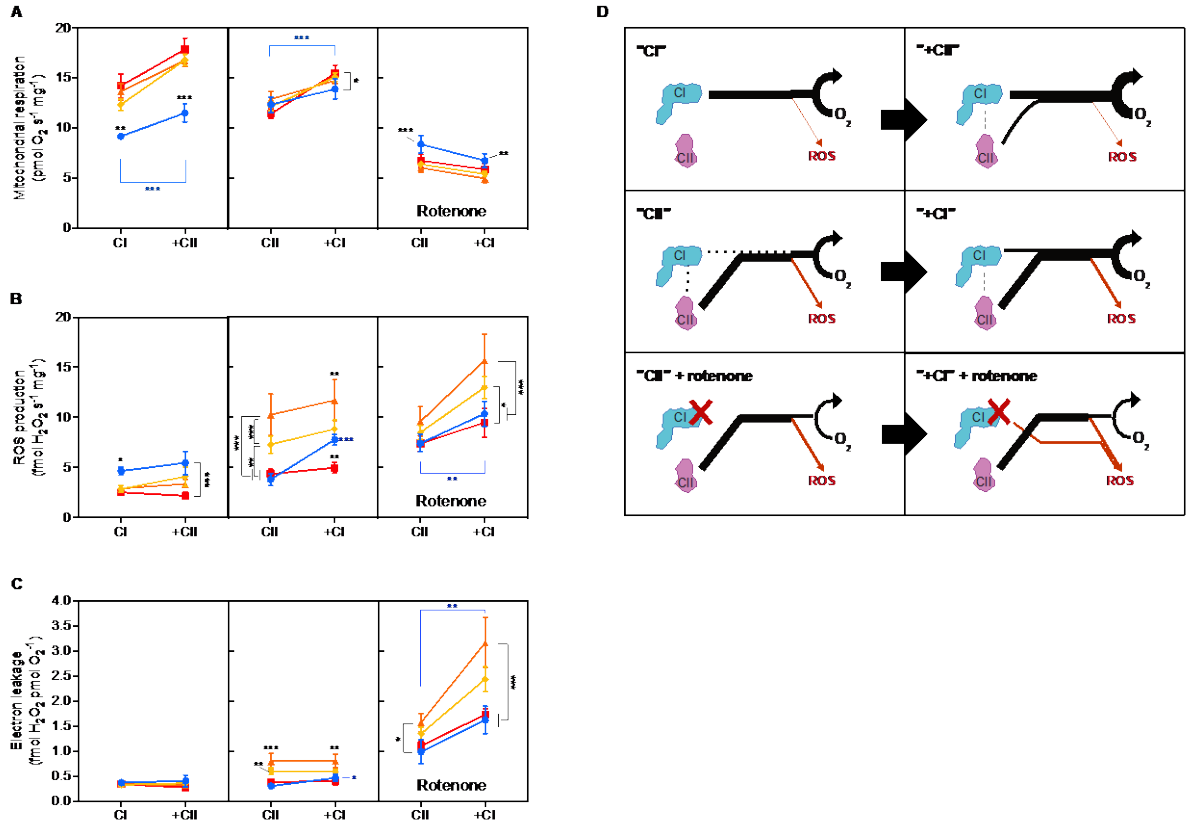

Figure 21. The contribution of the mitochondrial complex I (CI) and complex II (CII) to respiration and electron leakage for ROS formation. In permeabilised brain of four triplefin fish species, mitochondrial respiration (A) and ROS production (B) were measured simultaneously in three different settings. Firstly, with ADP and CI substrates (pyruvate, malate and glutamate; "CI"), and subsequently, additional succinate ("+CII"; left panel). Secondly, with ADP and CII substrate ("CII") and subsequently, additional CI substrates ("+CI"). Finally, the latter was repeated in the presence of the CI inhibitor rotenone. (C) The electron leakage was calculated as ROS per O_2 consumed. (D) Graphical representation of the results. The flux of electron supported by CI or CII is represented in black. A portion of this flux not directed to respiration, electron leak (orange), is directed to ROS production. Since CII product supposedly further contributes to feeding CI, this was represented in dash. We note that the origin of electron leakage is here arbitrary. Data in A, B&C are presented as mean of 6 individuals ± s.e.m. Statistical difference tested with two-way ANOVA repeated measures followed by Turkey's *post-hoc* test and presented in black for the difference between species, and blue for the effect of the additional complex, as *, ** and *** for $P < 0.05$, 0.01 and 0.001, respectively.

We note that CII only (i.e. without CI substrates) mediated higher electron leakage and ROS production than when respiration was already partially fuelled by CI ($P < 0.05$). The comparisons among pathways and their additive effects to ROS production revealed that while +CI and CI had similar production rates, +CII was lower than CII in all species of fish ($P < 0.05$; **Fig. 20A**).

With rotenone (**Fig. 21** right panels), respiration rates fuelled by CII were halved relative to without rotenone ($P < 0.001$), yet remained the highest in *F. varium* relative to the HTS ($P <$

0.001). Electron leakage was 75% higher in *F. lapillum* relative to *F. varium* (**Fig. 21C**; $P < 0.05$). While addition of CI substrates did not affect respiration, they increased electron leakage and ROS production in all fish species ($P < 0.01$), which were 2-fold higher in *F. lapillum* relative to *B. medius* and *F. varium*.

4.3.4. The role of succinate concentration

Mitochondrial respiration and ROS production were measured with increasing succinate concentrations (**Fig. 22**). Overall, mitochondrial respiration was the lowest at Leak state (**Fig. 21A** & **Table 3**; $P < 0.001$) and there were no differences among species (**Table 3**). In the OxPhos state, the three HTS had higher succinate supported respiration rates (**Fig. 21A**; $P < 0.05$) and higher affinities (i.e. lower $aK_{M,S}$) for succinate relative to *F. varium* (**Table 3**; $P < 0.001$). However, the catalytic efficiency was four time higher in *F. varium* relative to the HTS ($P < 0.001$). Exposure to AR significantly decreased OxPhos O_2 flux in the three HTS ($P < 0.001$), and two-way ANOVA revealed interactions with succinate concentration ($F_{63,315} = 3.39$; $P < 0.001$). While exposure to AR did not affect maximum respiration nor $aK_{M,S}$ in *F. varium*, it decreased the apparent $aK_{M,S}$ and O_2 flux in the three HTS ($P < 0.001$). AR also doubled $K_{cat,S}$ in all species, with *F. varium* maintain the highest catalytic rate (10.3 s^{-1} mg^{-1} as opposed to an average of ~2.5 s^{-1} mg^{-1} in HTS; $P < 0.001$; **Table 3**).

Succinate mediated ROS production (**Fig. 22B**) and electron leak (**Fig. 22C**) were higher in the Leak state in all species ($P < 0.001$). While in OxPhos, succinate mediated a slight increase in ROS production associated with an increase in electron leakage in *F. varium*, succinate decreased ROS production in *B. medius*. Above 0.5 mM succinate, ROS production remained unchanged in all species. AR did not affect the specific ROS production nor the electron leak, independently of succinate concentration (**Fig. 22B & 22C**).

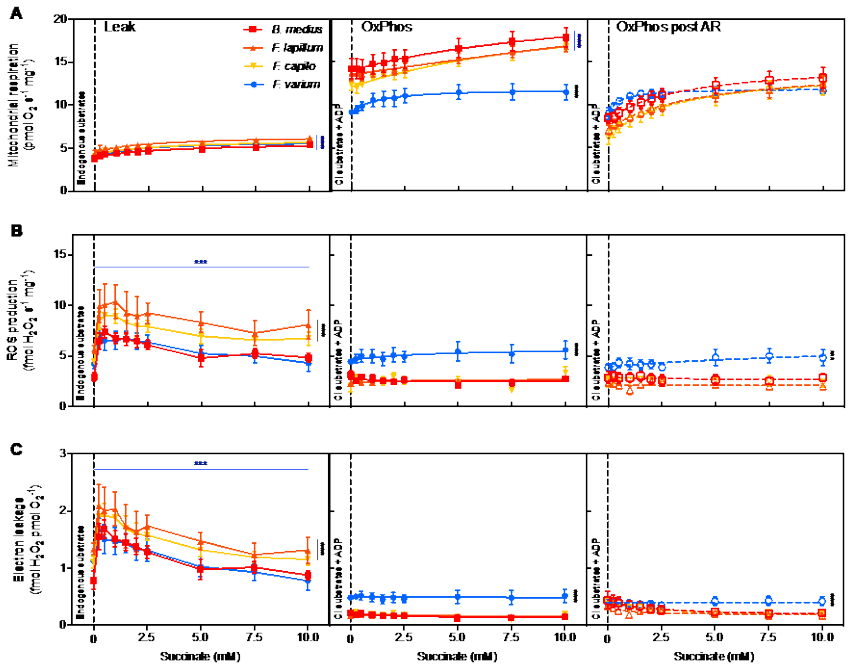

Figure 22. Succinate supported respiration but not ROS production is supressed post to anoxia-reoxygenation (AR) in hypoxia-tolerant triplefin fishes. Mitochondrial respiration (A), ROS production (B) and electron leakage (C) were assessed on permeabilised brain in Leak (endogenous substrates, no ADP nor other substrates added), OxPhos controls (additional ADP and other substrates) and OxPhos post an event of anoxia-reoxygenation ("post-AR") with graded succinate. Data are presented as the means of 6 individuals ± s.e.m. Warmer colours represent a greater hypoxia-tolerance. Statistical difference tested with two-way ANOVA repeated measures followed by Turkey's *post-hoc* test and presented in black for the difference between species within a state, and blue for the difference between state within the same species, as *** for $P < 0.001$.

4.4. Discussion

As with other aerobic tissues mitochondria within brain are the main O_2 consumers and likely are significant sources of ROS in particular if oxidising succinate has accumulated following anoxia. Much attention has been focused on mitochondrial function in mammalian models in hypoxia or following anoxia, yet their physiological role in other vertebrates such as fish, has been much less explored. Moreover, interpretations of ROS production are often criticised from the perspective that most cells function at low PO_2, and many experiments are conducted at elevated PO_2 where ROS production is elevated and likely overestimated (Makrecka-Kuka, Krumschnabel et al. 2015). This current study reveals that below 2.05 kPa (i.e. intracellular PO_2), ROS production was similar among triplefin species, despite a higher rate of electron leakage in the hypoxia-sensitive species. However, in hyperoxia, combined CI-linked substrates and succinate oxidation mediates less ROS in the brain of hypoxia-tolerant triplefins *in vitro*, including below 2 mM succinate, concentration that anoxic fish encounter *in vivo* (Johnston and Bernard 1983). HTS also had higher mitochondrial respiratory capacities relative to the hypoxia-sensitive fish on the cusp of anoxia, and electron transfer was more efficiently directed to respiration and not to ROS production. These findings suggest that New

Zealand hypoxia-tolerant fish benefit from more efficient mitochondria that may help to sustain repeated hypoxic episodes, and likely avoid oxidative damage on approaching anoxia, upon re-oxygenation and in hyperoxic conditions.

4.4.1. The ROS dependence on PO_2

As ROS production is dependent on O_2 tension (discussed in Makrecka-Kuka, Krumschnabel et al. 2015), we assessed the influence of PO_2 on ROS production and found a positive correlation between the ROS production and PO_2 within the range of 4.7-22 kPa (**Fig. 23**). However, mitochondrial respiration state (i.e. Leak or OxPhos) affected this O_2 dependence. The binding kinetics of electrons to O_2 in $O_2^{\cdot-}$ formation are dependent O_2 availability and transience of electrons in the ETS, which elevated reduction through hyperpolarisation of mitochondria, increases this transience, and potentiates electron leakage from the ETS to form ROS (Korshunov, Skulachev et al. 1997, Murphy 2009, Aon, Cortassa et al. 2010) (**Fig. 19**). Here, increased electron leakage was achieved *in vitro* through elevating substrate and O_2 levels, and through decreasing ADP levels (i.e. Leak state), which doubles the ROS production relative to the OxPhos state (**Fig. 23**).

Paradoxically, hypoxia has been suggested to potentiate mitochondrial ROS production (Guzy and Schumacker 2006, Murphy 2012, Zuo, Shiah et al. 2013). This mechanism is not clear in our data and others and has been critically discussed (Scandurra and Gnaiger 2010). In another study, ROS production measured with Amplex-Red™ assays, shows a linear relationship with PO_2, in the range between 64.6-4.3 kPa PO_2 (Grivennikova, Kareyeva et al. 2018). In this present study, ROS measurements were performed in real time from ~20.5 to 0 kPa PO_2, with more than 27,500 data points recorded between 4.3-0 kPa PO_2 (**Fig. 19B**), range within which mitochondria function within cells (Biro 2013). Within this range, the ROS-PO_2 relationship was better modelled using a three-parameter dose-response relationship ($P < 0.02$), which also do not support a potentiation of ROS production with the onset of hypoxia. However, the portion of electrons directed to ROS production (i.e. those not flowing to respiration) increased four-fold under 0.01 kPa PO_2, i.e. near anoxia (**Fig. 19C**). Although mitochondria are less likely to be exposed to such low oxygen tensions in most normoxic vertebrates (Palacios-Callender, Quintero et al. 2004, Benamar, Rolletschek et al. 2008), low PO_2 is likely reached in tissues of animals exposed to periods of environmental or functional hypoxia-anoxia (Hickey, Renshaw et al. 2012, Bundgaard, James et al. 2018), or pathologically in ischemic tissues exposed for at least several minutes (Chan 2001, Bainbridge, Tachtsidis et al. 2014).

We note that the amount of ROS produced by triplefin brain is small relative to other tissues, such as the heart of Wrasse species which produce ~25-fold more ROS (Iftikar and Hickey 2013). To our knowledge ROS production near anoxia has not yet been assessed in a range of species with varying tolerances to hypoxia. We conclude that the increased electron leakage near anoxia is likely due to the hyper-reduction of mitochondria, since substrate levels were high and O_2 limiting.

4.4.2. Intertidal triplefins produce less ROS than the subtidal species in a saturated medium.

Few studies have explored ROS production in fishes. Lower ROS levels were observed in isolated liver mitochondria of killifish (*Fundulus heteroclitus*) acclimatised for a month to hypoxia or intermitted hypoxia (Du, Mahalingam et al. 2016) and permeabilised ventricle fibres of the anoxia-tolerant epaulette shark (*Hemiscyllum ocellatum*) also depressed ROS release (Hickey, Renshaw et al. 2012). To our knowledge only those two studies have assessed ROS production *in vitro* in contexts of hypoxia tolerance in fish species. This present work shows that the intertidal triplefin species produced less ROS when phosphorylating in a fully aerated medium, which is likely hyperoxic for mitochondria *in vivo*.

The three HTS of triplefin fish displayed lower CI mediated ROS production relative to the HSS. A similar trait has been observed liver and skeletal muscle from a mammalian hypoxia-tolerant model, the ground squirrel, *Ictidomys tridecemlineatus* (Brown, Chung et al. 2012). It was also observed in heart mitochondria of the anoxia-tolerant turtle (*Trachemys scripta*), which lowered ROS production from CI was in part shown to be mediated by modification of specific residues within CI through S-nitrosylation (Bundgaard, James et al. 2018).

Such findings have mainly been assessed *in vitro* with O_2 concentrations above those that mitochondria would likely experience *in vivo*. This apparent experimental artefact has been discussed by Zenteno-Savin et al. (2002) who reported that aortic rings of diving seals, a model for ischemia-reperfusion and hypoxia tolerance, generated more ROS than tissues from pigs (Zenteno-Savin, Clayton-Hernandez et al. 2002). In this present study HTS generated less ROS than HSS at high PO_2. This indicates that excess mitochondrial ROS production may be prevented in HTS triplefins, which occupy rock pools that can become hyperoxic on sunny days. Although ROS production was similar across species at lower PO_2 where mitochondria likely function *in vivo* (i.e. PO_2 < 2.05 kPa), electron leakage near anoxia was greatest in the hypoxia sensitive species, indicating a better management of electrons in respiratory chains of the three more hypoxia tolerant species.

4.4.3. Species specific response to anoxia-reoxygenation

While complete O_2 deprivation may not be experienced in the brain of rock-pool triplefin fish, as anoxia does not appear to occur in rock pools (McArley, Hickey et al. 2018), we assessed the effect of 20 minutes anoxia *in vitro*. This time generally triggers mitochondria damage (Rouslin 1983). Unexpectedly, on reoxygenation OxPhos rates decreased in all HTS, and matched *F. varium* (**Fig. 20B**). Therefore, some damage may have occurred in HTS brain mitochondria following AR. However, Leak respiration rates were less affected and the RCR remained the highest in the truly intertidal species *B. medius* indicating greater stability of the inner mitochondrial membranes in this species. Exposure to AR decreased the electron leakage in the intertidal species of the *Forsterygion* genus, however *B. medius* had a similar response than *F. varium*. From these data, it appears that the response of the species within the *Fortserygion* genus follow a trend that correlates with hypoxia tolerance. However, the most HTS *B. medius*, species and phylogenetically more distant (Hickey, Lavery et al. 2009), had a response similar than *F. varium*. In triplefin fish species, the response to AR does not seem to be correlated with hypoxia-tolerance but appears to be species specific.

4.4.4. The role of succinate

In the absence of CI substrates (**Fig. 21** second panel) ROS production was surprisingly higher in *F. lapillum* and *F. capito* and no difference was apparent between *B. medius* and *F. varium*. However, with CI substrates present, succinate-mediated ROS was lower in the three more HTS relative to *F. varium* (**Fig. 22**), indicating that CI substrates and NADH, which increases in hypoxia (Garofalo, Cox et al. 1988) suppresses ROS production in the HTS, or elevates ROS production in HSS. Notably, with succinate and rotenone, ROS production was higher and electron leakage doubled in all species of fish (**Fig. 21**), and this is an artificial state unless CI is damaged to an equivalent state as when poisoned by rotenone. Perhaps these data illustrate the importance of mimicking substrates *in vivo*.

Following *in vitro* exposure to AR, the affinity for succinate, which was up to 20-fold higher in HTS controls, also decreased in the three HTS, though maximal succinate oxidation rates remained unchanged. Mitochondrial "metabolic depression" mediated through suppressed succinate oxidation rates has been reported in liver and skeletal muscle of hibernating ground squirrels in metabolic suppression during torpor (Brown, Chung et al. 2013), and in hypoxic reared, or selected drosophila (Ali, Hsiao et al. 2012). Since in hypoxia-sensitive mammalian brain, high succinate oxidation rates and associated elevated ROS production have been shown to be key mediators of ischemia-reperfusion injuries (Chouchani, Pell et al. 2014), the partial

suppression of succinate oxidation (**Table 3**) and associated diminished ROS production (**Fig. 22**) in hypoxia-tolerant triplefins appear to be a strategy against oxidative stress mediated by hypoxia-reoxygenation.

4.5. Conclusion

In this study, ROS production was assessed with the consideration of both O_2 and substrates availability. In this context, we demonstrate that at least at intracellular PO_2 that likely represent normoxia and hypoxia, decreasing ROS production does not appear to be an avoidance strategy for intertidal triplefin fishes. However, using simultaneous measures of respiration and ROS production we show that the efficiency of electron transfer is greater in HTS when entering anoxia. Moreover, succinate supported efficiencies of ROS production is better in HTS, and that this is possibly dependent on substrates that mediate NADH supply. In addition, in hyperoxic conditions, intertidal triplefins may avoid oxidative stress with a lower ROS production relative to the subtidal species. In ecological contexts, intertidal triplefin fish can better manage the hypoxia-reoxygenation and hyperoxia, which occurs in rock pools.

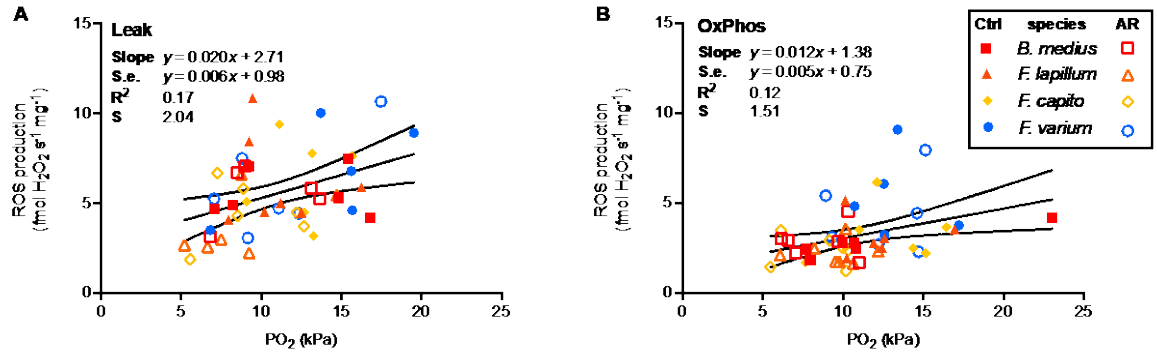

Figure 23. The dependence of the ROS production to the oxygen tension. In permeabilised brain, the ROS production was measure fluorometrically on mitochondria at OxPhos state (high substrates levels and ADP) and Leak state (inhibition of the $ATP_{F0\text{-}F1}$ with olygomycin). Each dot represents the measurement of an individual from the rock-pool species *B. medius* (red), the intertidal species *F. lapillum* (orange) and *F. capito* (yellow) and the subtidal species *F. varium* (blue), having experienced an episode of anoxia-reoxygenation ("AR", empty symbols) and in control groups ("Ctrl", filled symbols). The linear correlation between ROS production and the PO_2 at which ROS production was extracted was tested with the least squares fit and displayed with 95% confidence intervals.

Chapter 5. : Mitochondrial plasticity in the cerebellum of two anoxia-tolerant sharks: Contrasting responses to anoxia/reoxygenation.

Published in *Journal of Experimental Biology:* DEVAUX, J. B. L., RENSHAW, G. M. C. & HICKEY, A. J. R. 2019. “Mitochondrial plasticity in the cerebellum of two anoxia-tolerant sharks: Contrasting responses to anoxia/reoxygenation” 2019. Doi: 10.1242/jeb.191353 Published 4 March 2019;

5.1. Introduction

An adequate and continuous supply of oxygen is fundamental to fuelling vertebrate respiration. If the supply of oxygen is severely diminished in mammalian species, survival is limited to a few minutes unless they have adaptations to survive deep-sea diving, hibernation or stress-induced torpor. In the absence of specialised biochemical and physiological readjustments, hypoxia or anoxia can compromise cellular energy supplies, triggering signal cascades that result in organ failure and subsequently death. Sub-cellularly, anoxia can result in irreversible damage to mitochondria (Javadov 2015, Andrienko, Pasdois et al. 2017) which can induce the release cytochrome *c*, an initiator of cell death by apoptosis (Kinnally, Peixoto et al. 2011). Furthermore, majority of cell damage occurs during the re-introduction of normal oxygen levels (Kalogeris, Baines et al. 2012). Mitochondrial dysfunction does not always lead to cell death, for example, diminished mitochondrial transmembrane potential can be re-established by 72 hours post-stress (Tuan, Hsu et al. 2008).

In species that evolved their anoxia tolerance at temperatures close to 0°C, the duration of extreme anoxia-tolerance can extend to months, because hypothermia slows enzymatic reactions, diffusion and energy consuming processes, all of which spare energetic resources (Rubinsky 2003). However, the increase in energy consumption associated with increased metabolic rates in species adapted to higher temperatures (~20-25°C), diminishes the survival time for anoxia-tolerant species to a few days or even hours (Lutz and Nilsson 1997). On tropical reef platforms temperatures of up to 35^{o}C have been observed (Potts and Swart 1984) and remarkably some are inhabited by hypoxia and anoxia-tolerant reef sharks that have evolved their survival mechanisms in the absence of cold-induced survival mechanisms (Nilsson and Renshaw 2004). Only a few fish have evolved survival mechanisms that protect them from hypoxia and anoxia in tropical environments, such as: African lakes (Chapman et al., 2002), the Amazon (Val 1998, Richards, Wang et al. 2007, Val, Gomes et al. 2015), and warm coral reef waters (Renshaw, Kerrisk et al. 2002, Routley, Nilsson et al. 2002, Nilsson and Ostlund-Nilsson 2004). Since some of these tropical hypoxia and anoxia-tolerant species can survive several hours of hypoxia at mammalian temperatures in contrast to the a few minutes that humans are able to tolerate, they make useful experimental models in which to examine protective mechanisms.

The epaulette shark (*Hemiscyllium ocellatum*) and its close relative the grey carpet shark (*Chiloscyllium punctatum*) represent ancestral vertebrates and are the only elasmobranch species reported to tolerate prolonged anoxia or hypoxia at tropical temperatures (Wise,

Mulvey et al. 1998, Chapman and Renshaw 2009). The grey carpet shark (CGS) is distributed in northern Australian waters and is widely distributed in Indo-West Pacific regions (Dudgeon 2016) while the epaulette shark (ES) is restricted to northern Australian waters and New Guinea (Chapman and Renshaw 2009, Last 2009, Bennett 2015). Both species have been observed on reef flats during the day. While the ES has been observed hunting and feeding on reef flats during nocturnal hypoxic conditions, it has not been confirmed whether the GCS occupy this niche on nocturnal low tides. However, under experimental conditions the GCS can sustain around 1h anoxia at 25°C, while the ES routinely survives 2.5h (Renshaw, Kerrisk et al. 2002, Routley, Nilsson et al. 2002, Chapman, Harahush et al. 2011). The ES is capable of metabolic depression and neuronal hypometabolism in response to diminished oxygen (Mulvey and Renshaw 2000, Stenslokken, Milton et al. 2008) through mediators such as adenosine receptors (Renshaw et al., 2002). Neuronal hypometabolism and temporary blindness may act to diminish the demand for ATP (Mulvey and Renshaw 2000, Stenslokken, Milton et al. 2008). The ES increased the production of NO in response to hypoxia, which could enhance oxygen delivery (as discussed in Renshaw and Dyson 1999, Nilsson and Renshaw 2004) and depresses mitochondrial O_2 consumption (Brown 1995, Cooper and Brown 2008). In addition, ES are naturally exposed to cycles of nocturnal hypoxia in their natural environment (Nilsson and Renshaw 2004), which has been demonstrated pre-condition this species for longer future exposures to hypoxia with early entry into ventilatory and metabolic depression (Routley, Nilsson et al. 2002).

In contrast, the GCS maintain their metabolic and ventilation rates, and rapidly increased their haematocrit in response to anoxia, most likely *via* splenic contractions (Chapman and Renshaw 2009). It was suggested that the O_2 from stored red blood cells could be released which would ultimately increase the supply of oxygen to metabolically active organs when the O_2 supply is compromised.

It has been proposed that oxidative damage originates during re-oxygenation from an increase in mitochondria derived reactive oxygen species ("ROS"; illustrated in **Fig. 29**), potentially triggering apoptosis and necrosis (Murphy 2009). While laboratory-based anoxic stress can be well tolerated by both shark species (Chapman and Renshaw 2009), there is evidence of re-oxygenation induced oxidative damage in the ES (Renshaw, Kutek et al. 2012) even though the ES produced less reactive species than other elasmobranchs (Hickey, Renshaw et al. 2012). In mammals, it has been demonstrated that succinate accumulates in highly metabolic ischemic organs (at least in the brain, heart, liver and kidney) as a result of the ischemia induced reversal of the succinate dehydrogenase (SDH i.e. mitochondrial complex II or CII) and the partial

inhibition of the malate/aspartate shuttle (Chouchani, Pell et al. 2014). Upon reperfusion, succinate is oxidised at elevated rates and this drives excess ROS production by the reversal of electron flow at complex I (CI) (discussed in Andrienko, Pasdois et al. 2017). This succinate-induced ROS can cause oxidative damage that alters mitochondrial function (Paradies, Petrosillo et al. 2002) (illustrated in **Fig. 29**). These detrimental effects of reperfusion in the presence of excess succinate may be further enhanced at elevated temperatures (De Groot and Rauen 2007).

Intriguingly, the anoxia-tolerant ES displayed greater mitochondria membrane stability after an anoxic event than the hypoxia-sensitive shovelnose ray (*Aptychotrema rostrata*) (Hickey, Renshaw et al. 2012). It was proposed that the high mitochondrial membrane stability observed in the ES would act to maintain oxidative phosphorylation (*Oxphos*) efficiency and decrease ROS production post-anoxia, which would decrease oxidative damage mediated by re-oxygenation (Hickey, Renshaw et al. 2012). Although ES heart mitochondria are robust in response to an anoxic challenge, the effect of succinate build-up and ROS production on mitochondria respiratory complexes and mitochondrial efficiency in other highly metabolic tissues such as the brain, have yet to be determined. The cerebellum is one of the most vulnerable regions of the brain to damage from a hypoxic insult (Cervós-Navarro and Diemer 1991). The loss of the righting reflex, controlled by the cerebellum, is the first sign of physiological shut down and evidence suggests that such cerebellar shut down acts to conserve brain energy charge (Renshaw, Kerrisk et al. 2002). In addition, the ES cerebellum: (i) increases the transcription of pro-survival genes in response to recurrent hypoxic preconditioning (Rytkonen, Renshaw et al. 2012); and (ii) makes protective proteomic readjustments following episodes of either hypoxic or anoxic preconditioning (Dowd, Renshaw et al. 2010). It should be noted that cytochrome oxidase levels are significantly decreased by exposure to diminished oxygen, representing neuronal hypometabolism (Mulvey and Renshaw 2000), which implies that mitochondria turn down ETS activity in response to hypoxia. This questions whether cerebellum mitochondria are plastic in their response to diminished oxygen and whether they can subsequently recover

To test whether mitochondrial plasticity is likely to be involved in the tolerance of the ES and/or the GCS brain to anoxia, we investigated the tolerance of mitochondria in whole preparations from the cerebellum of each species to an acute episode of anoxia/re-oxygenation (AR) with and without elevated succinate levels. More specifically, we compared the mitochondrial respiratory capacity and the mitochondrial plasticity (readjustment of respiratory pathway from CI and CII) in responses to graded levels of exogenous succinate in mitochondria

exposed to either AR or maintained with sufficient O_2 (controls). Using high resolution respirometry, we tested the hypothesis that the cerebellum mitochondria from ES cerebellum would be more resilient to AR compared to those from the GCS and that ES mitochondria would adjust their respiratory characteristics in response to graded exogenous succinate rather than exhibit high CII succinate oxidation rates during reoxygenation. This is the first report describing both i) the normal activity of ES and GCS intact mitochondrial population in the cerebellum; and ii) their responses to an anoxic challenge followed by re-oxygenation. Both experiments were carried out with graded exogenous succinate.

5.2. Materials and methods

5.2.1. Animals and housing

Six sub-adult ES with a mean of 490 ± 83 g were purchased from Cairns Marine (Cairns, Australia) while seven sub-adult GCS with a mean of 138 ± 31 g were provided by Sea World (Main Beach, Gold Coast, Australia). Sharks were held in 300L tanks containing aerated sea water maintained at 22°C and fed daily with fresh raw shrimps. After a week of acclimation, sharks were starved for two days prior to euthanasia and the commencement of high-performance mitochondrial respirometry. The sharks were measured and weighed post-euthanasia and the cerebellum was weighed prior to homogenisation.

5.2.2. Cerebellum preparation

Tissue homogenates which avoided shear stress, were chosen over other methods of preparation (i.e. permeabilised brain or isolated mitochondria) because they retain i) mitochondrial integrity; ii) all sub-populations of mitochondrial in situ; and iii) conserve potential cellular regulators of mitochondrial function (Kondrashova, Zakharchenko et al. 2009). However, while including the overall mitochondrial characteristics of different sub-populations contained in the shark cerebellum, any potential differences in mitochondrial density were not assessed. Consequently, the reported difference in respiration rates between the two sharks provide information on the overall mitochondrial capacity within a fixed mass of shark cerebellum, and is not intended to examine differences between mitochondrial units (i.e. adjustments within a mitochondrion).

Sharks were euthanized by the addition of 15 ml of 5% benzocaine, dissolved in ethanol, to 1L sea-water for a final dose of 750 mg benzocaine/L. After ventilation ceased, the absence of response to fin pinch test and the loss of righting reflex indicated that euthanasia was complete,

then the spinal cord was sectioned at the cranio-vertebral junction and sharks were rapidly dissected. The cerebellum was rapidly removed and immersed in ice-cold biopsy buffer (in mM: 2.77 CaK_2EGTA, 7.23 K_2EGTA, 5.77 Na_2ATP, 6.56 $MgCl_2.6H_2O$, 20 taurine, 15 Na_2Phosphocreatine, 20 imidazole, 0.5 DTT, 50 KMES, and 50 Sucrose, pH 7.1 at 30°C) (Hickey, Renshaw et al. 2012). Then the cerebellum was gently blotted, to remove excess blood and it was weighed into ~150 mg pieces in 800 µl cold MiR05 respiration medium (containing, in mM: 0.5 EGTA, 3 $MgCl_2.6H_2O$, 60 K-lactobionate, 20 taurine, 10 KH_2PO_4, 2.5 HEPES, 700 sucrose and 1g l^{-1} BSA essentially free fatty acid, pH 7.2 at 22°C). A portion of the diced cerebellum was gently homogenised by triturating the small pieces through a 10ml syringe with decreasing gauge needles (16-25 gauge) and allowed to recover for an hour in cold MiR05 prior to use in respirometry experiments.

5.2.3. Respirometry experiments

A multiple substrate uncoupler inhibitor protocol (SUIT) was performed to assess the effect of AR on: (i) The total proton leak (L_{Total}) and the inducible proton leak through adenine nucleotide translocase (L_{ANT}); (ii) complex I (CI) mediated respiration and O_2 flux (JO_2) attributed to OxPhos with and without succinate build-up; (iii) the electron transport system (ETS) capacity and (iv) CII capacity (**Fig. 24**). Electron inputs from either complex I or complex II can be assessed in SUIT protocols with the sequential reconstitution of TCA cycle pathways by the addition of complex specific substrates. The contribution of each complex to ETS reflects putative mitochondrial plasticity because it represents the readjustment of convergent electron pathways to OxPhos (detailled in Gnaiger 2014). The addition of succinate and rotenone in the absence of CI substrate, mediates oxaloacetate accumulation and further competitively inhibits CII (Harris and Manger 1969). In this study, the CII contribution to OxPhos was determined by the additive effect of excess succinate to CI-mediated OxPhos (with pyruvate, malate and glutamate) because additive electrons flow from CI to the Q-junction converges according to a $NADH^+$:succinate ratio of at least 4:1 (Gnaiger 2014).

Whole homogenates from the cerebellum of either GCS or ES (100 µl corresponding to 10-15 mg tissue) were added to the 2 ml chambers of Oroboros O2ks™ respirometers containing aerated MiR05 media at 20°C (261.92 µM O_2 at 101.5 kPa barometric pressure). After signal stabilisation, 20 min recovery was sufficient to exhaust routine respiration, which remaining exhausted respiration was subtracted from the other mitochondrial states. Then, mitochondria CI-linked substrates, pyruvate and malate were added at saturated concentrations (10 and 5 mM respectively) to assess the non-phosphorylating state mediated by CI inputs (L_{CI}).

Oxidative phosphorylation supported by pyruvate and malate (PM OxPhos) was then triggered by the addition of 700 µM ADP and the additional effect of glutamate on mitochondrial respiration was tested by the addition of 10 mM glutamate (CI-*Oxphos*). To test mitochondrial tolerance to anoxia-reoxygenation (AR), mitochondria were allowed to deplete the chamber O_2 then maintained in anoxia for 20 minutes following re-oxygenation (Hickey, Renshaw et al. 2012), the control group had fully aerated medium.

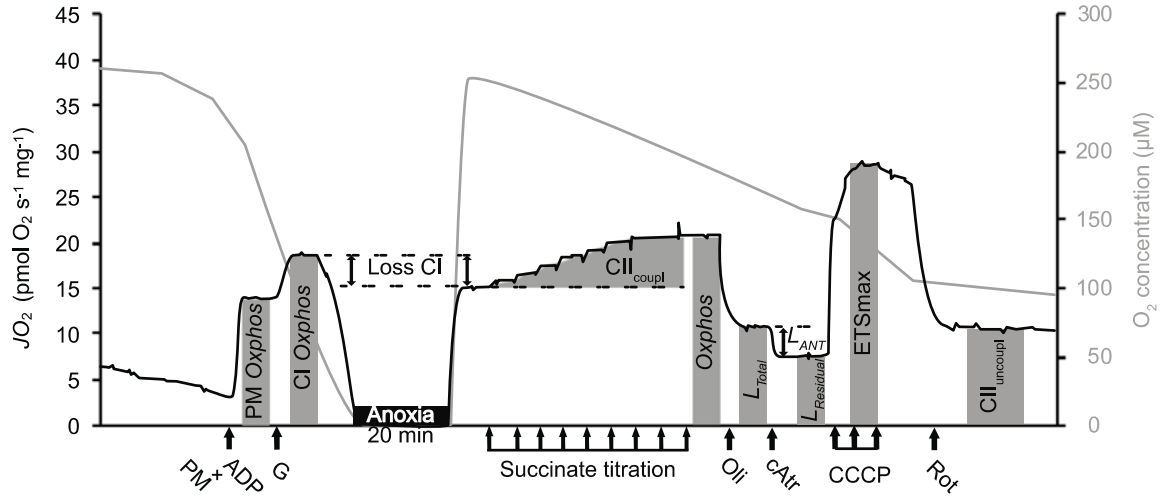

Figure 24. Representative trace of the substrate uncoupler inhibitor protocol used to measure mitochondrial respiration rates (JO_2) of cerebellum homogenate from grey carpet sharks and epaulette sharks. Samples were introduced into the 2 ml respirometer chambers and were allowed to recover for 20 min. Excess pyruvate, malate and ADP were injected to put mitochondria into Complex I (CI) mediated oxidative phosphorylation (PM-*Oxphos*). The additive effect of glutamate was tested by inclusion in the CI substrate addition (CI-*Oxphos*). The sample was permitted to deplete O_2 until anoxia, and a reference chamber was maintained between 100-250 µM O_2 (trace not shown). The chamber was then re-oxygenated after 20 min (up to ~220 µM O_2 for both control and anoxic groups). The loss in CI mediated JO_2 (Loss CI) was calculated by anoxia exposure followed by reoxygenation (AR). Succinate was then titrated up to 10 mM to measure the contribution of CII to CI+CII-*Oxphos* ($CII_{coupled}$). At the conclusion of the experiment, oligomycin (Oli) was added to induce mitochondria in total Leak state (L_{Total}) and the contribution of the adenine nucleotide translocase (L_{ANT}) was calculated as the difference between L_{Total} and the residual leak ($L_{Residual}$), which was reached after the addition of the ANT inhibitor carboxy-atractyloside (cAtr). Finally, the mitochondria were chemically uncoupled with the titration of CCCP to determine maximum ETS capacities (ETS_{max}). Finally, rotenone was added (Rot, a CI inhibitor) to measure the uncoupled CII capacity ($CII_{uncoupled}$).

The amount of tissue in the homogenates (~10-15 mg) was chosen as this permitted anoxic levels to be reached within 30-50 min. After acute anoxic exposure, chambers were exposed to ambient air to re-oxygenate the media up to ~220 µM O_2 and recommence respiration. Once CI-*Oxphos* fluxes post-anoxia were determined, a succinate titration (0-10 mM) was started using an automated titration pump to mimic gradual succinate accumulation. To determine the contribution of AR to altered mitochondrial function, the control tissues were exposed to succinate titration alone in fully aerated medium. Oligomycin was added (Oli, 5 µM) to determine total *Leak* respiration from combined CI and CII inputs (L_{Total}). The fraction of proton leak through the adenine nucleotide translocase (L_{ANT}) was then determined as the difference between L_{Total} and the residual leak ($L_{Residual}$), measured by the addition of carboxy-

atractyloside (cAtr, 5 µM) to inhibit the ANT. Respiration was then uncoupled from OxPhos using three injections of the protonopore carbonyl cyanide m-chlorophenyl hydrazone (CCCP, 0.5 µM each) to determine the ETS capacity (ETS_{max}). Then, CII capacity uncoupled from OxPhos ($CII_{uncoupled}$) was assessed by the addition of the CI inhibitor rotenone (0.5 µM), as this represents the maximum capacity of CII to fuel the ETS with electrons, without limitations of the phosphorylating system, and without competition for the Q-pool (Gnaiger 2014). A representative trace of the SUIT protocol and its corresponding effects on mitochondrial respiration is presented in **Fig. 24**.

5.2.4. Data and statistical analysis

Respirometry fluxes were calculated in real-time with DatLab 6.0 software and expressed in pmol O2 s-1 mg-1. The data and calculations were transferred to Microsoft Excel (Office vs15.38). The complex I contribution to OxPhos was calculated as the difference between CI-Oxphos and LCI. The CII respiration coupled to OxPhos (CIIcoupled) was calculated as the difference between OxPhos and CI-Oxphos. The respiratory or acceptor control ratio (RCR) is a function of OxPhos coupling efficiency of a system (Gnaiger 2014) and was calculated by the formula OxPhos/Leak. To estimate whereas damage to ETS may affect OxPhos, we calculated the net OxPhos control ratio (nOCR) as (Oxphos - Leak)/ETS. Dose response curves for succinate were fitted with the least-squares method using GraphPad Prism 7.0. In addition to the maximum respiration rate derived from the addition of succinate (CIIcoupled) and the apparent Km ("aKmS"; determined as the succinate concentration at which respiration was half of CIIcoupled) the catalytic efficiency of CII ("CIIcat"; proxy for enzymatic efficiency, generally represented as Vmax / Km), was also presented and calculated as CII_{coupl}/aKm_s.

It should be noted that the use of the term "mitochondria", expressed here, does not refer to normalised mitochondrial entities (i.e. if mitochondrial density were established) but denotes the all of mitochondrial populations in situ within the cerebellar homogenates. Therefore, mitochondrial characteristics interpreted from respiration rates in the present study, yield information about the capacity of mitochondria in the overall tissue, which better indicate the responses that are likely occur in shark cerebellum in vivo. It cannot be assumed that all of the results are directly related to mitochondrial adjustments at the organelle level. The data that was used to calculate a number of ratios associated with mitochondrial complexes and leak states did not require quantification of mitochondrial density and the discussion of results is largely based on these ratios

The Shapiro-Wilk test was used to test for normal distributions. SPSS 23.0 or GraphPad Prism 7.0 were used to perform a student t-test when equality of variances was verified. Two-way ANOVA repeated measure and post-hoc with Turkey multiple comparison were performed to compare the effect of substrates-inhibitor on mitochondrial states, to compare the effect of AR on CI contribution and to compare the additive effect of succinate build-up on mitochondrial respiration rates across species. A significant difference was accepted at $p < 0.05$.

5.3. Results

5.3.1. Shark morphology

Table 2. Morphology of the two anoxia tolerant sharks. Body length, body mass (BM) and the ratio of the cerebellum to BM for the two anoxia tolerant shark species, grey carpet shark and the epaulette shark. The mass of the cerebellum was normalised to body mass for comparison between species. Results expressed as mean ± s.e. Significant differences between species (#) or between control and post-anoxia (*) tested with independent t-tests, $p < 0.01$).

	Body length (cm)	Body mass (g)	Cerebellum (mg) /BM (g)
Grey carpet (6)	53.00 ± 7.57	138.25 ± 30.68	8.58 ± 1.50 *
Male (2)	56.00 ± 0.01	121.91 ± 19.74	8.01 ± 0.06
Female (4)	51.00 ± 9.25	143.70 ± 31.72	8.78 ± 1.69
Epaulette (6)	67.17 ± 4.15 *	490.57 ± 82.91 *	1.19 ± 0.13
Male (3)	68.25 ± 0.25	485.57 ± 68.32	1.24 ± 0.14
Female (3)	66.63 ± 4.99	495.57 ± 95.03	1.13 ± 0.10

Sub-adult GCS and ES were used for this study. While the ES had a greater mean body mass than GCS (**Table 4**), the mean proportion of cerebella mass to body mass was greater in the GCS than in the ES. Neither length nor mass or sex affected mitochondrial function (factorial ANOVA, homogeneity of variance verified with Levene's test).

5.3.2. Interspecies comparison of cerebellar mitochondrial respiration in fully aerated medium.

While the stepwise addition of substrates or inhibitors influenced mitochondrial respiration ($F_{7,42} = 153$, $p < 0.001$; **Fig 25**) Turkey post-hoc tests revealed no significant differences in leak states (L_{Total} and L_{ANT}) or OxPhos states (CI-*Oxphos* and OxPhos) between these two closely related carpet shark species. However, ES homogenates had a significantly higher ETS capacity (ETS_{max}) per mass tissue than GCS mitochondria ($p < 0.001$). The ETS_{max} was ~20% and ~75% higher than OxPhos in the GSC and ES, respectively ($p < 0.003$).

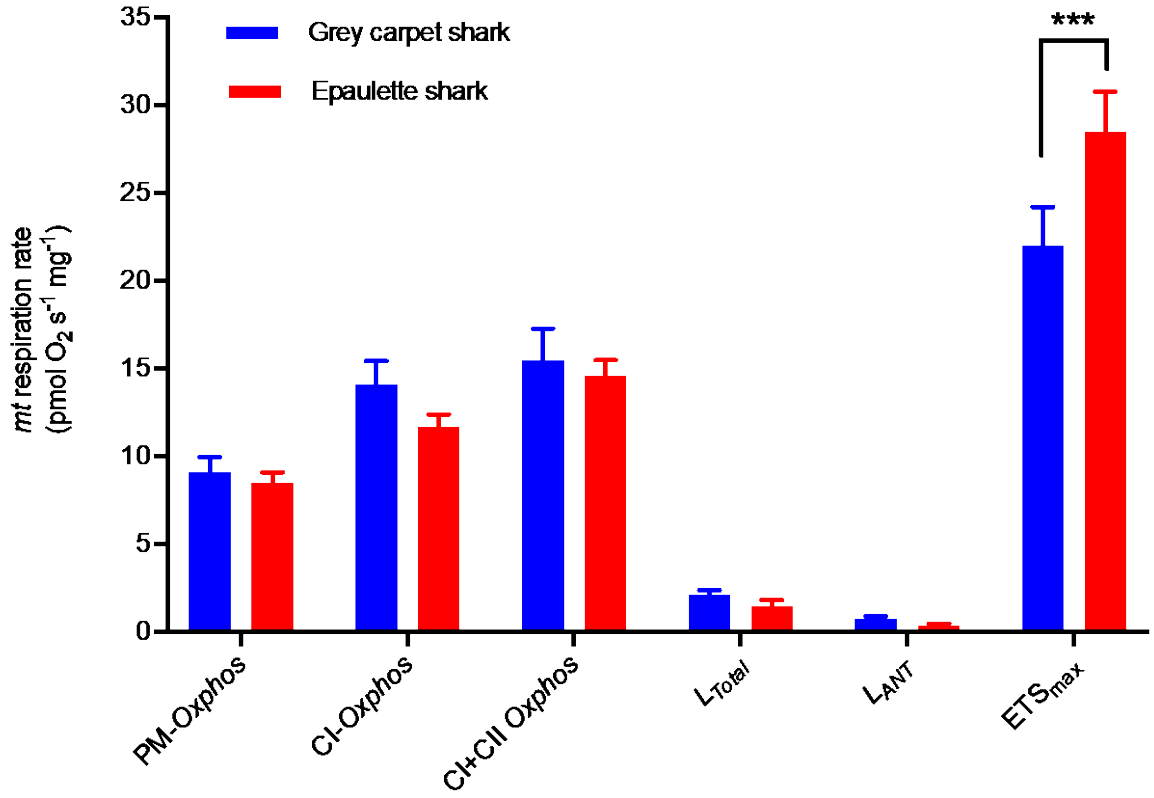

Figure 25. Mitochondrial respiration rates in homogenates of the cerebellum from two anoxia-tolerant sharks. In PM-*Oxphos*, there was no difference in respiration rates between grey carpet sharks mitochondria (blue) and epaulette sharks mitochondria (red). The addition of excess glutamate to reach CI-*Oxphos* followed by excess succinate to reach *Oxphos* state, each mediated and increase of ~6 pmol O_2 s^{-1} mg^{-1} in both species of sharks. The addition of oligomycin to measure total leak (L_{Total}) decreased JO_2 similarly in both sharks. Adenosine nucleotide translocase mediated Leak flux (L_{ANT}), was also similar in grey carpet and epaulette sharks. However, epaulette sharks mitochondria had greater ETS capacity. Refer to the Fig. 1 legend for details on the method. Significant difference tested with two-way ANOVA and post-hoc test with Turkey correction indicated as *** at $p < 0.001$.

5.3.3. Effect of anoxia/reoxygenation on mitochondria complexes in the two closely related carpet sharks.

The overall responses of OxPhos and ETS to AR as well as the contribution of CI and CII to OxPhos were analysed and compared for each species. While OxPhos was significantly decreased by AR in GCS homogenates ($p < 0.001$), OxPhos was maintained post AR in ES homogenates ($p = 0.15$; **Fig. 26**). In response to AR, the ETS_{max} was significantly decreased in both shark species with a decrease of ~31-34% ($p < 0.01$) relative to the pre-anoxic state (**Table 4**).

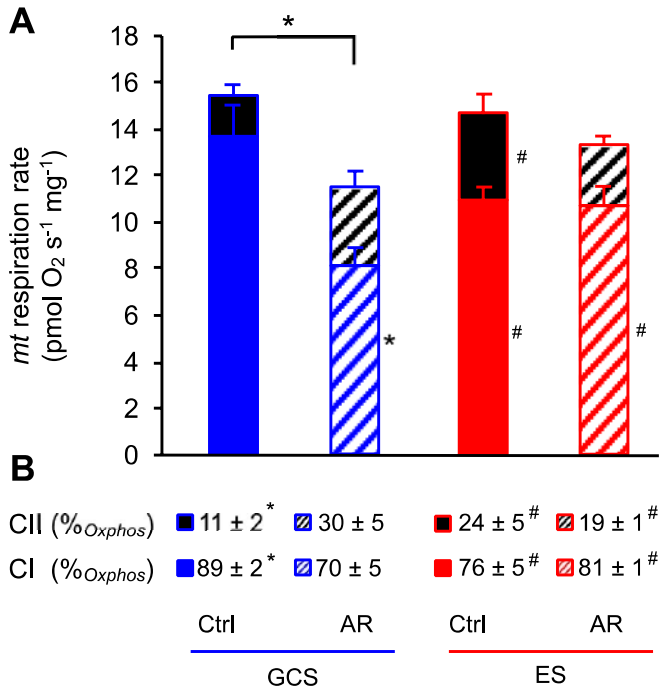

Figure 26. Contribution of complex I and complex II to Oxphos before and after exposure to anoxia/re-oxygenation. (A) Absolute respiration rates mediated by CI (coloured) and CII (black and white) and (B) the relative contributions of each complex to Oxphos, in cerebellar homogenates of GCS (blue) and ES (red) maintained in normoxia ('Ctrl', filled) or exposed to an episode of anoxia/reoxygenation ('AR', dashed). The CI contribution to respiration was determined in the presence of excess CI-linked substrates (pyruvate, malate and glutamate) followed by ADP while the CII contribution was calculated by the additive effect of succinate on CI-mediated Oxphos respiration rates. Data in (A) represent the absolute respiration rates mediated by CI and CII, the sum of which corresponds to Oxphos rates and expressed in pmol O_2 s^{-1} mg^{-1}. Data in (B) correspond to the relative contribution of each complexes to Oxphos rates in tissue either exposed to saturated O_2 or exposed to an episode of AR. Results are expressed as mean (n = 6) ± s.e. Significant difference ($p < 0.05$) are indicated as * between treatments (Control or AR) or as # between shark species (neighbouring histograms). The additive effect of both complexes is shown as stacked histograms, tested with two-way ANOVA test with Turkey correction for multiple comparison.

In mitochondria from GCS cerebella, there was a significant 31% decrease in CI respiration following AR with saturated CI substrates (**Fig. 26**), which was not compensated for by the 2.7-fold increase in the CII contribution to OxPhos ($p < 0.001$; **Fig. 26**). We note that this could account for the significant decrease of CI + CII *OxPhos* by 26% (corresponding to ~4 pmol O_2 s^{-1} mg^{-1}; $p = 0.04$; **Fig. 26**). Despite this loss in respiration, RCRs and nOCRs were not affected by AR ($p > 0.6$, **Table 2**). In contrast, CI mediated respiration was unaffected by AR in mitochondria from ES cerebella (**Table 4& Fig. 26**) and while the level of OxPhos respiration was preserved (**Fig. 26**), RCRs were significantly decreased indicating an increase in uncoupled respiration in OxPhos ($p = 0.007$, **Table 4**). OxPhos capacity was also greater in the ES cerebella following AR with a conserved ~91% capacity compared to ~74% in GCS mitochondria ($p = 0.05$; % **Fig. 26**).

The contribution of CII to respiration was also tested in two settings (**Table 4**), coupled to OxPhos (i.e. actual contribution to OxPhos) and uncoupled to OxPhos (full CII capacity to contribute to ETS). In GCS homogenates not exposed to AR, $CII_{coupled}$ respiration was ~2 pmol O_2 s^{-1} mg^{-1} and accounted for only 21% of $CII_{uncoupled}$ ($p < 0.001$). While post AR the $CII_{coupled}$ increased by ~80% ($p = 0.03$) and matched $CII_{uncoupled}$, CII overall was diminished by 60% ($p < 0.001$). In contrast, $CII_{coupled}$ reached its full capacity in ES homogenates not exposed to AR

and equated $CII_{uncoupled}$ (~3.5 pmol O_2 s^{-1} mg^{-1}). Post AR however, $CII_{coupled}$ flux was decreased by 35% and equated to 30% $CII_{uncoupled}$ only (p = 0.02).

5.3.4. Apparent proton leak.

In the normoxic control groups for ES and GCS, the L_{Total} was similar between species (p = 0.65; **Fig. 25** & **Fig. 27**). However, while AR did not affect L_{Total} in the GCS *mt*, it significantly increased L_{Total} by ~58% in ES mitochondria (p = 0.02; **Fig. 27**). There was no apparent difference in L_{ANT} between the control groups for two species during pre-AR respiration (**Fig. 27**). However, following AR the ES mitochondria showed a significant ~4-fold increase in L_{ANT} (p = 0.035) while L_{ANT} was unchanged in the mitochondria of GCS. Since the $L_{Residual}$ was similar in both species and not affected by AR (p > 0.5) the increase in L_{Total} in ES mitochondria reflected the increase in L_{ANT}.

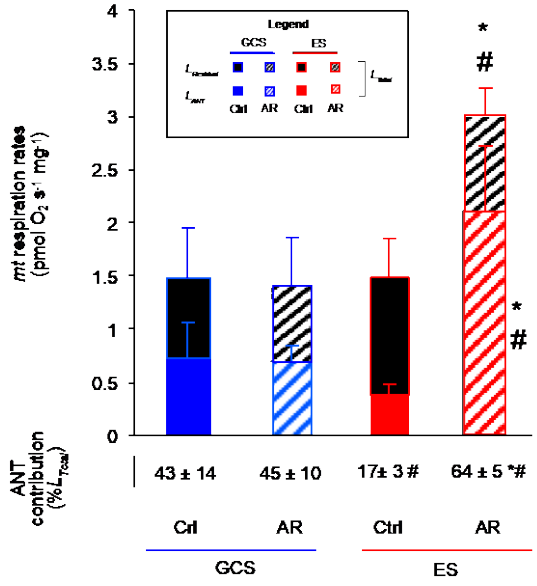

Figure 27. Mitochondrial respiration attributed to proton leak and the contribution of the adenine nucleotide translocase (ANT). Two components of proton leak were measured in cerebellar homogenates from GCS (blue) and ES (red) that were either exposed to normoxia (Ctrl) or anoxia-reoxygenation (AR). Oligomycin was added to put phosphorylating mitochondria into the Leak state (L_{Total}). The portion of proton leak though ANT (L_{ANT}) was calculated as the difference between L_{Total} and the residual leak ($L_{Residual}$), reached after the addition of carboxy-atractyloside. Both rates are expressed as pmol O_2 s^{-1} mg^{-1} with the relative contribution of L_{ANT} to L_{Total} (values below main graph). Results presented as mean (n = 6) ± s.e. Significant difference (p < 0.05) indicated as * between groups (Ctrl and AR) and as # between species, tested with independent t-tests.

5.3.5. Effects of titrated exogenous succinate on oxygen flux.

Both the succinate concentration and exposure to AR influenced CII mediated JO_2 ($F_{3.52}$, p = 0.015) (**Fig. 28**). In control groups, the apparent Km to succinate was similar between the two species (aKm_S ~0.4-0.9 mM). However, the $CII_{coupled}$ flux was two-fold higher in ES cerebella than in GCS cerebella (p < 0.001). In GCS, the CII fuelled respiration was significantly increased post-AR at succinate concentrations above 2 mM (p < 0.05). A Turkey post-hoc test revealed that the maximum CII-mediated respiration was significantly increased from 0.5 to 2.5 mM succinate in GCS (p < 0.05). Conversely in ES, AR mediated a significant decrease in CII fuelled respiration at succinate concentrations above 0.5 mM (p < 0.01), and the maximum CII mediated respiration was decreased at succinate concentrations above 2.5

mM (controls) or above 2 mM succinate in cerebellar preparations exposed to AR (**Fig. 28**). Exposure to AR increased the apparent Km to succinate in GCS mitochondria ($p < 0.001$) but not in ES mitochondria, in which aKm_S was unchanged (**Table 2**). While aKm_S was doubled in both species after exposure to AR, the capacity of CII to oxidise succinate CII_{cat} was maintained in GCS compared to their controls, while CII_{cat} was significantly decreased by ~35% relative to control groups in ES ($p < 0.001$; **Table 5**).

Table 3. Effects of anoxia/reoxygenation on mitochondrial function in cerebellum homogenates of grey carpet and epaulette sharks. The mitochondria in AR homogenates and their controls held with sufficient O_2 were uncoupled from Oxphos in the presence of rotenone to determine the CII capacity uncoupled from *Oxphos*. Three parameters of the CII capacity coupled to Oxphos were extracted using dose response curves fitted with the least-squared method and the maximum respiration rate mediated by succinate ($CII_{coupled}$) and the succinate concentration at which JO_2 is half of CII-JO_{2max} (aKm_S) were extracted using Prism7.0. The CII catalytic efficiency (CII_{cat}) was then calculated as $CII_{coupled}$ divided by aKm_S. The respiratory control ratios (RCR) is an estimation of mitochondria coupling and was calculated using the formula *Oxphos*/Leak. Net oxidative control ration was calculated as (*Oxphos*-Leak)/ETS_{max} and represents the net Oxphos capacity relative to ETS capacity. Results are expressed as mean ± s.e. Significant differences ($p < 0.05$) indicated as (*) between AR and controls or as (#) between shark species, tested with independent t-tests.

	$CII_{uncoupl}$ (pmol O_2 s^{-1} mg^{-1})	Characteristics of CII_{coupl}			ETS_{max} (pmol O_2 s^{-1} mg^{-1})	RCR	nOCR
		aKm (mM)	CII_{coupl} (pmol O_2 s^{-1} mg^{-1})	CII_{cat}			
Grey carpet shark (n = 7)							
Control	9.1 ± 0.9$^{\#}$	0.42 ± 0.18	2.0 ± 0.4$^{\#}$	4.83	22.0 ± 2.0$^{\#}$	7.9 ± 1.6	0.59 ± 0.02$^{\#}$
Anoxia/re-oxygenation	3.8 ± 0.6$^{*\#}$	1.12 ± 0.30*	3.6 ± 0.7$^{*\#}$	3.23	14.6 ± 0.9$^{*\#}$	7.4 ± 1.3*	0.66 ± 0.03$^{*\#}$
Epaulette shark (n = 7)							
Control	3.2 ± 0.5$^{\#}$	0.90 ± 0.48	4.0 ± 1.1$^{\#}$	4.47	28.5 ± 2.1$^{\#}$	9.7 ± 1.1	0.48 ± 0.04$^{\#}$
Anoxia/re-oxygenation	5.5 ± 0.6$^{*\#}$	1.37 ± 0.18	2.6 ± 0.3$^{*\#}$	1.69$^{*\#}$	19.8 ± 1.2$^{*\#}$	4.7 ± 0.7*	0.51 ± 0.03$^{\#}$

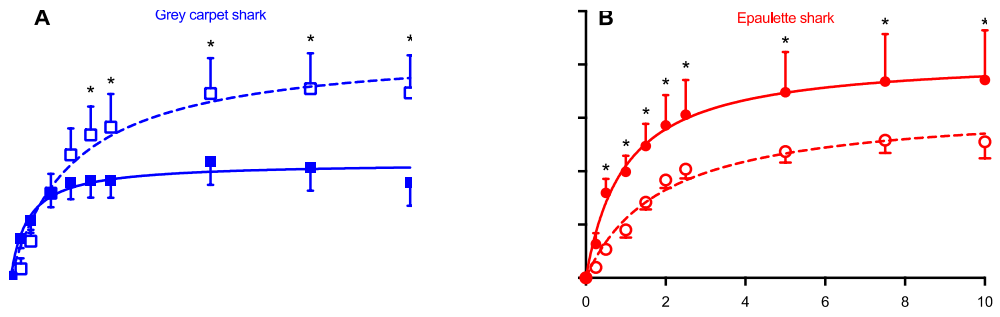

Figure 28. Comparison of complex II respiration rates mediated by increased succinate levels. In mitochondria at normoxia ("ctrl", solid lines) or exposed to anoxia/re-oxygenation ("AR", dashed line) in cerebellum of (A) grey carpet sharks or (B) epaulette sharks. mitochondria respiration in cerebella homogenates from grey carpet sharks (blue) and epaulette sharks (red) was measured in the presence of excess CI substrates (pyruvate, malate and glutamate) and ADP. Then, succinate was titrated up to 10 mM so that CII supported JO_2 could be measured. The additive effect of succinate on JO_2 is here represented with dose-response fitted curves extracted using GraphPad Prism with the least squares method. While AR mediated an increase in CII respiration in mitochondria from grey carpet sharks, CII respiration was decreased in mitochondria of the epaulette sharks. The effect of succinate increments and AR were tested with a two-way ANOVA repeated measure test.

5.4. Discussion

Ultimately, surviving hypoxia or anoxia depends on an animal's ability to conserve energy stores by limiting their ATP demands and/or their ability to produce sufficient ATP despite O_2 limitations and the arrest of OxPhos (Boutilier 2001). Notably, the ES had a smaller cerebellum relative to their body mass than the GCS (**Table 4**). The metabolic scaling theory based on the relationship between body mass and metabolic rate (reviewed in Agutter and Wheatley 2004) would support the notion that the cerebellum of ES may have lower demands for ATP and therefore require less O_2 to sustain cerebellar function than the cerebellum of GCS. In addition, the ES has the ability to undergo metabolic depression with clear evidence of neuronal hypometabolism (Mulvey and Renshaw 2000, Stenslokken, Milton et al. 2008), which most likely enables the ES to withstand a longer exposure to limited environmental O_2. Although both species of carpet sharks are known to survive prolonged anoxia, the sharks displayed contrasting physiological responses in response to AR (Chapman and Renshaw 2009). The *ex vivo* data collected in this study revealed that the contrasting mitochondrial plasticity of these two species of anoxia tolerant sharks parallels their *in vivo* physiological responses to anoxia: i) the mitochondria from the ES, capable of metabolic depression, decreased it metabolism of succinate in response to AR; while ii) the mitochondria from the GCS, which does not enter metabolic depression, not only continued to use succinate but also increased the rate of succinate metabolism in response to AR

5.4.1. Mitochondrial integrity with regard to anoxia/re-oxygenation

Cerebellum of the two carpet sharks displayed similar mitochondrial characteristics before exposure to AR *in vitro* (**Fig. 25**). While the data was not corrected for any differences in mitochondrial density, this finding implies that the cerebellum from both species had the same ability to produce ATP after AR. Both sharks had relatively high (reserve) ETS capacity (i.e. ETS > OxPhos), indicating that the cerebellum of both sharks can accommodate some damage to their ETS without a detrimental effect to OxPhos and ATP production rates. ETS damage may occur during reoxygenation because in the presence of O_2, electron leakage enhances ROS production and damage to lipids within biological membranes and this compromises ETS (Paradies, Petrosillo et al. 2002, Musatov and Robinson 2012, Murphy 2016). We note that the ES cerebellum had a 20% greater ETS capacity than the GCS, which is likely to confer a substantial advantage against ROS damage in response to AR, due to the maintenance of high coupling and low leak state.

While AR decreased ETS by ~30% in both shark species, only the OxPhos rate in GCS cerebellum was affected with a 26% decrease. Previous work using permeabilised ES heart ventricle fibres, showed a ~20% to ~60% loss of ETS capacity relative to OxPhos following an anoxic exposure, with minimal change in OxPhos (Hickey, Renshaw et al. 2012) indicating a consistent response to anoxia in ES mitochondrial populations across cerebellum and heart tissues. Surprisingly, GCS homogenate respiration was more tightly coupled to OxPhos (greater RCR) than the ES homogenate. Furthermore, the net OxPhos ratio suggests similar ATP production efficiencies (i.e. similar nOCR) between the sharks. Overall, while OxPhos rates were lowered in both species, respiration in GCS was better coupled to OxPhos and hence more efficiently directed to ATP production. In contrast, respiration was less coupled to OxPhos in ES cerebellum but OxPhos rates were maintained post AR. Taken together, these data demonstrate that cerebella mitochondria exposed to AR appeared to experience ETS damage in both sharks, however ATP production rates may remain preserved with contrasting response between shark species.

5.4.2. Leak and contribution of the ANT

Proton leak results from protons dissipating passively or actively across the inner mitochondrial membrane without passing through the $ATP_{F0\text{-}F1}$ synthase, and therefore mediates a loss in coupling efficiencies of mitochondria (Divakaruni and Brand 2011). The total leak (L_{Total}, mediated with oligomycin) is similar for both species and represents around 10% of OxPhos rates, which corresponds to levels previously measures in ES heart mitochondria (Hickey, Renshaw et al. 2012). Although anoxia followed by reoxygenation did not affect total proton leak in the GCS cerebellum, AR significantly increased the total proton leak in ES cerebellum to 18% of OxPhos rates.

While counterintuitive, we note that increased proton leak can be beneficial, as it likely prevents elevated ROS production under reduced states (Rolfe and Brand 1997, Ali, Hsiao et al. 2012), such as with elevated succinate with anoxia (Chouchani, Pell et al. 2014). Up to a third of total proton leakage occurs through the ANT (Brand, Pakay et al. 2005, Azzu, Parker et al. 2008). The portion of L_{Total} attributed to the ANT increased from 43% pre-anoxia to 63% after AR in the ES. Similar increases have been observed in rodents displaying enhanced leak through the mitochondrial transition pore (and at least in part through the ANT) after repeated anoxia re-oxygenation episodes (Navet, Mouithys-Mickalad et al. 2006).

Proton leak through the ANT may reflect ADP-ATP exchange rates (Chinopoulos, Kiss et al. 2014). This increase may therefore favour ADP-ATP exchange between mitochondria and the

cytosol and restore cytosolic ATP and mitochondria ADP contents (Klingenberg 2008). Overexpression of the ANT, *via* the activation of cell-protective pathways (ERK and AKT), has been shown to protect mammalian cardiomyocytes exposed to hypoxia (Winter, Klumpe et al. 2016) or oxidative stress (Klumpe, Savvatis et al. 2016). While the specific mechanisms of ANT regulation in ES mitochondria were not assessed in this study, elevated leak should decrease reverse electron flow, decrease localised O_2 concentration and therefore prevent increased ROS production (Brookes 2005), and possibly temporarily increasing ATP-ADP exchange (**Fig. 29**).

5.4.3. Mitochondrial plasticity and complex contribution following AR

The capacity of CI and CII to feed the ETS with electrons is essential for the OxPhos. CI has been shown to be sensitive to anoxia (Rouslin 1983, Paradies, Petrosillo et al. 2004, Chen, Camara et al. 2007, Giusti, Converso et al. 2008) and the most sensitive mitochondrial complex to ROS damage (Hardy, Clark et al. 1990, McLennan and Degli Esposti 2000, Paradies, Petrosillo et al. 2004). In this study, CI contribution was tested prior to and after 20min anoxia. While the contribution of CI to OxPhos was similar for both species in normoxia, in the GCS mitochondria the CI capacity decreased by ~30% following AR (**Fig. 26**). The loss of CI JO_2 capacity was not fully compensated for by CII and resulted in an overall 26% loss in OxPhos capacity in the GCS mitochondria. However, the ES mitochondria which appeared to have a greater ETS reserve capacity also retained proportionately more CI supported flux following AR, despite a suppression in CII flux. Hence, O_2 utilisation in ES mitochondria is more efficiently transferred to proton pumping, essential for OxPhos.

In general, enhanced CII activity has been proposed to lead to a greater electron leakage from CII post-anoxia (Quinlan, Orr et al. 2012, Zakharchenko, Zakharchenko et al. 2013, Tretter, Patocs et al. 2016), which may impact CI capacity through ROS-mediated oxidation of cardiolipin (Paradies, Petrosillo et al. 2002). In hypoxia-tolerant drosophila, the suppression of CII activity decreased ROS production and was proposed to improve long-term survival in hypoxia (Ali, Hsiao et al. 2012). Hence, the data on CII suppression in ES following AR could have a role in preventing damage to CI upon reoxygenation (**Fig. 29**). In contrast, within the GCS cerebellum, CII was more sensitive to AR, yet provided a greater contribution to respiration than CI.

5.4.4. Succinate accumulation

In normoxic conditions, succinate is better utilised by the ES mitochondria with a greater CII contribution to OxPhos than GCS mitochondria (**Fig. 26**). Following anoxia, succinate is oxidised more rapidly by GCS mitochondria with increased apparent CII catalytic efficiencies. At high concentration (i.e above 2 mM), which approximate concentrations in ischemic mammalian brain (Folbergrova, Ljunggren et al. 1974, Benzi, Arrigoni et al. 1979, Benzi, Pastoris et al. 1982), succinate also mediated higher O_2 flux in GCS (**Fig. 27**). As enhanced succinate oxidation rates on reoxygenation can trigger reverse electron flow to CI, which impairs the mitochondrial function in murine model (Starkov 2005, Chouchani, Pell et al. 2014), this may explain why CI capacities were decreased post-AR in the GCS.

In contrast, the overall mitochondrial succinate oxidation rates in the ES cerebellum were lowered in response to AR even with incremented succinate concentrations and this may suppress ROS production in the ES cerebellum (**Fig. 29**). Greater CII catalytic efficiency at low succinate concentrations also suggests that succinate is better utilised by ES cerebellum than by the GCS, which may prevent its accumulation. The downregulation of succinate dehydrogenase activity also occurs within ES rectal glands after hypoxic exposure (Dowd, Renshaw et al. 2010), and lowered succinate dehydrogenase has been shown to be protective against ischemia-reperfusion injuries in other animal models (Wojtovich and Brookes 2008, Ali, Hsiao et al. 2012, Pfleger, He et al. 2015). Succinate oxidation is also depressed in hibernating squirrels, which experience reperfusion-like injury on arousal (Brown, Chung et al. 2012, Brown, Chung et al. 2013). While this is yet unknown whereas succinate accumulates in the cerebellum of the sharks, inhibition of succinate oxidation may reflect the metabolic suppression observed in the ES (Renshaw and Dyson 1999, Renshaw, Kerrisk et al. 2002, Chapman, Harahush et al. 2011) furthermore it may account for the preconditioning effect initiated by a first anoxic exposure which remodelled responses to subsequent insults on a cellular level (Dowd, Renshaw et al. 2010, Rytkonen, Renshaw et al. 2012).

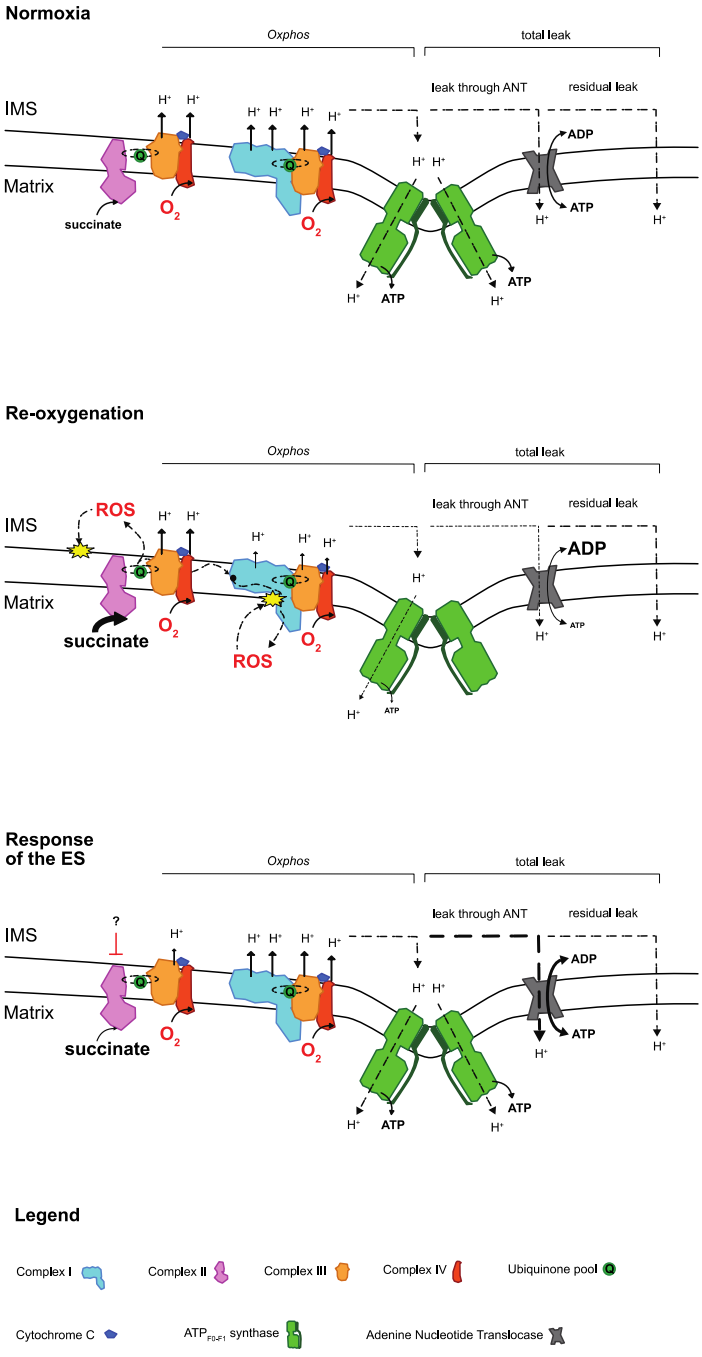

Figure 29. Oxygen, proton and adenine nucleotide fluxes in the mitochondrial electron transport system. In normoxic conditions, proton pumping is mediated through complex I (CI) and complex II (CII) linked systems and the consumption of O_2. The gradient of proton, more concentrated in the inter-membrane space (IMS), is utilised by the $ATP_{F0\text{-}F1}$ synthase via the process known as oxidative phosphorylation (Oxphos) to produce ATP. Some protons may leak through the membrane or transmembrane proteins, one of which being the adenine-nucleotide translocase (ANT), which mediates the ADP and ATP exchange between the matrix and the IMS. The proton leak through the ANT (L_{ANT}) and other proton leakage (residual leak) uncouple respiration from Oxphos and this results in the loss capacity to produce ATP for a given rate of respiration. After an episode of anoxia, succinate accumulates and upon re-oxygenation, succinate oxidation rate accelerates, which mediates an enhanced ROS production from CII, but also a "reverse electron flow" to CI (Chouchani, Pell et al. 2014). This likely affects CI stability and results in an overall loss of capacity for proton pumping and Oxphos. In contrast with most vertebrates, mitochondria from the epaulette shark (ES) cerebellum somehow decrease succinate oxidation rate post-AR and CI linked system capacity is maintained. The L_{ANT} was also increased post-AR and this results in the maintenance of Oxphos. The results obtained from this study suggests that the response of GCS mitochondria sits between the re-oxygenation and the ES panels. While succinate oxidation rates were increased post AR and CI-linked system capacity was decreased, the GCS maintained Oxphos rates similar to those of the ES, with a greater utilisation of O_2 for *Oxphos* (lower L_{ANT} and similar $L_{Residual}$ relative to the ES).

5.5. Conclusion

Contrasting responses of the GCS and the ES cerebella to AR with and without elevated succinate levels highlight key attributes of mitochondrial plasticity used by two tropical anoxia-tolerant species. Despite damage reflected by the decrease in ETS capacity post-AR in both species, OxPhos rates were not changed in the ES mitochondria and were only marginally lower in GCS mitochondria. In this respect, brain mitochondria in these two species are

comparatively more robust than heart mitochondria from the anoxia sensitive shovelnose ray (Hickey, Renshaw et al. 2012).

GCS mitochondria were surprisingly more efficient in directing O_2 flux to OxPhos which could result in a greater capacity to produce ATP post-AR. A contrasting strategy which would maintain ATP levels post-AR was observed in ES mitochondria which had higher active proton leak rates associated with higher ADP/ATP exchange rates. Such a strategy would help to rapidly restore cytosolic energy stores post-AR.

The data revealed that CI was more robust to AR in ES cerebellum than in GCS cerebellum and that the partial inhibition of CII in the ES may represent the initiation of metabolic depression. Furthermore, CII inhibition in the ES would likely prevent reverse electron flow to CI. Such inhibition is likely to not only preserve CI integrity but also to limit ROS production during AR.

This study provides insights into the mitochondria physiology and plasticity in the brains of two anoxia tolerant tropical species which can tolerate hypoxia at temperatures close to that of the mammals. An understanding of how mitochondria plasticity occurs in tropical anoxia tolerant species could lead to novel therapeutic strategies to prevent ischemia-reperfusion injuries the mammalian brain

Chapter 6. Summary and future directions

6.1. Summary

At the end of the O_2 cascade, mitochondria balance O_2 utilisation for life's energy support and paradoxically, death. Various aerobic species can sustain acute exposure to O_2 limitation, however not without a cost. Hypoxia and anoxia rapidly mediate a cascade of events that compromise cell physiology, tissue function and ultimately an organism's life. However, some species occupy habitat frequently exposed to dramatic O_2 fluctuations and have evolved adaptations to avoid damages from hypoxia-reoxygenation. Using a comparative approach, I assessed multiple facets of the mitochondrial function to determine whether mitochondria are involved in the hypoxia-tolerance of intertidal triplefin fishes that occupy hypoxic to hyperoxic tidal rock-pools of the New Zealand coastline, and anoxia-tolerant sharks occupying anoxic lagoons and reef flats of tropical Australian islands.

Tolerance to hypoxia may arise from a multitude of adaptive adjustments, but the interactions between subcellular remodelling and hypoxia-tolerance are yet not clearly defined. The mitochondrion plays an important role in O_2 utilisation and energy release, with adaptive modifications occasionally shared among hypoxia-tolerant species. In my second chapter, I sought to determine whether mitochondrial adaptations could explain the hypoxia-tolerance of intertidal New Zealand triplefin fishes. Using a comparative approach, I chose two intertidal triplefin fish (*Bellapiscis medius* and *Forsterygion lapillum*) supposedly accustom to hypoxia-reoxygenation exposures, and two subtidal species (*F. varium* and *F. malcomi*), which live in stable normoxic waters. Using whole animal respirometry, we verified hypoxia-tolerance in the intertidal fish, with delayed loss of equilibrium, linearly and highly correlated (R^2=0.92) with lower critical O_2 tension of O_2 consumption rates (P_{crit}). I then used high-resolution respirometry to assess mitochondrial characteristics in homogenate and permeabilised brain. While no correlation was found between mitochondrial O_2 binding affinity (mP_{50}) and P_{crit}, OxPhos and mitochondrial O_2 catalytic efficiency were higher in the intertidal species. At the end of the O_2 cascade, activity of cytochrome *c* oxidase (CCO) appeared species-specific, with the highest rate in *B. medius* and lowest rates in *F. lapillum*. Although no correlation to hypoxia-tolerance was verified at the enzymatic levels, I showed that greater mitochondrial oxidative capacities likely sustain brain energy demand of intertidal triplefins and allows their survival in hypoxic rock-pools at low tide.

The vertebrate brain is generally very sensitive to acidosis, so a hypoxia-induced decrease in pH is likely to have an effect on brain mitochondria. Mitochondrial respiration (JO_2) is required to generate an electrical gradient ($\Delta\Psi m$) and a pH gradient to power ATP synthesis, yet the impact of pH modulation on brain mitochondrial function has remained largely unexplored, even in model organisms typically used in medical research. As intertidal fishes within rock pools routinely experience hypoxia and reoxygenation, they would most likely experience frequent changes in cellular pH. Hence, in my third chapter I compared four New Zealand triplefin fish species ranging from intertidal hypoxia-tolerant species to subtidal hypoxia-sensitive species. I predicted that the hypoxia-tolerant fish would tolerate acidosis better than the hypoxia-sensitive ones in terms of sustaining mitochondrial structure and function. Using respirometers coupled to fluorimeters and pH electrodes, I titrated lactic-acid to decrease the pH of the media, and simultaneously recorded JO_2, $\Delta\Psi m$ and H^+ buffering capacities within permeabilized brain and swelling of mitochondria isolated from non-permeabilised brains. I then measured ATP synthesis rates in the most hypoxia-tolerant species (*Bellapiscus medius*) and the hypoxia-sensitive (*Forsterygion varium*) at pH 7.25 and 6.65. Brain mitochondria from hypoxia-tolerant species did have greater H^+ buffering capacities than mitochondria from the hypoxia-sensitive fish (~10 mU $pH.mg_{protein}^{-1}$). Mitochondria from hypoxia-tolerant fish also swelled by 40% when exposed to a decrease of 1.5 pH units, and JO_2 was depressed by up to 15%. However, they were able to maintain $\Delta\Psi m$ near -120 mV.

This work also was unique in that it accounted for changes in mitochondrial volume, a property that has largely been ignored and that alters the estimation of $\Delta\Psi m$. I also estimated the work, in terms of charges moved across the mitochondrial inner-membrane. These estimates suggested that with acidosis, mitochondria from hypoxia-tolerant species may in part harness extra-mitochondrial H^+ to maintain $\Delta\Psi m$, and could therefore support ATP production. This was confirmed with elevated ATP synthesis rates and enhanced P:O ratios at pH 6.65 relative to pH 7.25. In contrast, mitochondrial volumes and $\Delta\Psi m$ decreased downward pH 6.9 in mitochondria from the hypoxia-sensitive species and paradoxically, JO_2 increased (~25%) but ATP synthesis and P:O ratios were depressed at pH 6.65. This indicates a loss of coupling in the HSS with acidosis. Overall, I showed that the mitochondria of these intertidal fish have adaptations that enhance ATP synthesis efficiency under acidic conditions such as those that occur in hypoxic or reoxygenated brain.

Oxygen is essential for the majority of complex lifeforms however, O_2 is paradoxically reactive and toxic in excess and also interacts with electrons in the mitochondrial electron transport system to form reactive oxygen species (ROS). The latter is dependent on O_2 concentration and also the mitochondrial complex II substrate succinate, which accumulates in hypoxic aerobic tissues such as brain. Intertidal species are repetitively exposed to dramatic O_2 fluctuations and likely have evolved strategies to avoid oxidative damage due to hypoxia, reoxygenation and also hyperoxia. Intertidal rock pool fish therefore provide useful models to search for adaptions to ranging O_2. Mitochondrial ROS production has traditionally been assessed in O_2 saturated media, and at concentrations where mitochondria likely do not typically function *in vivo*. In my fourth chapter, I evaluated mitochondrial electron leakage and ROS production in permeabilised brain of intertidal and subtidal triplefin fish species from hyperoxia to anoxia, and assessed the effect of anoxia-reoxygenation and the influence of increasing succinate concentrations. At elevated PO_2, brains of the intertidal triplefin fish released less ROS than subtidal species, however at typical intracellular PO_2, net ROS production was similar among all species. However, following *in vitro* anoxia-reoxygenation electron transfer mediated by gradual succinate titration was better directed, or more efficiently channelled through the ETS to O_2, and not to ROS production in brains from the intertidal species. Overall, I revealed that intertidal species better manage electrons within the ETS and likely avoid oxidative damage in hyperoxic rock-pools on sunny days.

In the previous chapters, we highlighted the mitochondrial adaptations that triplefin fish species have evolved to cope rock-pool O_2 fluctuations. Triplefins have evolved from a common ancestor that arose 12-25 million years ago. In my fifth chapter, I aimed to answer whether some "recent" adaptations observed in triplefins were also carried by "older" hypoxia-tolerant species. Two carpet sharks, the epaulette shark (*Hemiscyllium ocellatum*; ES) and the grey carpet shark (*Chiloscyllium punctatum*; GCS) have evolved for around 150 million years, from the Upper Jurassic when the earth was holding twice less O_2 than today. While both are tolerant to anoxia, the two sharks display different adaptive responses to prolonged anoxia: the ES enters into an energy conserving metabolic depression, while the GCS temporarily elevates its haematocrit in order to prolonging oxygen delivery and sustain metabolism.

I used high-resolution respirometry to investigate mitochondrial function in the cerebellum, a highly metabolically active organ that is oxygen sensitive and vulnerable to injury after anoxia/re-oxygenation anoxia-reoxygenation. I titrated succinate into cerebellar preparations *in vitro*, with or without pre-exposure to anoxia-reoxygenation, and examined the activity of mitochondrial complexes. Like most vertebrates, GCS mitochondria significantly increased

succinate oxidation rates, with impaired complex I function post- anoxia-reoxygenation. In contrast, ES mitochondria inhibited succinate oxidation rates and both complex I and II capacities were conserved, resulting in preservation of oxidative phosphorylation capacity post anoxia-reoxygenation. In this chapter, I showed that the divergent mitochondrial plasticity elicited by elevated succinate post anoxia-reoxygenation parallels the inherently divergent physiological adaptations of these animals to prolonged anoxia, namely the absence (GCS) and presence of metabolic depression (ES). In addition, the responses exhibited by both sharks contrast from the responses observed in triplefin fish species (chapter four), suggesting that mitochondrial adaptations involved in hypoxia-tolerance i) differ from those involved in tolerance to anoxia, or ii) are not universal to hypoxia-tolerant species but appears phylogenetically specific.

Overall, this work has provided fundamental knowledge on some mitochondrial traits that intertidal fish and sharks appeared to have evolved for cheating death when O_2 becomes limited. In eco-physiological contexts, identification of such adaptations to hypoxia and hyperoxia can be used to predict species' survival capacities in naturally and anthropogenically zones currently affected by climate shifts. In a clinical context, understanding the evolution of metabolic mechanisms underlying hypoxia and hyperoxia-tolerance in natural systems may provide insights on how best to resolve anoxic complications such as those occurring post ischemia-reperfusion (i. g. stroke, cardiac arrest, and transplant).

6.2. Limitations and future directions

This present work has brought fundamental knowledge on some aspects of the mitochondrial function in hypoxia and anoxia tolerant species, and this work is of relevance in biomedical contexts. This work has been shared to the general public in the form of published articles (chapter three and five), with the remaining chapters yet to be accepted for publication. Although the findings that arose are interesting and scientifically relevant, there are limitations that must be considered.

Overall, the mitochondrial function was assessed *in vitro* conditions, with saturating substrates and O_2. Such conditions may not be strictly representative of the mitochondrial environment *in vivo*, and while this is informative on the maximum mitochondrial capacity, mitochondria may not be pushed to such extremes within cells. The use of respirometry has opened the door to the assessment of mitochondrial bioenergetics and physiology (Severinghaus and Astrup

1986). However, it involves tissue/cellular preparation that likely alter mitochondrial function, as they are extracted from their host cells, tissues and conditions within the organism (Picard, Taivassalo et al. 2011). The assessment of mitochondrial pathways and respiratory control also requires the use of mitochondrial substrates directly available to mitochondria, and in "unlimited" concentrations that, such as discussed in chapter four, are unlikely reached *in vivo* (Gnaiger 2014). This is required to sustain "constant" flux or apparent steady states. Nonetheless, high-resolution respirometry mainly employed in this thesis, is a standard procedure, recognised to assess mitochondrial physiology and respiratory controls and suitable for comparative physiology studies (Gnaiger 2007, Pesta and Gnaiger 2012), such as those presented in this thesis. While this would be a great additive approach, it is to mention that the study of mitochondrial physiology within tissue is yet not without issues. *In vivo* O_2 saturation, measured by near-infrared or magnetic resonance spectroscopy, and whole body O_2 consumption rates are currently the two approaches available to measure O_2 kinetics attributed to mitochondrial respiration *in vivo*, although the challenge remains in how to differentiate O_2 supply and demand rates (Lanza and Nair 2010).

Other characteristics of mitochondrial physiology such as membrane potential (Logan, Pell et al. 2016), ATP synthesis (Xu, Close et al. 2016), redox state (Mayevsky and Rogatsky 2007) and ROS production (Salin, Auer et al. 2017) can be also be measured *in vivo*. Although, some of these measurements may involve the use of fluorescent dye(s), spin traps (Lanza and Nair 2009, Lanza and Nair 2010), these invariably interact with the studied compound (i.e ROS) and therefore may prevent, quench or exacerbate the compounds effects. As an example, dyes used to monitor real-time ROS production may act as anti-oxidants and may prevent oxidative damage, or physiological response that would normally occur (Griendling, Touyz et al. 2016). Despite these limits, the assessment of mitochondrial function *in vivo* would undeniably bring an additional perspective, more representative of the mitochondrial characteristics and response within cells. In the context of mitochondrial adaptations involved in hypoxia-tolerance, a further study would be to assess the response of mitochondrial populations within tissues of animals exposed to O_2 fluctuation they would experience within their natural habitat. Over the course of this thesis, I used non-invasive spectrophotometry to measure NADH auto-fluorescence **Figure 30**, which non-invasively gives estimates of the redox state within cells without a probe (Mayevsky 2015). Fish were placed on a holder with a wet cloth and intubated with continuous flow of oxygenated sea-water. LEDs at 350-360nm were then used to follow fluorescence using an inexpensive USB camera with a UV and 400-450nm band-pass filter.

This was placed immediately above a fish's head and the signal recorded of the fluorescence emitted for accumulating reduced nicotinamides (NAD(P)H). Sea-water PO_2 was then progressively decreased to 7% air saturation, maintained for 30min and fully reoxygenated.

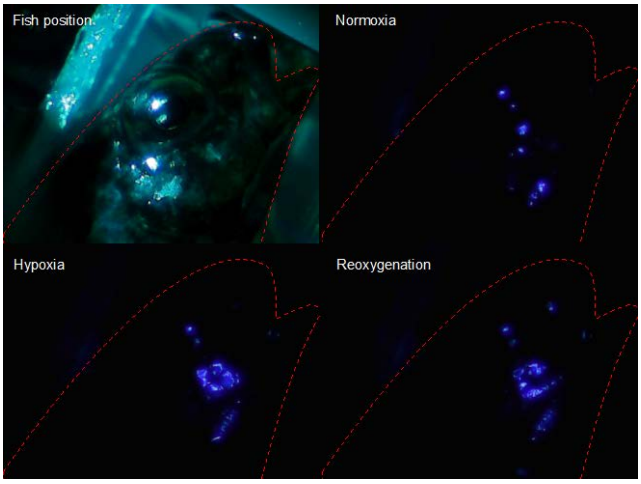

Figure 30. *In vivo* change in redox state of a triplefin fish (*F. lapillum*) exposed to progressive hypoxia (7% air saturated water) and reoxygenation.

While a change in fluorescence was apparent between states **Fig. 30**, the overall set-up could have been improved, with the amelioration of the photo-sensitivity, wavelength selectivity and definition. This study could perhaps be further improved with additional measurements of mitochondrial cytochromes and globins, which have absorption spectra that can be detectable *in vivo* (Banaji, Mallet et al. 2008).

In my third chapter, I assessed the effect of extra-mitochondrial pH on the mitochondrial function and discovered that intertidal triplefin (partially) use acidosis to drive ATP synthesis. During this study, I came across a problematic involved in ΔΨm calculation that requires measurement of the mitochondrial (volume xlix). Mitochondrial volumes (Vol_{mt}) have been estimated in set respiration states with the sucrose or mannitol-impermeable space and tritiated water (Nicholls, Grav et al. 1972, Cohen, Cheung et al. 1987, Bednarczyk, Barker et al. 2008, Casteilla, Devin et al. 2011), or by computer assisted imaging (Perkins, Sun et al. 2009, Peddie and Collinson 2014). However, mitochondria are dynamic organelles, and vary in size and form, and change differently in different tissues and metabolic states and even have different populations in some tissues (e.g. heart) (Benard, Faustin et al. 2006, Woods 2017, Porat-Shliom, Harding et al. 2019). Physiological conditions alters fusion/fission rates (Ernster and Schatz 1981, Cereghetti and Scorrano 2006, Friedman and Nunnari 2014), with changes in respiration state (Hackenbrock 1968, Fujii, Nodasaka et al. 2004), ion concentrations (Kristian, Gertsch et al. 2000) and metabolic water produced by the reduction of O_2 (Casteilla, Devin et al. 2011). Mitochondrial K^+ channels can also regulate Vol_{mt} (Das, Parker et al. 2003, Fujii, Nodasaka et al. 2004, Bednarczyk, Barker et al. 2008), and these can open the mitochondrial transition pore (mPTP) to swell the matrix compartment (Halestrap 2009). Therefore, Vol_{mt} is likely dynamic, and alters ΔΨm. Given the difficulty to assess mitochondrial volume (Peddie and Collinson 2014), only few studies have considered changes in mitochondrial volume in ΔΨm calculation (Kowaltowski, Cosso et al. 2002, Casteilla, Devin et al. 2011). Others assumed mitochondrial volume constant (Chinopoulos, Vajda et al. 2009, Chinopoulos, Kiss et al. 2014), with estimates taken from the literature on similar models (Galli, Lau et al. 2013), or more surprisingly, taken from a different model and different tissues (Poburko, Santo-Domingo et al. 2011).

Using my own data, I noted that error in Vol_{mt} estimates can drastically affect ΔΨm, and this may lead to misinterpretation of the data **Figure 31**. In my third chapter, I calculated Vol_{mt} knowing the distribution of the dye used to assess ΔΨm, and made the only assumption that ΔΨm equates -120 mV at OxPhos state (Kaim and Dimroth 1999, Huttemann, Lee et al. 2008). Changes in Vol_{mt} were measured using light scattering/absorption techniques (detailed in xlix.). The limitation resides in the fact that changes in Vol_{mt} were measured on isolated mitochondria, while ΔΨm was measured in permeabilised brain and while both preparations were exposed to the same conditions, the response of isolated mitochondria may differ from in response in permeabilised tissues. Indeed, mitochondria function as an active network, as they

are in close contact with cytosolic and cytoskeletal elements (Rizzuto, Pinton et al. 1998, Friedman and Nunnari 2014). The isolation process disrupts this environment and may also select the mitochondrial population(s), in that some mitochondria may be more robust to fast centrifuge spins (Picard, Taivassalo et al. 2011). Considering this, we did note that O_2 flux were similarly affected in both preparations and although mitochondria isolated from triplefin brain may have been affected by the isolation process, their response remained similar to these within permeabilised brain. This comforted the scientific relevance of our method employed in Chapter 3, and allowed me to propose a new process that considers changes in Vol_{mt} to better estimate ΔΨm.

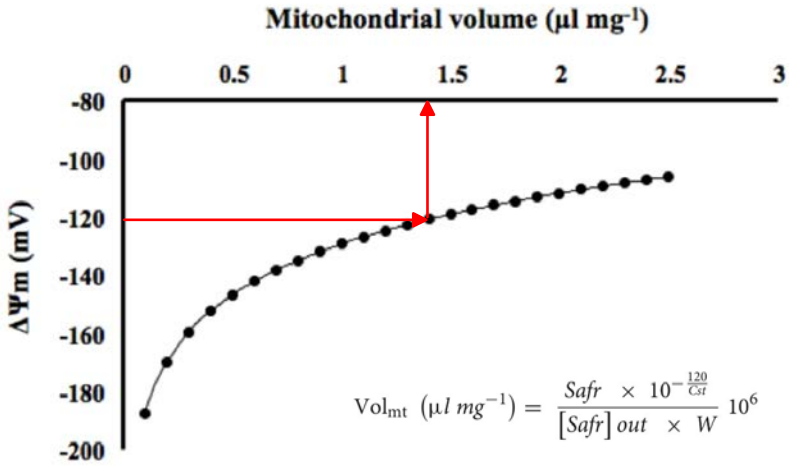

Figure 31. Effect of changes in mitochondrial volume (Vol_{mt}) on membrane potential (ΔΨm). Model calculated from our experiments on mitochondria from *B. medius* brain. At OxPhos state, ΔΨm was assumed to be at -120mV. This allowed the back-calculation of Vol_{mt}, calculated to be equal to 1.4 µl.mg^{-1} average. From this, a change in Vol_{mt} reports change in ΔΨm.

In this same chapter, I demonstrated that mitochondria in intertidal but not subtidal triplefins partially harness acidosis and utilise extra-mitochondrial protons to drive ATP synthesis. While I showed clear evidence of the contrasted mitochondrial responses between intertidal and subtidal species, the specific mechanisms behind the physiology remains unknown. Lactate mediated respiration was higher in intertidal species. Lactate, imported by different monocarboxylic acid transporter isoforms (MCTs), with different apparent affinities for lactate could alter substrate import rates into mitochondria. This could alter $NAD^+/NADH_2$ pools and therefore respiration rates (Kane 2014). Of all isoforms, MCT2 has the highest affinity to lactate and its expression is regulated rapidly (within minutes) of changes of tumour

intracellular pH (Caruso, Koch et al. 2017). Caruso et al (2017) have reported evidence of the pH-sensitive facilitation of the astrocyte-neurone lactate shuttling. Furthermore, MCT2 present in vertebrate neurones has recently been shown to be sensitive to pH, lactate, hypoxia and glycolytic substrates in glioblastoma (Caruso, Koch et al. 2017). Although MCT isoforms have not been assessed in this study, we propose that brain mitochondria in intertidal triplefin fish may differ in MCT expression and this could alter respiration and swelling of mitochondria, and the buffering of cytosolic acidosis. Notably in *Saccharomyces cerevisiae* exposed to acidosis, extra-mitochondrial proton accumulation (i.e. in the cytosol) may increase osmotic pressures and trigger mitochondrial shrinkage (Martinez de Maranon, Tourdot-Marechal et al. 2001), which is a response that was observed in the subtidal species.

The second mechanism may involve mPTP opening, which mediates direct proton transfer from the cytosol to the matrix. Modulations of mPTP is controlled by matrix pH and $\Delta\Psi m$ (Bernardi, Krauskopf et al. 2006). The voltage dependent anion channel (VDAC), which contributes to mPTP shows a strong sensitivity to acidosis on the cytosolic side, while the matrix side is almost insensitive to changes in pH (Teijido, Rappaport et al. 2014). In intertidal fish mitochondria, cytosolic acidosis may more readily trigger VDAC and further mPTP opening, allowing protons to diffuse to the matrix and this may actively buffer cytosolic pH. Notably, mPTP opening mediates mitochondrial swelling (Bernardi 1999), a response observed in brain mitochondria of intertidal triplefins. The opening of mPTP along with the inhibition of CI supported JO_2 also appears to be protective against ROS production and Ca^{2+} accumulation (Briston, Roberts et al. 2017), both also occurring with hypoxia exposure (Javadov 2015). While mitochondrial channel activity has not been assessed in this chapter, the response of phosphorylating mitochondria to lactate suggests the involvement of lactate-mediated regulation in HTS and HSS, which modulates proton conductance in HTS and HSS brain.

Along with lactate, glutamate has also been shown to decrease mitochondrial pH in astrocytes (Azarias, Perreten et al. 2011). While glutamate is an amino acid and mitochondrial substrate, it is also the most excitatory neurotransmitter in the vertebrate brain (Meldrum 2000) and activates neuronal AMPA, NMDA and EAAC receptors (Meldrum 2000). Glutamate is normally captured by astrocytes and converted to glutamine, and then transferred as a fuel to surrounding neurons (Petroff, Errante et al. 2002). Glutamate can be a useful substrate in mitochondria as it may be imported via the ARALAR complex (Ca^{2+}-dependent mitochondrial

aspartate-glutamate transporter) and converted into α-keto-glutarate, which is a component of the citric acid cycle (Ramos, del Arco et al. 2003). Despite its potential use for energy release in brain, the accumulation of glutamate in the synaptic cleft may contribute to brain damage occurring after cerebral ischemia (Johnston, Trescher et al. 2001, Schubert and Piasecki 2001, Hinzman, Thomas et al. 2010, Mehta, Prabhakar et al. 2013). Glutamate toxicity plays a major role in excitotoxicity and is involved in epilepsy, amnesia, anxiety and psychosis (Meldrum 2000). Glutamate clearance is therefore essential to avoid brain damage. It has been shown that the anoxia-tolerant freshwater turtle remodels its brain function by depressing glutamatergic neuronal activity (Hogg, Hawrysh et al. 2014). Such metabolic depression has also been revealed in the anoxia tolerant Epaulette shark (Dowd, Renshaw et al. 2010), although it remains unknown whether glutamate levels are depressed or not.

During my PhD, I assessed some key-components of the mitochondrial glutamate metabolism. Unpublished results revealed that, relative to subtidal triplefins, i) glutamate-mediate JO_2 were greater in HTS Figure 32.A, ii) glutamate dehydrogenase activity Figure 32.B and iii) glutamate levels were lower in the brain of intertidal triplefins exposed to hypoxia Figure 32.C. This suggests that intertidal fish have a greater ability to clear glutamate, supposedly in excess in hypoxia, and utilise this fuel as a substrate for ATP production.

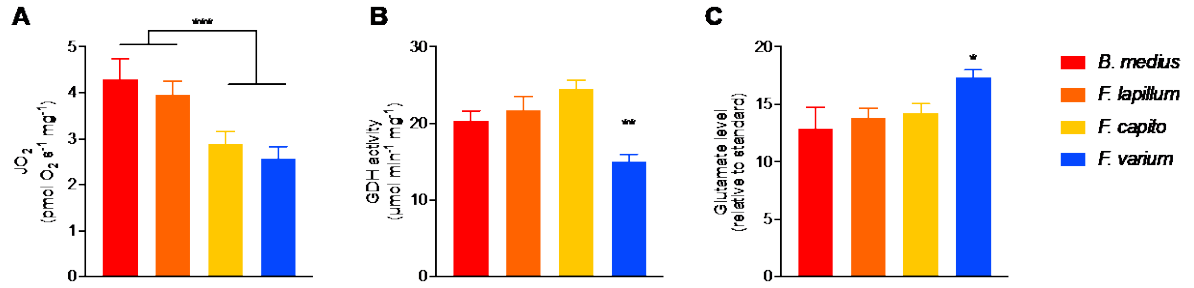

Figure 32. Glutamate metabolism in the brain of four triplefin fish species. A) Mitochondrial respiration, B) glutamate dehydrogenase activity and C) glutamate levels in the intertidal species (warm colours) and subtidal species (blue colour). Data presented as mean of 8 individuals ± s.e.m. Statistical difference tested with one-way ANOVA and represented in APA.

Glutamate accumulation activates AMPA and NMDA receptors allowing the excess entry of Na^+ and Ca^{2+} (Sandoval, Gonzalez et al. 2011, Tang and Xing 2013). The raise in intracellular $[Ca^{2+}]$ ($[Ca^{2+}]_i$) leads to an ionic imbalance, cellular depolarisation, activation of second messenger pathways and the disturbance of other physiological pathways (Berridge, Bootman

et al. 1998, Arundine and Tymianski 2004). In neurones, $[Ca^{2+}]_i$ fluctuates as its influx depends on the electrical activity of the brain, but the resting state modulates $[Ca^{2+}]_i$ within the nano- to micromolar, with only 0.1% Ca^{2+} present as a free ion (Carafoli and Lehninger 1971). The endoplasmic reticulum is the major Ca^{2+} store and actively imports the cation when concentrations exceed 100 nM (Michalak, Groenendyk et al. 2009). However, mitochondria also contribute to Ca^{2+} regulation/buffering and buffer at around 10-130 nmol.mg^{-1} of mitochondrial protein. At physiological levels (200-500 nM), Ca^{2+} enhances OxPhos by regulating dehydrogenases from the TCA by decreasing their apparent Km but by also enhancing pyruvate oxidation at the PDH complex, which helps the maintenance of $\Delta\Psi m$ required for ATP production (Gellerich, Gizatullina et al. 2010). At over ~500 nM mitochondria commence Ca^{2+} buffering (Gellerich, Gizatullina et al. 2012), but $[Ca^{2+}]_i$ above this appears to lead to pathological states when $[Ca^{2+}]_i$ over 1-3µM (Gellerich, Gizatullina et al. 2013). In this context, I assessed mitochondrial Ca^{2+} buffering capacities in the triplefin species used in Chapter 3&4. Using Calcium-Green™, I measured free Ca^{2+} in the chamber of the O2k containing MiR05 thermostated at 20°C, and titrated $CaCl_2$ onto 5 mg permeabilised triplefin brain. The fluorescence signal was normalised by the mass of wet tissue and plotted against control (medium only) Figure 33.

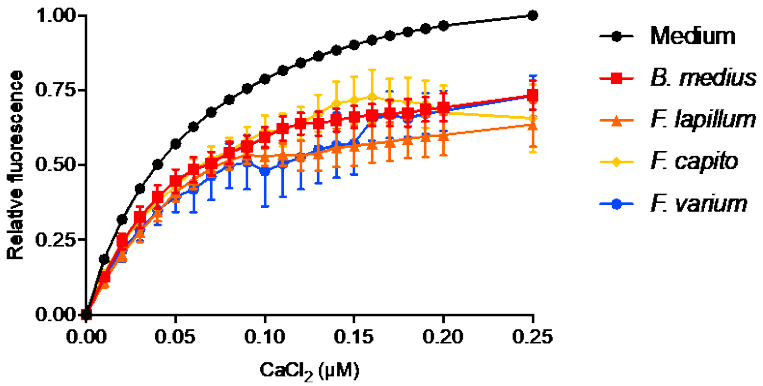

Figure 33. Calcium buffering capacities in four triplefin fish species with graded degree of hypoxia-tolerance. $CaCl_2$ was titrated onto 5 mg permeabilised brain and Magnesium-Green™ was used to track changes in Mg^{2+} free contained in the medium.

From this, no difference was found among the species, as they had similar Ca^{2+} buffering capacities. Taken together with glutamate metabolism, the results suggests that hypoxic Ca^{2+} accumulation is likely avoided by a greater glutamate clearance in the brain of intertidal species.

In this thesis, we confirmed that the mitochondrial function is likely involved in the hypoxia-tolerance of triplefin fish species and anoxia-tolerant sharks, with responses relevant to their ecophysiology. The knowledge gained from these studies opens the door to revealing other traits of the mitochondrial function to identify the interactions and influence weigh of each trait to hypoxia-tolerance in these species. In a clinical context, understanding the evolution of metabolic mechanisms underlying hypoxia and hyperoxia-tolerance in natural systems may provide insights on how best to resolve anoxic complications (i.e ischemia-reperfusion injuries). In eco-physiological contexts, identification of hypoxia and hyperoxia-tolerance strategies can be used to predict species' survival capacities in naturally and anthropogenically oxygen depleted zones.

References

A.L. Val, M. N. P. S., V. M. F. Almeida-Val (1998). "Hypoxia adaptation in fish of the Amazon: a never-ending task." South African journal of zoology. Suid-Afrikaanse tydskrif vir dierkunde. **33**(2): 107-114.

Agutter, P. S. and D. N. Wheatley (2004). "Metabolic scaling: consensus or controversy?" Theor Biol Med Model **1**: 13.

Akerman, K. E. and M. K. Wikstrom (1976). "Safranine as a probe of the mitochondrial membrane potential." FEBS Lett **68**(2): 191-197.

Ali, S. S., M. Hsiao, H. W. Zhao, L. L. Dugan, G. G. Haddad and D. Zhou (2012). "Hypoxia-adaptation involves mitochondrial metabolic depression and decreased ROS leakage." PLoS One **7**(5): e36801.

Altmann, R. (1890). "Die Elementarorganismen und ihre Beziehungen zu den Zellen." Leipzig, Germany: Veit & Co.

Anastacio, M. M., E. M. Kanter, C. M. Makepeace, A. D. Keith, H. Zhang, R. B. Schuessler, C. G. Nichols and J. S. Lawton (2013). "Relationship between mitochondrial matrix volume and cellular volume in response to stress and the role of ATP-sensitive potassium channel." Circulation **128**(11 Suppl 1): S130-135.

Andrienko, T. N., P. Pasdois, G. C. Pereira, M. J. Ovens and A. P. Halestrap (2017). "The role of succinate and ROS in reperfusion injury - A critical appraisal." J Mol Cell Cardiol **110**: 1-14.

Anesti, V. and L. Scorrano (2006). "The relationship between mitochondrial shape and function and the cytoskeleton." Biochim Biophys Acta **1757**(5-6): 692-699.

Aon, M. A., S. Cortassa and B. O'Rourke (2010). "Redox-optimized ROS balance: a unifying hypothesis." Biochim Biophys Acta **1797**(6-7): 865-877.

Arundine, M. and M. Tymianski (2004). "Molecular mechanisms of glutamate-dependent neurodegeneration in ischemia and traumatic brain injury." Cell Mol Life Sci **61**(6): 657-668.

Azarias, G., H. Perreten, S. Lengacher, D. Poburko, N. Demaurex, P. J. Magistretti and J. Y. Chatton (2011). "Glutamate transport decreases mitochondrial pH and modulates oxidative metabolism in astrocytes." J Neurosci **31**(10): 3550-3559.

Azzu, V., N. Parker and M. D. Brand (2008). "High membrane potential promotes alkenal-induced mitochondrial uncoupling and influences adenine nucleotide translocase conformation." Biochem J **413**(2): 323-332.

Bainbridge, A., I. Tachtsidis, S. D. Faulkner, D. Price, T. Zhu, E. Baer, K. D. Broad, D. L. Thomas, E. B. Cady, N. J. Robertson and X. Golay (2014). "Brain mitochondrial oxidative metabolism during and after cerebral hypoxia-ischemia studied by simultaneous phosphorus magnetic-resonance and broadband near-infrared spectroscopy." Neuroimage **102 Pt 1**: 173-183.

Banaji, M., A. Mallet, C. E. Elwell, P. Nicholls and C. E. Cooper (2008). "A model of brain circulation and metabolism: NIRS signal changes during physiological challenges." PLoS Comput Biol **4**(11): e1000212.

Barnes, B. M. (1989). "Freeze avoidance in a mammal: body temperatures below 0 degree C in an Arctic hibernator." Science **244**(4912): 1593-1595.

Barros, L. F. (2013). "Metabolic signaling by lactate in the brain." Trends Neurosci **36**(7): 396-404.

Beavis, A. D., R. D. Brannan and K. D. Garlid (1985). "Swelling and contraction of the mitochondrial matrix. I. A structural interpretation of the relationship between light scattering and matrix volume." J Biol Chem **260**(25): 13424-13433.

Bednarczyk, P., G. D. Barker and A. P. Halestrap (2008). "Determination of the rate of K(+) movement through potassium channels in isolated rat heart and liver mitochondria." Biochim Biophys Acta **1777**(6): 540-548.

Behrens, J. W. and J. F. Steffensen (2007). "The effect of hypoxia on behavioural and physiological aspects of lesser sandeel, Ammodytes tobianus (Linnaeus, 1785)." Marine Biology **150**(6): 1365-1377.

Benamar, A., H. Rolletschek, L. Borisjuk, M. H. Avelange-Macherel, G. Curien, H. A. Mostefai, R. Andriantsitohaina and D. Macherel (2008). "Nitrite-nitric oxide control of mitochondrial respiration at the frontier of anoxia." Biochim Biophys Acta **1777**(10): 1268-1275.

Benard, G., B. Faustin, E. Passerieux, A. Galinier, C. Rocher, N. Bellance, J. P. Delage, L. Casteilla, T. Letellier and R. Rossignol (2006). "Physiological diversity of mitochondrial oxidative phosphorylation." Am J Physiol Cell Physiol **291**(6): C1172-1182.

Benda, C. (1898). " "Ueber die Spermatogenese der Vertebraten und höherer Evertebraten, II. Theil: Die Histiogenese der Spermien"." Archiv für Anatomie und Physiologie **73**: 393-398.

Bennett, M. B., Kyne, P.M. & Heupel, M.R. (2015). "Hemiscyllium ocellatum. The IUCN Red List of Threatened Species 2015: e.T41818A68625284.", from http://dx.doi.org/10.2305/IUCN.UK.2015-4.RLTS.T41818A68625284.en.

Benov, L. (2001). "How superoxide radical damages the cell." Protoplasma **217**(1-3): 33-36.

Bento, L. M., M. M. Fagian, A. E. Vercesi and J. A. Gontijo (2007). "Effects of NH4Cl-induced systemic metabolic acidosis on kidney mitochondrial coupling and calcium transport in rats." Nephrol Dial Transplant **22**(10): 2817-2823.

Benzi, G., E. Arrigoni, F. Marzatico and R. F. Villa (1979). "Influence of some biological pyrimidines on the succinate cycle during and after cerebral ischemia." Biochem Pharmacol **28**(17): 2545-2550.

Benzi, G., O. Pastoris and M. Dossena (1982). "Relationships between gamma-aminobutyrate and succinate cycles during and after cerebral ischemia." J Neurosci Res **7**(2): 193-201.

Bernardi, P. (1999). "Mitochondrial transport of cations: channels, exchangers, and permeability transition." Physiol Rev **79**(4): 1127-1155.

Bernardi, P. (2018). "Why F-ATP Synthase Remains a Strong Candidate as the Mitochondrial Permeability Transition Pore." Front Physiol **9**: 1543.

Bernardi, P., A. Krauskopf, E. Basso, V. Petronilli, E. Blachly-Dyson, F. Di Lisa and M. A. Forte (2006). "The mitochondrial permeability transition from in vitro artifact to disease target." FEBS J **273**(10): 2077-2099.

Berridge, M. J., M. D. Bootman and P. Lipp (1998). "Calcium--a life and death signal." Nature **395**(6703): 645-648.

Berridge, M. V., M. J. McConnell, C. Grasso, M. Bajzikova, J. Kovarova and J. Neuzil (2016). "Horizontal transfer of mitochondria between mammalian cells: beyond co-culture approaches." Current Opinion in Genetics & Development **38**: 75-82.

Berridge, Michael V., Remy T. Schneider and Melanie J. McConnell (2016). "Mitochondrial Transfer from Astrocytes to Neurons following Ischemic Insult: Guilt by Association?" Cell Metabolism **24**(3): 376-378.

Bhowmick, S., J. T. Moore, D. L. Kirschner and K. L. Drew (2017). "Arctic ground squirrel hippocampus tolerates oxygen glucose deprivation independent of hibernation season even when not hibernating and after ATP depletion, acidosis, and glutamate efflux." J Neurochem **142**(1): 160-170.

Bickler, P. E. and L. T. Buck (2007). "Hypoxia tolerance in reptiles, amphibians, and fishes: life with variable oxygen availability." Annu Rev Physiol **69**: 145-170.

Bienert, G. P. and F. Chaumont (2014). "Aquaporin-facilitated transmembrane diffusion of hydrogen peroxide." Biochim Biophys Acta **1840**(5): 1596-1604.

Biro, G. P. (2013). From the Atmosphere to the Mitochondrion: The Oxygen Cascade. Hemoglobin-Based Oxygen Carriers as Red Cell Substitutes and Oxygen Therapeutics. H. W. Kim and A. G. Greenburg. Berlin, Heidelberg, Springer Berlin Heidelberg**:** 27-53.

Bogdanis, G. C., M. E. Nevill, L. H. Boobis and H. K. Lakomy (1996). "Contribution of phosphocreatine and aerobic metabolism to energy supply during repeated sprint exercise." J Appl Physiol **80**(3): 876-884.

Boutilier, R. G. (2001). "Mechanisms of cell survival in hypoxia and hypothermia." J Exp Biol **204**(Pt 18): 3171-3181.

Boveris, A. (1977). "Mitochondrial production of superoxide radical and hydrogen peroxide." Adv Exp Med Biol **78**: 67-82.

Brahimi-Horn, M. C. and J. Pouyssegur (2007). "Oxygen, a source of life and stress." FEBS Lett **581**(19): 3582-3591.

Brand, M. D., K. M. Brindle, J. A. Buckingham, J. A. Harper, D. F. Rolfe and J. A. Stuart (1999). "The significance and mechanism of mitochondrial proton conductance." Int J Obes Relat Metab Disord **23 Suppl 6**: S4-11.

Brand, M. D. and M. P. Murphy (1987). "Control of electron flux through the respiratory chain in mitochondria and cells." Biol Rev Camb Philos Soc **62**(2): 141-193.

Brand, M. D. and D. G. Nicholls (2011). "Assessing mitochondrial dysfunction in cells." Biochem J **435**(2): 297-312.

Brand, M. D., J. L. Pakay, A. Ocloo, J. Kokoszka, D. C. Wallace, P. S. Brookes and E. J. Cornwall (2005). "The basal proton conductance of mitochondria depends on adenine nucleotide translocase content." Biochem J **392**(Pt 2): 353-362.

Briston, T., M. Roberts, S. Lewis, B. Powney, M. S. J, G. Szabadkai and M. R. Duchen (2017). "Mitochondrial permeability transition pore: sensitivity to opening and mechanistic dependence on substrate availability." Sci Rep **7**(1): 10492.

Brookes, P. S. (2005). "Mitochondrial H(+) leak and ROS generation: an odd couple." Free Radic Biol Med **38**(1): 12-23.

Brown, G. C. (1995). "Nitric oxide regulates mitochondrial respiration and cell functions by inhibiting cytochrome oxidase." FEBS Lett **369**(2-3): 136-139.

Brown, J. C., D. J. Chung, K. R. Belgrave and J. F. Staples (2012). "Mitochondrial metabolic suppression and reactive oxygen species production in liver and skeletal muscle of hibernating thirteen-lined ground squirrels." Am J Physiol Regul Integr Comp Physiol **302**(1): R15-28.

Brown, J. C., D. J. Chung, A. N. Cooper and J. F. Staples (2013). "Regulation of succinate-fuelled mitochondrial respiration in liver and skeletal muscle of hibernating thirteen-lined ground squirrels." J Exp Biol **216**(Pt 9): 1736-1743.

Bundgaard, A., A. M. James, W. Joyce, M. P. Murphy and A. Fago (2018). "Suppression of reactive oxygen species generation in heart mitochondria from anoxic turtles: the role of complex I S-nitrosation." J Exp Biol **221**(Pt 8).

Cadenas, E. and K. J. Davies (2000). "Mitochondrial free radical generation, oxidative stress, and aging." Free Radic Biol Med **29**(3-4): 222-230.

Carafoli, E. and A. L. Lehninger (1971). "A survey of the interaction of calcium ions with mitochondria from different tissues and species." Biochem J **122**(5): 681-690.

Carter, H. N., C. C. Chen and D. A. Hood (2015). "Mitochondria, muscle health, and exercise with advancing age." Physiology (Bethesda) **30**(3): 208-223.

Caruso, J. P., B. J. Koch, P. D. Benson, E. Varughese, M. D. Monterey, A. E. Lee, A. M. Dave, S. Kiousis, A. E. Sloan and S. P. Mathupala (2017). "pH, Lactate, and Hypoxia: Reciprocity in Regulating High-Affinity Monocarboxylate Transporter Expression in Glioblastoma." Neoplasia **19**(2): 121-134.

Casteilla, L., A. Devin, A. Carriere, B. Salin, J. Schaeffer and M. Rigoulet (2011). "Control of mitochondrial volume by mitochondrial metabolic water." Mitochondrion **11**(6): 862-866.

Cereghetti, G. M. and L. Scorrano (2006). "The many shapes of mitochondrial death." Oncogene **25**(34): 4717-4724.

Cervós-Navarro, J. and N. H. Diemer (1991). "Selective vulnerability in brain hypoxia." Critical reviews in neurobiology **6**(3): 149-182.

Chan, P. H. (2001). "Reactive oxygen radicals in signaling and damage in the ischemic brain." J Cereb Blood Flow Metab **21**(1): 2-14.

Chapman, C. A., B. K. Harahush and G. M. Renshaw (2011). "The physiological tolerance of the grey carpet shark (Chiloscyllium punctatum) and the epaulette shark (Hemiscyllium ocellatum) to anoxic exposure at three seasonal temperatures." Fish Physiol Biochem **37**(3): 387-399.

Chapman, C. A. and G. M. Renshaw (2009). "Hematological responses of the grey carpet shark (Chiloscyllium punctatum) and the epaulette shark (Hemiscyllium ocellatum) to anoxia and re-oxygenation." J Exp Zool A Ecol Genet Physiol **311**(6): 422-438.

Chapman, L. J., C. A. Chapman, F. G. Nordlie and A. E. Rosenberger (2002). "Physiological refugia: swamps, hypoxia tolerance and maintenance of fish diversity in the Lake Victoria region." Comp Biochem Physiol A Mol Integr Physiol **133**(3): 421-437.

Chapman, L. J. and D. J. McKenzie (2009). Chapter 2 Behavioral Responses and Ecological Consequences. Fish Physiology. A. P. F. Jeffrey G. Richards and J. B. Colin, Academic Press. **Volume 27:** 25-77.

Chen, Q., A. K. Camara, D. F. Stowe, C. L. Hoppel and E. J. Lesnefsky (2007). "Modulation of electron transport protects cardiac mitochondria and decreases myocardial injury during ischemia and reperfusion." Am J Physiol Cell Physiol **292**(1): C137-147.

Chen, Y., Jr., N. G. Mahieu, X. Huang, M. Singh, P. A. Crawford, S. L. Johnson, R. W. Gross, J. Schaefer and G. J. Patti (2016). "Lactate metabolism is associated with mammalian mitochondria." Nat Chem Biol **advance online publication**(11): 937-+.

Chinopoulos, C., A. A. Gerencser, M. Mandi, K. Mathe, B. Torocsik, J. Doczi, L. Turiak, G. Kiss, C. Konrad, S. Vajda, V. Vereczki, R. J. Oh and V. Adam-Vizi (2010). "Forward operation of adenine nucleotide translocase during F0F1-ATPase reversal: critical role of matrix substrate-level phosphorylation." FASEB J **24**(7): 2405-2416.

Chinopoulos, C., G. Kiss, H. Kawamata and A. A. Starkov (2014). "Measurement of ADP-ATP exchange in relation to mitochondrial transmembrane potential and oxygen consumption." Methods Enzymol **542**: 333-348.

Chinopoulos, C., S. Vajda, L. Csanady, M. Mandi, K. Mathe and V. Adam-Vizi (2009). "A novel kinetic assay of mitochondrial ATP-ADP exchange rate mediated by the ANT." Biophys J **96**(6): 2490-2504.

Chouchani, E. T., V. R. Pell, E. Gaude, D. Aksentijevic, S. Y. Sundier, E. L. Robb, A. Logan, S. M. Nadtochiy, E. N. Ord, A. C. Smith, F. Eyassu, R. Shirley, C. H. Hu, A. J. Dare, A. M. James, S. Rogatti, R. C. Hartley, S. Eaton, A. S. Costa, P. S. Brookes, S. M. Davidson, M. R. Duchen, K. Saeb-Parsy, M. J. Shattock, A. J. Robinson, L. M. Work, C. Frezza, T. Krieg and M. P. Murphy (2014). "Ischaemic accumulation of succinate controls reperfusion injury through mitochondrial ROS." Nature **515**(1476-4687 (Electronic)): 431-+.

Claireaux, G. and D. Chabot (2016). "Responses by fishes to environmental hypoxia: integration through Fry's concept of aerobic metabolic scope." J Fish Biol **88**(1): 232-251.

Clarke, A. and N. M. Johnston (1999). "Scaling of metabolic rate with body mass and temperature in teleost fish." Journal of Animal Ecology **68**(5): 893-905.

Clements, K. (2006). Triplefins. New Zealand Geographic, Kowhai Media Ltd.

Cogliati, S., J. A. Enriquez and L. Scorrano (2016). "Mitochondrial Cristae: Where Beauty Meets Functionality." Trends Biochem Sci **41**(3): 261-273.

Cohen, N. S., C. W. Cheung and L. Raijman (1987). "Measurements of mitochondrial volumes are affected by the amount of mitochondria used in the determinations." Biochemical Journal **245**(2): 375-379.

Cook, D. G., F. I. Iftikar, D. W. Baker, A. J. Hickey and N. A. Herbert (2013). "Low-O(2) acclimation shifts the hypoxia avoidance behaviour of snapper (Pagrus auratus) with only subtle changes in aerobic and anaerobic function." J Exp Biol **216**(Pt 3): 369-378.

Cook, G. A. L., Carol M. (1968). "Oxygen". The Encyclopedia of the Chemical Elements. C. A. Hampel. Library of Congress of the United States, New York: Reinhold Book Corporation**:** 499–512.

Cooper, C. E. and G. C. Brown (2008). "The inhibition of mitochondrial cytochrome oxidase by the gases carbon monoxide, nitric oxide, hydrogen cyanide and hydrogen sulfide: chemical mechanism and physiological significance." J Bioenerg Biomembr **40**(5): 533-539.

Cooper, G. M. (2000). The cell a molecular approach. Sunderland, Mass. : Bethesda, MD : NCBI\ \ \, Sunderland, Mass. : Sinauer Associates ; Bethesda, MD : NCBI c2000.\.

Cox, G. K., E. Sandblom, J. G. Richards and A. P. Farrell (2011). "Anoxic survival of the Pacific hagfish (Eptatretus stoutii)." J Comp Physiol B **181**(3): 361-371.

Cumming, H. and N. A. Herbert (2016). "Gill structural change in response to turbidity has no effect on the oxygen uptake of a juvenile sparid fish." Conserv Physiol **4**(1): cow033.

Danovaro, R., A. Dell'Anno, A. Pusceddu, C. Gambi, I. Heiner and R. M. Kristensen (2010). "The first metazoa living in permanently anoxic conditions." BMC Biol **8**: 30.

Das, M., J. E. Parker and A. P. Halestrap (2003). "Matrix volume measurements challenge the existence of diazoxide/glibencamide-sensitive KATP channels in rat mitochondria." J Physiol **547**(Pt 3): 893-902.

Davies, K. M., C. Anselmi, I. Wittig, J. D. Faraldo-Gomez and W. Kuhlbrandt (2012). "Structure of the yeast F1Fo-ATP synthase dimer and its role in shaping the mitochondrial cristae." Proc Natl Acad Sci U S A **109**(34): 13602-13607.

Davies, K. M., M. Strauss, B. Daum, J. H. Kief, H. D. Osiewacz, A. Rycovska, V. Zickermann and W. Kuhlbrandt (2011). "Macromolecular organization of ATP synthase and complex I in whole mitochondria." Proc Natl Acad Sci U S A **108**(34): 14121-14126.

De Groot, H. and U. Rauen (2007). "Ischemia-reperfusion injury: processes in pathogenetic networks: a review." Transplant Proc **39**(2): 481-484.

Degli Esposti, M. (1998). "Inhibitors of NADH-ubiquinone reductase: an overview." Biochim Biophys Acta **1364**(2): 222-235.

Dickinson, B. C. and C. J. Chang (2011). "Chemistry and biology of reactive oxygen species in signaling or stress responses." Nat Chem Biol **7**(8): 504-511.

Dienel, G. A. (2012). "Brain lactate metabolism: the discoveries and the controversies." J Cereb Blood Flow Metab **32**(7): 1107-1138.

Divakaruni, A. S. and M. D. Brand (2011). "The regulation and physiology of mitochondrial proton leak." Physiology (Bethesda) **26**(3): 192-205.

Dowd, W. W., G. M. Renshaw, J. J. Cech, Jr. and D. Kultz (2010). "Compensatory proteome adjustments imply tissue-specific structural and metabolic reorganization following episodic hypoxia or anoxia in the epaulette shark (Hemiscyllium ocellatum)." Physiol Genomics **42**(1): 93-114.

Du, S. N., S. Mahalingam, B. G. Borowiec and G. R. Scott (2016). "Mitochondrial physiology and reactive oxygen species production are altered by hypoxia acclimation in killifish (Fundulus heteroclitus)." J Exp Biol **219**(Pt 8): 1130-1138.

Duchen, M. R. (2012). "Mitochondria, calcium-dependent neuronal death and neurodegenerative disease." Pflugers Arch **464**(1): 111-121.

Dudgeon, C. L., Bennett, M.B. & Kyne, P.M. (2016). "Chiloscyllium punctatum. The IUCN Red List of Threatened Species 2016: e.T41872A68616745.", from http://dx.doi.org/10.2305/IUCN.UK.2016-1.RLTS.T41872A68616745.en.

Edited by Greenwood, N. N., Earnshaw, A. (1997). 14 - Oxygen. Chemistry of the Elements (Second Edition). N. N. Greenwood and A. Earnshaw. Oxford, Butterworth-Heinemann**:** 600-644.

Emsley, J. (2011). Nature's Building Blocks: An A-Z Guide to the Elements, OUP Oxford.

Ernster, L. and G. Schatz (1981). "Mitochondria: a historical review." J Cell Biol **91**(3 Pt 2): 227s-255s.

Eubel, H., J. Heinemeyer, S. Sunderhaus and H. P. Braun (2004). "Respiratory chain supercomplexes in plant mitochondria." Plant Physiol Biochem **42**(12): 937-942.

Farrell, A. P. and J. G. Richards (2009). Chapter 11 Defining Hypoxia: An Integrative Synthesis of the Responses of Fish to Hypoxia. Fish Physiology. A. P. F. Jeffrey G. Richards and J. B. Colin, Academic Press. **Volume 27:** 487-503.

Feary, D., M. Wellenreuther and K. Clements (2009). "Trophic ecology of New Zealand triplefin fishes (Family Tripterygiidae)." Marine Biology **156**(8): 1703-1714.

Feary, D. A. C., K. D. (2006). "Habitat use by triplefin species (Tripterygiidae) on rocky reefs in New Zealand." Journal of Fish Biology **69**(4): 1031-1046.

Fenical, W. (1983). Marine Plants: A Unique and Unexplored Resource. Plants: the potentials for extracting protein, medicines, and other useful chemicals. Institute of MArine Ressources Scripps Institution of Oceanography University of California , San Diego, DIANE Publishing.

Folbergrova, J., B. Ljunggren, K. Norberg and B. K. Siesjo (1974). "Influence of complete ischemia on glycolytic metabolites, citric acid cycle intermediates, and associated amino acids in the rat cerebral cortex." Brain Res **80**(2): 265-279.

Fricke, R. (1994). Tripterygiid Fishes of Australia, New Zealand and the Southwest Pacific Ocean (Teleostei).

Friedman, J. R. and J. Nunnari (2014). "Mitochondrial form and function." Nature **505**(7483): 335-343.

Fujii, F., Y. Nodasaka, G. Nishimura and M. Tamura (2004). "Anoxia induces matrix shrinkage accompanied by an increase in light scattering in isolated brain mitochondria." Brain Res **999**(1): 29-39.

Gallagher, C. N., K. L. Carpenter, P. Grice, D. J. Howe, A. Mason, I. Timofeev, D. K. Menon, P. J. Kirkpatrick, J. D. Pickard, G. R. Sutherland and P. J. Hutchinson (2009). "The human brain utilizes lactate via the tricarboxylic acid cycle: a 13C-labelled microdialysis and high-resolution nuclear magnetic resonance study." Brain **132**(Pt 10): 2839-2849.

Galli, G. L., G. Y. Lau and J. G. Richards (2013). "Beating oxygen: chronic anoxia exposure reduces mitochondrial F1FO-ATPase activity in turtle (Trachemys scripta) heart." J Exp Biol **216**(Pt 17): 3283-3293.

Galli, G. L. and J. G. Richards (2014). "Mitochondria from anoxia-tolerant animals reveal common strategies to survive without oxygen." J Comp Physiol B **184**(3): 285-302.

Gamperl, A. K. and W. R. Driedzic (2009). Chapter 7 Cardiovascular Function and Cardiac Metabolism. Fish Physiology. J. G. Richards, A. P. Farrell and J. B. Colin, Academic Press. **Volume 27:** 301-360.

Garland, T., Jr., A. F. Bennett and E. L. Rezende (2005). "Phylogenetic approaches in comparative physiology." J Exp Biol **208**(Pt 16): 3015-3035.

Garlid, K. D. and A. D. Beavis (1985). "Swelling and contraction of the mitochondrial matrix. II. Quantitative application of the light scattering technique to solute transport across the inner membrane." J Biol Chem **260**(25): 13434-13441.

Garofalo, O., D. W. Cox and H. S. Bachelard (1988). "Brain levels of NADH and NAD+ under hypoxic and hypoglycaemic conditions in vitro." J Neurochem **51**(1): 172-176.

Garrido, C., L. Galluzzi, M. Brunet, P. E. Puig, C. Didelot and G. Kroemer (2006). "Mechanisms of cytochrome c release from mitochondria." Cell Death Differ **13**(9): 1423-1433.

Gáspár, S. (2011). Detection of Superoxide and Hydrogen Peroxide from Living Cells Using Electrochemical Sensors. Oxidative Stress: Diagnostics, Prevention, and Therapy, American Chemical Society. **1083:** 289-309.

Gates, T. A., E. Gorscak and P. J. Makovicky (2019). "New sharks and other chondrichthyans from the latest Maastrichtian (Late Cretaceous) of North America." Journal of Paleontology: 1-19.

Gellerich, F. N., Z. Gizatullina, T. Gainutdinov, K. Muth, E. Seppet, Z. Orynbayeva and S. Vielhaber (2013). "The control of brain mitochondrial energization by cytosolic calcium: the mitochondrial gas pedal." IUBMB Life **65**(3): 180-190.

Gellerich, F. N., Z. Gizatullina, S. Trumbeckaite, H. P. Nguyen, T. Pallas, O. Arandarcikaite, S. Vielhaber, E. Seppet and F. Striggow (2010). "The regulation of OXPHOS by extramitochondrial calcium." Biochim Biophys Acta **1797**(6-7): 1018-1027.

Gellerich, F. N., Z. Gizatullina, S. Trumbekaite, B. Korzeniewski, T. Gaynutdinov, E. Seppet, S. Vielhaber, H. J. Heinze and F. Striggow (2012). "Cytosolic Ca2+ regulates the energization of isolated brain mitochondria by formation of pyruvate through the malate-aspartate shuttle." Biochem J **443**(3): 747-755.

Giusti, S., D. P. Converso, J. J. Poderoso and S. Fiszer de Plazas (2008). "Hypoxia induces complex I inhibition and ultrastructural damage by increasing mitochondrial nitric oxide in developing CNS." Eur J Neurosci **27**(1): 123-131.

Gnaiger, E. (2007). "Mitochondrial pathways and respiratory control." Textbook on Mitochondrial Physiology, edited by E Gnaiger Innsbruck, Austria: OROBOROS MiPNet: 1-95.

Gnaiger, E. (2008). Polarographic Oxygen Sensors, the Oxygraph, and High-Resolution Respirometry to Assess Mitochondrial Function. Drug-Induced Mitochondrial Dysfunction.

Gnaiger, E. (2014). "Mitochondrial Pathways and Respiratory Control: An Introduction to OXPHOS Analysis." OROBOROS MiPNet Publications **1**.

Gnaiger, E., A. V. Kuznetsov, S. Schneeberger, R. Seiler, G. Brandacher, W. Steurer and R. Margreiter (2000). Mitochondria in the Cold. Life in the Cold: Eleventh International Hibernation Symposium. G. Heldmaier and M. Klingenspor. Berlin, Heidelberg, Springer Berlin Heidelberg**:** 431-442.

Gnaiger, E., B. Lassnig, A. Kuznetsov, G. Rieger and R. Margreiter (1998). "Mitochondrial oxygen affinity, respiratory flux control and excess capacity of cytochrome c oxidase." J Exp Biol **201**(Pt 8): 1129-1139.

Gorman, G. S., P. F. Chinnery, S. DiMauro, M. Hirano, Y. Koga, R. McFarland, A. Suomalainen, D. R. Thorburn, M. Zeviani and D. M. Turnbull (2016). "Mitochondrial diseases." Nature Reviews Disease Primers **2**: 16080.

Gorr, T. A., D. Wichmann, J. Hu, M. Hermes-Lima, A. F. Welker, N. Terwilliger, J. F. Wren, M. Viney, S. Morris, G. E. Nilsson, A. Deten, J. Soliz and M. Gassmann (2010). "Hypoxia tolerance in animals: biology and application." Physiol Biochem Zool **83**(5): 733-752.

Greaves, L. C. and R. W. Taylor (2006). "Mitochondrial DNA mutations in human disease." IUBMB Life **58**(3): 143-151.

Griendling, K. K., R. M. Touyz, J. L. Zweier, S. Dikalov, W. Chilian, Y. R. Chen, D. G. Harrison, A. Bhatnagar and S. American Heart Association Council on Basic Cardiovascular (2016). "Measurement of Reactive Oxygen Species, Reactive Nitrogen Species, and Redox-Dependent Signaling in the Cardiovascular System: A Scientific Statement From the American Heart Association." Circ Res **119**(5): e39-75.

Grivennikova, V. G., A. V. Kareyeva and A. D. Vinogradov (2018). "Oxygen-dependence of mitochondrial ROS production as detected by Amplex Red assay." Redox Biol **17**: 192-199.

Guzy, R. D. and P. T. Schumacker (2006). "Oxygen sensing by mitochondria at complex III: the paradox of increased reactive oxygen species during hypoxia." Exp Physiol **91**(5): 807-819.

Hackenbrock, C. R. (1968). "Ultrastructural bases for metabolically linked mechanical activity in mitochondria : II. Electron transport-linked ultrastructural transformations in mitochondria." J Cell Biol **37**(2): 345-369.

Halestrap, A. P. (1975). "The mitochondrial pyruvate carrier. Kinetics and specificity for substrates and inhibitors." Biochem J **148**(1): 85-96.

Halestrap, A. P. (2009). "What is the mitochondrial permeability transition pore?" J Mol Cell Cardiol **46**(6): 821-831.

Halliwell, B. (1977). "Generation of hydrogen peroxide, superoxide and hydroxyl radicals during the oxidation of dihydroxyfumaric acid by peroxidase." Biochem J **163**(3): 441-448.

Hancock, C. N., W. Liu, W. G. Alvord and J. M. Phang (2016). "Co-regulation of mitochondrial respiration by proline dehydrogenase/oxidase and succinate." Amino Acids **48**(3): 859-872.

Hardy, D. L., J. B. Clark, V. M. Darley-Usmar and D. R. Smith (1990). "Reoxygenation of the hypoxic myocardium causes a mitochondrial complex I defect." Biochem Soc Trans **18**(4): 549.

Harris, E. J. and J. R. Manger (1969). "Intersubstrate competitions and evidence for compartmentation in mitochondria." Biochem J **113**(4): 617-628.

Hickey, A. J. and K. D. Clements (2003). "Key metabolic enzymes and muscle structure in triplefin fishes (Tripterygiidae): a phylogenetic comparison." J Comp Physiol B **173**(2): 113-123.

Hickey, A. J. and K. D. Clements (2005). "Genome size evolution in New Zealand triplefin fishes." J Hered **96**(4): 356-362.

Hickey, A. J., S. D. Lavery, D. A. Hannan, C. S. Baker and K. D. Clements (2009). "New Zealand triplefin fishes (family Tripterygiidae): contrasting population structure and mtDNA diversity within a marine species flock." Mol Ecol **18**(4): 680-696.

Hickey, A. J., G. M. Renshaw, B. Speers-Roesch, J. G. Richards, Y. Wang, A. P. Farrell and C. J. Brauner (2012). "A radical approach to beating hypoxia: depressed free radical release from heart fibres of the hypoxia-tolerant epaulette shark (Hemiscyllum ocellatum)." J Comp Physiol B **182**(1): 91-100.

Hillered, L., L. Ernster and B. K. Siesjo (1984). "Influence of in vitro lactic acidosis and hypercapnia on respiratory activity of isolated rat brain mitochondria." J Cereb Blood Flow Metab **4**(3): 430-437.

Hilton, Z. (2010). Physiological adaptation in the radiation of New Zealand triplefin fishes (Family Tripterygiidae). PhD PhD, University of Auckland.

Hilton, Z., K. D. Clements and A. J. Hickey (2010). "Temperature sensitivity of cardiac mitochondria in intertidal and subtidal triplefin fishes." J Comp Physiol B **180**(7): 979-990.

Hilton, Z., M. Wellenreuther and K. D. Clements (2008). "Physiology underpins habitat partitioning in a sympatric sister-species pair of intertidal fishes." Functional Ecology **22**(6): 1108-1117.

Hinzman, J. M., T. C. Thomas, J. J. Burmeister, J. E. Quintero, P. Huettl, F. Pomerleau, G. A. Gerhardt and J. Lifshitz (2010). "Diffuse brain injury elevates tonic glutamate levels and potassium-evoked glutamate release in discrete brain regions at two days post-injury: an enzyme-based microelectrode array study." J Neurotrauma **27**(5): 889-899.

Hochachka, P. W., L. T. Buck, C. J. Doll and S. C. Land (1996). "Unifying theory of hypoxia tolerance: molecular/metabolic defense and rescue mechanisms for surviving oxygen lack." Proc Natl Acad Sci U S A **93**(18): 9493-9498.

Hogg, D. W., P. J. Hawrysh and L. T. Buck (2014). "Environmental remodelling of GABAergic and glutamatergic neurotransmission: rise of the anoxia-tolerant turtle brain." J Therm Biol **44**: 85-92.

Holt, I. J., A. E. Harding and J. A. Morgan-Hughes (1988). "Deletions of muscle mitochondrial DNA in patients with mitochondrial myopathies." Nature **331**(6158): 717-719.

Huttemann, M., I. Lee, A. Pecinova, P. Pecina, K. Przyklenk and J. W. Doan (2008). "Regulation of oxidative phosphorylation, the mitochondrial membrane potential, and their role in human disease." J Bioenerg Biomembr **40**(5): 445-456.

Iftikar, F. I. and A. J. Hickey (2013). "Do mitochondria limit hot fish hearts? Understanding the role of mitochondrial function with heat stress in Notolabrus celidotus." PLoS One **8**(5): e64120.

Jackson, D. C. (2004). "Surviving extreme lactic acidosis: the role of calcium lactate formation in the anoxic turtle." Respir Physiol Neurobiol **144**(2-3): 173-178.

Jackson, D. C., C. V. Herbert and G. R. Ultsch (1984). "The Comparative Physiology of Diving in North American Freshwater Turtles. II. Plasma Ion Balance during Prolonged Anoxia." Physiological Zoology **57**(6): 632-640.

Jagendorf, A. T. and E. Uribe (1966). "ATP formation caused by acid-base transition of spinach chloroplasts." Proc Natl Acad Sci U S A **55**(1): 170-177.

Jastroch, M., A. S. Divakaruni, S. Mookerjee, J. R. Treberg and M. D. Brand (2010). "Mitochondrial proton and electron leaks." Essays Biochem **47**: 53-67.

Javadov, S. (2015). "The calcium-ROS-pH triangle and mitochondrial permeability transition: challenges to mimic cardiac ischemia-reperfusion." Front Physiol **6**: 83.

Jena, N. R. (2012). "DNA damage by reactive species: Mechanisms, mutation and repair." J Biosci **37**(3): 503-517.

Jensen, P. K. (1966). "Antimycin-insensitive oxidation of succinate and reduced nicotinamide-adenine dinucleotide in electron-transport particles. I. pH dependency and hydrogen peroxide formation." Biochim Biophys Acta **122**(2): 157-166.

Johansson, D., G. Nilsson, Ouml and E. Rnblom (1995). "Effects of anoxia on energy metabolism in crucian carp brain slices studied with microcalorimetry." J Exp Biol **198**(Pt 3): 853-859.

Johnston, I. A. and L. M. Bernard (1983). "Utilization of the Ethanol Pathway in Carp Following Exposure to Anoxia." Journal of Experimental Biology **104**(1): 73.

Johnston, M. V., W. H. Trescher, A. Ishida and W. Nakajima (2001). "Neurobiology of hypoxic-ischemic injury in the developing brain." Pediatr Res **49**(6): 735-741.

Jokivarsi, K. T., H. I. Grohn, O. H. Grohn and R. A. Kauppinen (2007). "Proton transfer ratio, lactate, and intracellular pH in acute cerebral ischemia." Magn Reson Med **57**(4): 647-653.

Kagan, V. E., G. G. Borisenko, Y. Y. Tyurina, V. A. Tyurin, J. Jiang, A. I. Potapovich, V. Kini, A. A. Amoscato and Y. Fujii (2004). "Oxidative lipidomics of apoptosis: redox catalytic interactions of cytochrome c with cardiolipin and phosphatidylserine." Free Radic Biol Med **37**(12): 1963-1985.

Kaim, G. and P. Dimroth (1999). "ATP synthesis by F-type ATP synthase is obligatorily dependent on the transmembrane voltage." EMBO J **18**(15): 4118-4127.

Kale, J., E. J. Osterlund and D. W. Andrews (2018). "BCL-2 family proteins: changing partners in the dance towards death." Cell Death Differ **25**(1): 65-80.

Kalogeris, T., C. P. Baines, M. Krenz and R. J. Korthuis (2012). "Cell biology of ischemia/reperfusion injury." Int Rev Cell Mol Biol **298**: 229-317.

Kane, D. A. (2014). "Lactate oxidation at the mitochondria: a lactate-malate-aspartate shuttle at work." Front Neurosci **8**: 366.

Karlsson, A., L. S. Heier, B. O. Rosseland, B. Salbu and A. Kiessling (2011). "Changes in arterial PO2, physiological blood parameters and intracellular antioxidants in free-swimming Atlantic cod (Gadus morhua) exposed to varying levels of hyperoxia." Fish Physiol Biochem **37**(1): 249-258.

Karlsson, A., L. S. Heier, B. O. Rosseland, B. Salbu and A. Kiessling (2011). "Changes in arterial PO(2), physiological blood parameters and intracellular antioxidants in free-swimming Atlantic cod (Gadus morhua) exposed to varying levels of hyperoxia." Fish Physiol Biochem **37**(1): 249-258.

Katsura, K., B. Asplund, A. Ekholm and B. K. Siesjo (1992). "Extra- and Intracellular pH in the Brain During Ischaemia, Related to Tissue Lactate Content in Normo- and Hypercapnic rats." Eur J Neurosci **4**(2): 166-176.

Katsura, K., A. Ekholm, B. Asplund and B. K. Siesjo (1991). "Extracellular pH in the brain during ischemia: relationship to the severity of lactic acidosis." J Cereb Blood Flow Metab **11**(4): 597-599.

Katsura, K., A. Ekholm and B. K. Siesjo (1992). "Tissue PCO2 in brain ischemia related to lactate content in normo- and hypercapnic rats." J Cereb Blood Flow Metab **12**(2): 270-280.

Kaufman, D. P. and A. S. Dhamoon (2018). Physiology, Oxyhemoglobin Dissociation Curve. StatPearls. Treasure Island (FL).

Khacho, M., M. Tarabay, D. Patten, P. Khacho, J. G. MacLaurin, J. Guadagno, R. Bergeron, S. P. Cregan, M. E. Harper, D. S. Park and R. S. Slack (2014). "Acidosis overrides oxygen deprivation to maintain mitochondrial function and cell survival." Nat Commun **5**: 3550.

Khalifat, N., J. B. Fournier, M. I. Angelova and N. Puff (2011). "Lipid packing variations induced by pH in cardiolipin-containing bilayers: the driving force for the cristae-like shape instability." Biochim Biophys Acta **1808**(11): 2724-2733.

Khan, J. R., S. Pether, M. Bruce, S. P. Walker and N. A. Herbert (2014). "Optimum temperatures for growth and feed conversion in cultured hapuku (Polyprion oxygeneios) — Is there a link to aerobic metabolic scope and final temperature preference?" Aquaculture **430**: 107-113.

Kinnally, K. W., P. M. Peixoto, S.-Y. Ryu and L. M. Dejean (2011). "Is mPTP the gatekeeper for necrosis, apoptosis, or both?" Biochimica et biophysica acta **1813**(4): 616-622.

Kitzenberg, D., S. P. Colgan and L. E. Glover (2016). "Creatine kinase in ischemic and inflammatory disorders." Clin Transl Med **5**(1): 31.

Klingenberg, M. (2008). "The ADP and ATP transport in mitochondria and its carrier." Biochim Biophys Acta **1778**(10): 1978-2021.

Klumpe, I., K. Savvatis, D. Westermann, C. Tschope, U. Rauch, U. Landmesser, H. P. Schultheiss and A. Dorner (2016). "Transgenic overexpression of adenine nucleotide translocase 1 protects ischemic hearts against oxidative stress." J Mol Med (Berl) **94**(6): 645-653.

Kondrashova, M., M. Zakharchenko and N. Khunderyakova (2009). "Preservation of the in vivo state of mitochondrial network for ex vivo physiological study of mitochondria." Int J Biochem Cell Biol **41**(10): 2036-2050.

Korshunov, S. S., V. P. Skulachev and A. A. Starkov (1997). "High protonic potential actuates a mechanism of production of reactive oxygen species in mitochondria." FEBS Lett **416**(1): 15-18.

Kowaltowski, A. J., R. G. Cosso, C. B. Campos and G. Fiskum (2002). "Effect of Bcl-2 overexpression on mitochondrial structure and function." J Biol Chem **277**(45): 42802-42807.

Krab, K., H. Kempe and M. Wikstrom (2011). "Explaining the enigmatic KM for oxygen in cytochrome c oxidase: a kinetic model." Biochim Biophys Acta **1807**(3): 348-358.

Kraig, R. P. and R. J. Wagner (1987). "Acid-induced changes of brain protein buffering." Brain Res **410**(2): 390-394.

Kraut, J. A. and N. E. Madias (2014). "Lactic acidosis." N Engl J Med **371**(24): 2309-2319.

Krieg, B. J., S. M. Taghavi, G. L. Amidon and G. E. Amidon (2014). "In vivo predictive dissolution: transport analysis of the CO2 , bicarbonate in vivo buffer system." J Pharm Sci **103**(11): 3473-3490.

Kristian, T., J. Gertsch, T. E. Bates and B. K. Siesjo (2000). "Characteristics of the calcium-triggered mitochondrial permeability transition in nonsynaptic brain mitochondria: effect of cyclosporin A and ubiquinone O." J Neurochem **74**(5): 1999-2009.

Krumschnabel, G., A. Eigentler, M. Fasching and E. Gnaiger (2014). "Use of safranin for the assessment of mitochondrial membrane potential by high-resolution respirometry and fluorometry." Methods Enzymol **542**: 163-181.

Kuznetsov, A. V., G. Brandacher, W. Steurer, R. Margreiter and E. Gnaiger (2000). "Isolated rat heart mitochondria and whole rat heart as models for mitochondrial cold ischemia-reperfusion injury." Transplant Proc **32**(1): 45.

Kuznetsov, A. V., S. Schneeberger, R. Seiler, G. Brandacher, W. Mark, W. Steurer, V. Saks, Y. Usson, R. Margreiter and E. Gnaiger (2004). "Mitochondrial defects and heterogeneous cytochrome c release after cardiac cold ischemia and reperfusion." Am J Physiol Heart Circ Physiol **286**(5): H1633-1641.

Lambotte, L. (1977). "Effect of anoxia and ATP depletion on the membrane potential and permeability of dog liver." J Physiol **269**(1): 53-76.

Lancha Junior, A. H., S. Painelli Vde, B. Saunders and G. G. Artioli (2015). "Nutritional Strategies to Modulate Intracellular and Extracellular Buffering Capacity During High-Intensity Exercise." Sports Med **45 Suppl 1**: S71-81.

Lane, N. (2002). Oxygen : the molecule that made the world. Oxford, Oxford : Oxford University Press 2002.

Lane, N. (2015). The vital question why is life the way it is? London, London : Profile Books 2015.

Lanza, I. R. and K. S. Nair (2009). "Functional assessment of isolated mitochondria in vitro." Methods Enzymol **457**: 349-372.

Lanza, I. R. and K. S. Nair (2010). "Mitochondrial metabolic function assessed in vivo and in vitro." Curr Opin Clin Nutr Metab Care **13**(5): 511-517.

Larson, J., K. L. Drew, L. P. Folkow, S. L. Milton and T. J. Park (2014). "No oxygen? No problem! Intrinsic brain tolerance to hypoxia in vertebrates." J Exp Biol **217**(Pt 7): 1024-1039.

Last, P. R. (2009). Sharks and rays of Australia. Collingwood, Vic., Collingwood, Vic. CSIRO Publishing 2009.

Lau, G. Y., M. Mandic and J. G. Richards (2017). "Evolution of Cytochrome c Oxidase in Hypoxia Tolerant Sculpins (Cottidae, Actinopterygii)." Mol Biol Evol **34**(9): 2153-2162.

Lavoisier, A. (1777). Mémoire sur la combustion en général Mémoire.

Lee, H., S. B. Smith and Y. Yoon (2017). "The short variant of the mitochondrial dynamin OPA1 maintains mitochondrial energetics and cristae structure." J Biol Chem **292**(17): 7115-7130.

Lemarie, A., L. Huc, E. Pazarentzos, A. L. Mahul-Mellier and S. Grimm (2011). "Specific disintegration of complex II succinate:ubiquinone oxidoreductase links pH changes to oxidative stress for apoptosis induction." Cell Death Differ **18**(2): 338-349.

Logan, A., V. R. Pell, K. J. Shaffer, C. Evans, N. J. Stanley, E. L. Robb, T. A. Prime, E. T. Chouchani, H. M. Cocheme, I. M. Fearnley, S. Vidoni, A. M. James, C. M. Porteous, L. Partridge, T. Krieg, R. A. Smith and M. P. Murphy (2016). "Assessing the Mitochondrial Membrane Potential in Cells and In Vivo using Targeted Click Chemistry and Mass Spectrometry." Cell Metab **23**(2): 379-385.

Lohmann, K. (1929). "Über die Pyrophosphatfraktion im Muskel." Naturwissenschaften **17**(31): 624-625.

Luo, S., C. A. Valencia, J. Zhang, N. C. Lee, J. Slone, B. Gui, X. Wang, Z. Li, S. Dell, J. Brown, S. M. Chen, Y. H. Chien, W. L. Hwu, P. C. Fan, L. J. Wong, P. S. Atwal and T. Huang (2018). "Biparental Inheritance of Mitochondrial DNA in Humans." Proc Natl Acad Sci U S A **115**(51): 13039-13044.

Lushchak, V. I. and T. V. Bagnyukova (2006). "Effects of different environmental oxygen levels on free radical processes in fish." Comp Biochem Physiol B Biochem Mol Biol **144**(3): 283-289.

Lutz, P. L. and G. E. Nilsson (1997). "Contrasting strategies for anoxic brain survival--glycolysis up or down." J Exp Biol **200**(Pt 2): 411-419.

Ma, Y. L., X. Zhu, P. M. Rivera, O. Toien, B. M. Barnes, J. C. LaManna, M. A. Smith and K. L. Drew (2005). "Absence of cellular stress in brain after hypoxia induced by arousal from hibernation in Arctic ground squirrels." Am J Physiol Regul Integr Comp Physiol **289**(5): R1297-1306.

Madshus, I. H. (1988). "Regulation of intracellular pH in eukaryotic cells." Biochem J **250**(1): 1-8.

Makrecka-Kuka, M., G. Krumschnabel and E. Gnaiger (2015). "High-Resolution Respirometry for Simultaneous Measurement of Oxygen and Hydrogen Peroxide Fluxes in Permeabilized Cells, Tissue Homogenate and Isolated Mitochondria." Biomolecules **5**(3): 1319-1338.

Mandic, M., G. Y. Lau, M. M. Nijjar and J. G. Richards (2008). "Metabolic recovery in goldfish: A comparison of recovery from severe hypoxia exposure and exhaustive exercise." Comp Biochem Physiol C Toxicol Pharmacol **148**(4): 332-338.

Mandic, M., K. A. Sloman and J. G. Richards (2009). "Escaping to the surface: a phylogenetically independent analysis of hypoxia-induced respiratory behaviors in sculpins." Physiol Biochem Zool **82**(6): 730-738.

Mandic, M., B. Speers-Roesch and J. G. Richards (2013). "Hypoxia tolerance in sculpins is associated with high anaerobic enzyme activity in brain but not in liver or muscle." Physiol Biochem Zool **86**(1): 92-105.

Mandic, M., A. E. Todgham and J. G. Richards (2009). "Mechanisms and evolution of hypoxia tolerance in fish." Proc Biol Sci **276**(1657): 735-744.

Martin, W. F., F. L. Sousa and N. Lane (2014). "Evolution. Energy at life's origin." Science **344**(6188): 1092-1093.

Martinez de Maranon, I., R. Tourdot-Marechal and P. Gervais (2001). "Involvement of osmotic cell shrinkage on the proton extrusion rate in Saccharomyces cerevisiae." Int J Food Microbiol **67**(3): 241-246.

Masson, S. W. C., C. P. Hedges, J. B. L. Devaux, C. S. James and A. J. R. Hickey (2017). "Mitochondrial glycerol 3-phosphate facilitates bumblebee pre-flight thermogenesis." Scientific Reports **7**(1): 13107.

Mayevsky, A. (2015). Mitochondrial function in vivo evaluated by NADH fluorescence, Cham : Springer. 2015 ©2015.

Mayevsky, A. and G. G. Rogatsky (2007). "Mitochondrial function in vivo evaluated by NADH fluorescence: from animal models to human studies." Am J Physiol Cell Physiol **292**(2): C615-640.

McArley, T. J., A. J. R. Hickey and N. A. Herbert (2017). "Chronic warm exposure impairs growth performance and reduces thermal safety margins in the common triplefin fish (Forsterygion lapillum)." J Exp Biol **220**(Pt 19): 3527-3535.

McArley, T. J., A. J. R. Hickey and N. A. Herbert (2018). "Hyperoxia increases maximum oxygen consumption and aerobic scope of intertidal fish facing acutely high temperatures." The Journal of Experimental Biology.

McLennan, H. R. and M. Degli Esposti (2000). "The contribution of mitochondrial respiratory complexes to the production of reactive oxygen species." J Bioenerg Biomembr **32**(2): 153-162.

Mehta, A., M. Prabhakar, P. Kumar, R. Deshmukh and P. L. Sharma (2013). "Excitotoxicity: bridge to various triggers in neurodegenerative disorders." Eur J Pharmacol **698**(1-3): 6-18.

Meldrum, B. S. (2000). "Glutamate as a neurotransmitter in the brain: review of physiology and pathology." J Nutr **130**(4S Suppl): 1007S-1015S.

Meunier, B., B. White and L. D. Corkum (2013). "The role of fanning behavior in water exchange by a nest-guarding benthic fish before spawning." Limnology and Oceanography: Fluids and Environments\ **3**(1\): 198\-209\.

Michalak, M., J. Groenendyk, E. Szabo, L. I. Gold and M. Opas (2009). "Calreticulin, a multi-process calcium-buffering chaperone of the endoplasmic reticulum." Biochem J **417**(3): 651-666.

Mik, E. G. (2013). "Special article: measuring mitochondrial oxygen tension: from basic principles to application in humans." Anesth Analg **117**(4): 834-846.

Mik, E. G., T. Johannes, C. J. Zuurbier, A. Heinen, J. H. Houben-Weerts, G. M. Balestra, J. Stap, J. F. Beek and C. Ince (2008). "In vivo mitochondrial oxygen tension measured by a delayed fluorescence lifetime technique." Biophys J **95**(8): 3977-3990.

Miki, H. and Y. Funato (2012). "Regulation of intracellular signalling through cysteine oxidation by reactive oxygen species." J Biochem **151**(3): 255-261.

Mitchell, P. (1961). "Coupling of phosphorylation to electron and hydrogen transfer by a chemi-osmotic type of mechanism." Nature **191**: 144-148.

Mitchell, P. (2011). "Chemiosmotic coupling in oxidative and photosynthetic phosphorylation. 1966." Biochim Biophys Acta **1807**(12): 1507-1538.

Mittler, R. and B. A. Zilinskas (1991). "Purification and characterization of pea cytosolic ascorbate peroxidase." Plant Physiol **97**(3): 962-968.

Moore, J., C. Stanitski and P. Jurs (2009). Principles of Chemistry: The Molecular Science, Cengage Learning.

Mulvey, J. M. and G. M. Renshaw (2000). "Neuronal oxidative hypometabolism in the brainstem of the epaulette shark (Hemiscyllium ocellatum) in response to hypoxic pre-conditioning." Neurosci Lett **290**(1): 1-4.

Murphy, G. E., B. C. Lowekamp, P. M. Zerfas, R. J. Chandler, R. Narasimha, C. P. Venditti and S. Subramaniam (2010). "Ion-abrasion scanning electron microscopy reveals distorted liver mitochondrial morphology in murine methylmalonic acidemia." J Struct Biol **171**(2): 125-132.

Murphy, M. P. (2009). "How mitochondria produce reactive oxygen species." Biochem J **417**(1): 1-13.

Murphy, Michael P. (2009). "How mitochondria produce reactive oxygen species." Biochemical Journal **417**(Pt 1): 1-13.

Murphy, M. P. (2012). "Modulating mitochondrial intracellular location as a redox signal." Sci Signal **5**(242): pe39.

Murphy, M. P. (2016). "Understanding and preventing mitochondrial oxidative damage." Biochem Soc Trans **44**(5): 1219-1226.

Musatov, A. and N. C. Robinson (2012). "Susceptibility of mitochondrial electron-transport complexes to oxidative damage. Focus on cytochrome c oxidase." Free Radic Res **46**(11): 1313-1326.

Navet, R., A. Mouithys-Mickalad, P. Douette, C. M. Sluse-Goffart, W. Jarmuszkiewicz and F. E. Sluse (2006). "Proton leak induced by reactive oxygen species produced during in vitro anoxia/reoxygenation in rat skeletal muscle mitochondria." J Bioenerg Biomembr **38**(1): 23-32.

Nicholls, D. G., H. J. Grav and O. Lindberg (1972). "Mitochondrial from hamster brown-adipose tissue. Regulation of respiration in vitro by variations in volume of the matrix compartment." Eur J Biochem **31**(3): 526-533.

Nilsson, G. E. and S. Ostlund-Nilsson (2004). "Hypoxia in paradise: widespread hypoxia tolerance in coral reef fishes." Proc Biol Sci **271 Suppl 3**: S30-33.

Nilsson, G. E. and G. M. Renshaw (2004). "Hypoxic survival strategies in two fishes: extreme anoxia tolerance in the North European crucian carp and natural hypoxic preconditioning in a coral-reef shark." J Exp Biol **207**(Pt 18): 3131-3139.

Norin, T., H. Malte and T. D. Clark (2014). "Aerobic scope does not predict the performance of a tropical eurythermal fish at elevated temperatures." J Exp Biol **217**(Pt 2): 244-251.

Orrenius, S. and B. Zhivotovsky (2005). "Cardiolipin oxidation sets cytochrome c free." Nature Chemical Biology **1**: 188.

Pagel, M. (1997). "Inferring evolutionary processes from phylogenies." Zoologica Scripta **26**(4): 331-348.

Palacios-Callender, M., M. Quintero, V. S. Hollis, R. J. Springett and S. Moncada (2004). "Endogenous NO regulates superoxide production at low oxygen concentrations by modifying the redox state of cytochrome c oxidase." Proc Natl Acad Sci U S A **101**(20): 7630-7635.

Pamenter, M. E. (2014). "Mitochondria: a multimodal hub of hypoxia tolerance." Canadian Journal of Zoology **92**(7): 569-589.

Panov, A., Z. Orynbayeva, V. Vavilin and V. Lyakhovich (2014). "Fatty acids in energy metabolism of the central nervous system." Biomed Res Int **2014**: 472459.

Paradies, G., G. Petrosillo, M. Pistolese, N. Di Venosa, A. Federici and F. M. Ruggiero (2004). "Decrease in mitochondrial complex I activity in ischemic/reperfused rat heart: involvement of reactive oxygen species and cardiolipin." Circ Res **94**(1): 53-59.

Paradies, G., G. Petrosillo, M. Pistolese and F. M. Ruggiero (2002). "Reactive oxygen species affect mitochondrial electron transport complex I activity through oxidative cardiolipin damage." Gene **286**(1): 135-141.

Peddie, C. J. and L. M. Collinson (2014). "Exploring the third dimension: volume electron microscopy comes of age." Micron **61**: 9-19.

Pell, V. R., E. T. Chouchani, C. Frezza, M. P. Murphy and T. Krieg (2016). "Succinate metabolism: a new therapeutic target for myocardial reperfusion injury." Cardiovasc Res **111**(2): 134-141.

Pelster, B., C. M. Wood, E. Jung and A. L. Val (2018). "Air-breathing behavior, oxygen concentrations, and ROS defense in the swimbladders of two erythrinid fish, the facultative air-breathing jeju, and the non-air-breathing traira during normoxia, hypoxia and hyperoxia." J Comp Physiol B **188**(3): 437-449.

Perkins, G. A., M. G. Sun and T. G. Frey (2009). "Chapter 2 Correlated light and electron microscopy/electron tomography of mitochondria in situ." Methods Enzymol **456**: 29-52.

Perry, S. W., J. P. Norman, J. Barbieri, E. B. Brown and H. A. Gelbard (2011). "Mitochondrial membrane potential probes and the proton gradient: a practical usage guide." Biotechniques **50**(2): 98-115.

Pesta, D. and E. Gnaiger (2012). "High-resolution respirometry: OXPHOS protocols for human cells and permeabilized fibers from small biopsies of human muscle." Methods Mol Biol **810**: 25-58.

Petroff, O. A., L. D. Errante, D. L. Rothman, J. H. Kim and D. D. Spencer (2002). "Glutamate-glutamine cycling in the epileptic human hippocampus." Epilepsia **43**(7): 703-710.

Pfleger, J., M. He and M. Abdellatif (2015). "Mitochondrial complex II is a source of the reserve respiratory capacity that is regulated by metabolic sensors and promotes cell survival." Cell Death Dis **6**: e1835.

Pham, T., D. Loiselle, A. Power and A. J. Hickey (2014). "Mitochondrial inefficiencies and anoxic ATP hydrolysis capacities in diabetic rat heart." Am J Physiol Cell Physiol **307**(6): C499-507.

Philp, A., A. L. Macdonald and P. W. Watt (2005). "Lactate--a signal coordinating cell and systemic function." J Exp Biol **208**(Pt 24): 4561-4575.

Picard, M., T. Taivassalo, G. Gouspillou and R. T. Hepple (2011). "Mitochondria: isolation, structure and function." J Physiol **589**(Pt 18): 4413-4421.

Picard, M., T. Taivassalo, D. Ritchie, K. J. Wright, M. M. Thomas, C. Romestaing and R. T. Hepple (2011). "Mitochondrial structure and function are disrupted by standard isolation methods." PLoS One **6**(3): e18317.

Pileggi, C. A., C. P. Hedges, R. F. D'Souza, B. R. Durainayagam, J. F. Markworth, A. J. R. Hickey, C. J. Mitchell and D. Cameron-Smith (2018). "Exercise recovery increases skeletal muscle H2O2 emission and mitochondrial respiratory capacity following two-weeks of limb immobilization." Free Radic Biol Med **124**: 241-248.

Poburko, D., J. Santo-Domingo and N. Demaurex (2011). "Dynamic regulation of the mitochondrial proton gradient during cytosolic calcium elevations." J Biol Chem **286**(13): 11672-11684.

Porat-Shliom, N., O. J. Harding, L. Malec, K. Narayan and R. Weigert (2019). "Mitochondrial Populations Exhibit Differential Dynamic Responses to Increased Energy Demand during Exocytosis In Vivo." iScience **11**: 440-449.

Portier, P. (1918). Les symbiotes. Paris, Masson.

Potts, D. C. and P. K. Swart (1984). "Water temperature as an indicator of environmental variability on a coral reef." Limnology and Oceanography **29**(3): 504-516.

Power, A., N. Pearson, T. Pham, C. Cheung, A. Phillips and A. Hickey (2014). "Uncoupling of oxidative phosphorylation and ATP synthase reversal within the hyperthermic heart." Physiol Rep **2**(9).

Putnam, R. W. (2012). Chapter 17 - Intracellular pH Regulation A2 - Sperelakis, Nicholas. Cell Physiology Source Book (Fourth Edition). San Diego, Academic Press**:** 303-321.

Quinlan, C. L., A. L. Orr, I. V. Perevoshchikova, J. R. Treberg, B. A. Ackrell and M. D. Brand (2012). "Mitochondrial complex II can generate reactive oxygen species at high rates in both the forward and reverse reactions." J Biol Chem **287**(32): 27255-27264.

Quistorff, B., N. H. Secher and J. J. Van Lieshout (2008). "Lactate fuels the human brain during exercise." FASEB J **22**(10): 3443-3449.

Ramos, M., A. del Arco, B. Pardo, A. Martinez-Serrano, J. R. Martinez-Morales, K. Kobayashi, T. Yasuda, E. Bogonez, P. Bovolenta, T. Saheki and J. Satrustegui (2003). "Developmental changes in the Ca2+-regulated mitochondrial aspartate-glutamate carrier aralar1 in brain and prominent expression in the spinal cord." Brain Res Dev Brain Res **143**(1): 33-46.

Ravera, S., I. Panfoli, D. Calzia, M. G. Aluigi, P. Bianchini, A. Diaspro, G. Mancardi and A. Morelli (2009). "Evidence for aerobic ATP synthesis in isolated myelin vesicles." Int J Biochem Cell Biol **41**(7): 1581-1591.

Rehncrona, S. (1985). "Brain acidosis." Ann Emerg Med **14**(8): 770-776.

Rehncrona, S. (1985). The Deleterious Effect of Excessive Tissue Lactic Acidosis in Brain Ischemia. Controlled Hypotension in Neuroanaesthesia. D. Heuser, D. G. McDowall and V. Hempel. Boston, MA, Springer US**:** 63-69.

Rehncrona, S. and E. Kagstrom (1983). "Tissue lactic acidosis and ischemic brain damage." Am J Emerg Med **1**(2): 168-174.

Renshaw, G. M. and S. E. Dyson (1999). "Increased nitric oxide synthase in the vasculature of the epaulette shark brain following hypoxia." Neuroreport **10**(8): 1707-1712.

Renshaw, G. M., C. B. Kerrisk and G. E. Nilsson (2002). "The role of adenosine in the anoxic survival of the epaulette shark, Hemiscyllium ocellatum." Comp Biochem Physiol B Biochem Mol Biol **131**(2): 133-141.

Renshaw, G. M., A. K. Kutek, G. D. Grant and S. Anoopkumar-Dukie (2012). "Forecasting elasmobranch survival following exposure to severe stressors." Comp Biochem Physiol A Mol Integr Physiol **162**(2): 101-112.

Richards, J. G. (2011). "Physiological, behavioral and biochemical adaptations of intertidal fishes to hypoxia." J Exp Biol **214**(Pt 2): 191-199.

Richards, J. G., Y. S. Wang, C. J. Brauner, R. J. Gonzalez, M. L. Patrick, P. M. Schulte, A. R. Choppari-Gomes, V. M. Almeida-Val and A. L. Val (2007). "Metabolic and ionoregulatory responses of the Amazonian cichlid, Astronotus ocellatus, to severe hypoxia." J Comp Physiol B **177**(3): 361-374.

Rigoulet, M., E. D. Yoboue and A. Devin (2011). "Mitochondrial ROS generation and its regulation: mechanisms involved in H(2)O(2) signaling." Antioxid Redox Signal **14**(3): 459-468.

Riske, L., R. K. Thomas, G. B. Baker and S. M. Dursun (2017). "Lactate in the brain: an update on its relevance to brain energy, neurons, glia and panic disorder." Ther Adv Psychopharmacol **7**(2): 85-89.

Rizzuto, R., P. Pinton, W. Carrington, F. S. Fay, K. E. Fogarty, L. M. Lifshitz, R. A. Tuft and T. Pozzan (1998). "Close contacts with the endoplasmic reticulum as determinants of mitochondrial Ca2+ responses." Science **280**(5370): 1763-1766.

Robergs, R. A., F. Ghiasvand and D. Parker (2004). "Biochemistry of exercise-induced metabolic acidosis." Am J Physiol Regul Integr Comp Physiol **287**(3): R502-516.

Rogers, N. J., M. A. Urbina, E. E. Reardon, D. J. McKenzie and R. W. Wilson (2016). "A new analysis of hypoxia tolerance in fishes using a database of critical oxygen level (Pcrit)." Conservation Physiology **4**(1).

Rolfe, D. F. and M. D. Brand (1997). "The physiological significance of mitochondrial proton leak in animal cells and tissues." Biosci Rep **17**(1): 9-16.

Roos, A. and W. F. Boron (1981). "Intracellular pH." Physiol Rev **61**(2): 296-434.

Rosselin, M., P. Nunes-Hasler and N. Demaurex (2018). "Ultrastructural Characterization of Flashing Mitochondria." Contact **1**: 2515256418801423.

Rouslin, W. (1983). "Mitochondrial complexes I, II, III, IV, and V in myocardial ischemia and autolysis." Am J Physiol **244**(6): H743-748.

Routley, M. H., G. E. Nilsson and G. M. C. Renshaw (2002). "Exposure to hypoxia primes the respiratory and metabolic responses of the epaulette shark to progressive hypoxia." Comparative Biochemistry and Physiology Part A: Molecular & Integrative Physiology **131**(2): 313-321.

Rubinsky, B. (2003). "Principles of Low Temperature Cell Preservation." Heart Failure Reviews **8**(3): 277-284.

Rytkonen, K. T., G. M. Renshaw, P. P. Vainio, K. J. Ashton, G. Williams-Pritchard, E. H. Leder and M. Nikinmaa (2012). "Transcriptional responses to hypoxia are enhanced by recurrent hypoxia (hypoxic preconditioning) in the epaulette shark." Physiol Genomics **44**(22): 1090-1097.

Sagan, L. (1967). "On the origin of mitosing cells." J Theor Biol **14**(3): 255-274.

Salin, K., S. K. Auer, E. M. Villasevil, G. J. Anderson, A. G. Cairns, W. Mullen, R. C. Hartley and N. B. Metcalfe (2017). "Using the MitoB method to assess levels of reactive oxygen species in ecological studies of oxidative stress." Sci Rep **7**: 41228.

Sanderson, T. H., C. A. Reynolds, R. Kumar, K. Przyklenk and M. Huttemann (2013). "Molecular mechanisms of ischemia-reperfusion injury in brain: pivotal role of the mitochondrial membrane potential in reactive oxygen species generation." Mol Neurobiol **47**(1): 9-23.

Sandoval, R., A. Gonzalez, A. Caviedes, F. Pancetti, K. H. Smalla, T. Kaehne, L. Michea, E. D. Gundelfinger and U. Wyneken (2011). "Homeostatic NMDA receptor down-regulation via brain derived neurotrophic factor and nitric oxide-dependent signalling in cortical but not in hippocampal neurons." J Neurochem **118**(5): 760-772.

Scandurra, F. M. and E. Gnaiger (2010). Cell Respiration Under Hypoxia: Facts and Artefacts in Mitochondrial Oxygen Kinetics. Oxygen Transport to Tissue XXXI. E. Takahashi and D. F. Bruley. Boston, MA, Springer US**:** 7-25.

Scandurra, F. M. and E. Gnaiger (2010). "Cell respiration under hypoxia: facts and artefacts in mitochondrial oxygen kinetics." Adv Exp Med Biol **662**: 7-25.

Schubert, D. and D. Piasecki (2001). "Oxidative glutamate toxicity can be a component of the excitotoxicity cascade." J Neurosci **21**(19): 7455-7462.

Schulte, K., U. Kunter and M. J. Moeller (2015). "The evolution of blood pressure and the rise of mankind." Nephrol Dial Transplant **30**(5): 713-723.

Schurmann, H. and J. F. Steffensen (1997). "Effects of temperature, hypoxia and activity on the metabolism of juvenile Atlantic cod." Journal of Fish Biology **50**(6): 1166-1180.

Selivanov, V. A., J. A. Zeak, J. Roca, M. Cascante, M. Trucco and T. V. Votyakova (2008). "The role of external and matrix pH in mitochondrial reactive oxygen species generation." J Biol Chem **283**(43): 29292-29300.

Severinghaus, J. W. and P. B. Astrup (1986). "History of blood gas analysis. IV. Leland Clark's oxygen electrode." J Clin Monit **2**(2): 125-139.

Sharma, P., A. B. Jha, R. S. Dubey and M. Pessarakli (2012). "Reactive oxygen species, oxidative damage, and antioxidative defense mechanism in plants under stressful conditions." Journal of botany **2012**.

Sheng, Y., I. A. Abreu, D. E. Cabelli, M. J. Maroney, A. F. Miller, M. Teixeira and J. S. Valentine (2014). "Superoxide dismutases and superoxide reductases." Chem Rev **114**(7): 3854-3918.

Sielaff, H. and M. Borsch (2013). "Twisting and subunit rotation in single F(O)(F1)-ATP synthase." Philos Trans R Soc Lond B Biol Sci **368**(1611): 20120024.

Siesjo, B. K., G. Bendek, T. Koide, E. Westerberg and T. Wieloch (1985). "Influence of acidosis on lipid peroxidation in brain tissues in vitro." J Cereb Blood Flow Metab **5**(2): 253-258.

Solaini, G., A. Baracca, G. Lenaz and G. Sgarbi (2010). "Hypoxia and mitochondrial oxidative metabolism." Biochim Biophys Acta **1797**(6-7): 1171-1177.

Speers-Roesch, B., M. Mandic, D. J. E. Groom and J. G. Richards (2013). "Critical oxygen tensions as predictors of hypoxia tolerance and tissue metabolic responses during hypoxia exposure in fishes." Journal of Experimental Marine Biology and Ecology **449**: 239-249.

Speers-Roesch, B., E. Sandblom, G. Y. Lau, A. P. Farrell and J. G. Richards (2010). "Effects of environmental hypoxia on cardiac energy metabolism and performance in tilapia." Am J Physiol Regul Integr Comp Physiol **298**(1): R104-119.

Starkov, A. (2005). "Succinate in hypoxia-reperfusion induced tissue damage."

Steffensen, J. F. (1989). "Some errors in respirometry of aquatic breathers: How to avoid and correct for them." Fish Physiol Biochem **6**(1): 49-59.

Stenslokken, K. O., S. L. Milton, P. L. Lutz, L. Sundin, G. M. Renshaw, J. A. Stecyk and G. E. Nilsson (2008). "Effect of anoxia on the electroretinogram of three anoxia-tolerant vertebrates." Comp Biochem Physiol A Mol Integr Physiol **150**(4): 395-403.

Stuart, J. A., K. M. Brindle, J. A. Harper and M. D. Brand (1999). "Mitochondrial proton leak and the uncoupling proteins." J Bioenerg Biomembr **31**(5): 517-525.

Sun, S., H. Li, J. Chen and Q. Qian (2017). "Lactic Acid: No Longer an Inert and End-Product of Glycolysis." Physiology **32**(6): 453-463.

Talley, K. and E. Alexov (2010). "On the pH-optimum of activity and stability of proteins." Proteins **78**(12): 2699-2706.

Tan, W., P. Pasinelli and D. Trotti (2014). "Role of mitochondria in mutant SOD1 linked amyotrophic lateral sclerosis." Biochim Biophys Acta **1842**(8): 1295-1301.

Tang, X. J. and F. Xing (2013). "Calcium-permeable AMPA receptors in neonatal hypoxic-ischemic encephalopathy (Review)." Biomed Rep **1**(6): 828-832.

Taylor, R. W. and D. M. Turnbull (2005). "Mitochondrial DNA mutations in human disease." Nat Rev Genet **6**(5): 389-402.

Teijido, O., S. M. Rappaport, A. Chamberlin, S. Y. Noskov, V. M. Aguilella, T. K. Rostovtseva and S. M. Bezrukov (2014). "Acidification asymmetrically affects voltage-dependent anion channel implicating the involvement of salt bridges." J Biol Chem **289**(34): 23670-23682.

Teixeira, A. P., S. S. Santos, N. Carinhas, R. Oliveira and P. M. Alves (2008). "Combining metabolic flux analysis tools and 13C NMR to estimate intracellular fluxes of cultured astrocytes." Neurochem Int **52**(3): 478-486.

Tiefenthaler, M., A. Amberger, N. Bacher, B. L. Hartmann, R. Margreiter, R. Kofler and G. Konwalinka (2001). "Increased lactate production follows loss of mitochondrial membrane potential during apoptosis of human leukaemia cells." Br J Haematol **114**(3): 574-580.

Towe, K. M. (1970). "Oxygen-collagen priority and the early metazoan fossil record." Proceedings of the National Academy of Sciences **65**(4): 781-788.

Tretter, L., A. Patocs and C. Chinopoulos (2016). "Succinate, an intermediate in metabolism, signal transduction, ROS, hypoxia, and tumorigenesis." Biochim Biophys Acta **1857**(8): 1086-1101.

Tsujimoto, Y. (1998). "Role of Bcl-2 family proteins in apoptosis: apoptosomes or mitochondria?" Genes Cells **3**(11): 697-707.

Tuan, T. C., T. G. Hsu, M. C. Fong, C. F. Hsu, K. K. Tsai, C. Y. Lee and C. W. Kong (2008). "Deleterious effects of short-term, high-intensity exercise on immune function: evidence from leucocyte mitochondrial alterations and apoptosis." Br J Sports Med **42**(1): 11-15.

Tuppen, H. A., E. L. Blakely, D. M. Turnbull and R. W. Taylor (2010). "Mitochondrial DNA mutations and human disease." Biochim Biophys Acta **1797**(2): 113-128.

Turrens, J. F., A. Alexandre and A. L. Lehninger (1985). "Ubisemiquinone is the electron donor for superoxide formation by complex III of heart mitochondria." Archives of Biochemistry and Biophysics **237**(2): 408-414.

Val, A. L., K. R. Gomes and V. M. de Almeida-Val (2015). "Rapid regulation of blood parameters under acute hypoxia in the Amazonian fish Prochilodus nigricans." Comp Biochem Physiol A Mol Integr Physiol **184**: 125-131.

Val, A. L. S., M. N. P.; Almeida-Val, V. M. F. (1998). "Hypoxia adaptation in fish of the Amazon: a never-ending task." South African journal of zoology. Suid-Afrikaanse tydskrif vir dierkunde. **33**(2): 107-114.

Valls-Lacalle, L., I. Barba, E. Miro-Casas, J. J. Alburquerque-Bejar, M. Ruiz-Meana, M. Fuertes-Agudo, A. Rodriguez-Sinovas and D. Garcia-Dorado (2016). "Succinate dehydrogenase inhibition with malonate during reperfusion reduces infarct size by preventing mitochondrial permeability transition." Cardiovasc Res **109**(3): 374-384.

Vaughan-Jones, R. D. and K. W. Spitzer (2002). "Role of bicarbonate in the regulation of intracellular pH in the mammalian ventricular myocyte." Biochem Cell Biol **80**(5): 579-596.

Vornanen, M., J. A. W. Stecyk and G. E. Nilsson (2009). Chapter 9 The Anoxia-Tolerant Crucian Carp (Carassius Carassius L.). Fish Physiology. A. P. F. Jeffrey G. Richards and J. B. Colin, Academic Press. **Volume 27:** 397-441.

Walker, D. A. (2002). "'And whose bright presence' – an appreciation of Robert Hill and his reaction." Photosynthesis Research **73**(1): 51-54.

Webster, V. W. and M. Charlotte (1975). "Oxyconformers and oxyregulators: A quantitative index." Journal of Experimental Marine Biology and Ecology **17**(2): 103-110.

Weisiger, R. A. and I. Fridovich (1973). "Superoxide dismutase. Organelle specificity." J Biol Chem **248**(10): 3582-3592.

Wijermars, L. G., A. F. Schaapherder, S. Kostidis, R. C. Wust and J. H. Lindeman (2016). "Succinate Accumulation and Ischemia-Reperfusion Injury: Of Mice but Not Men, a Study in Renal Ischemia-Reperfusion." Am J Transplant **16**(9): 2741-2746.

Wilson, J. L. (1988). "Biochemistry; Third edition (Stryer, Lubert)." Journal of Chemical Education **65**(12): A337.

Winter, J., I. Klumpe, J. Heger, U. Rauch, H. P. Schultheiss, U. Landmesser and A. Dorner (2016). "Adenine nucleotide translocase 1 overexpression protects cardiomyocytes against hypoxia via increased ERK1/2 and AKT activation." Cell Signal **28**(1): 152-159.

Wise, G., J. M. Mulvey and G. M. C. Renshaw (1998). "Hypoxia tolerance in the epaulette shark (Hemiscyllium ocellatum)." Journal of Experimental Zoology **281**(1): 1-5.

Witt, A. M., F. S. Larsen and P. N. Bjerring (2017). "Accumulation of lactate in the rat brain during hyperammonaemia is not associated with impaired mitochondrial respiratory capacity." Metab Brain Dis **32**(2): 461-470.

Wojtovich, A. P. and P. S. Brookes (2008). "The endogenous mitochondrial complex II inhibitor malonate regulates mitochondrial ATP-sensitive potassium channels: implications for ischemic preconditioning." Biochim Biophys Acta **1777**(7-8): 882-889.

Wood, C. M. (2018). "The fallacy of the Pcrit – are there more useful alternatives?" The Journal of Experimental Biology **221**.

Woods, D. C. (2017). "Mitochondrial Heterogeneity: Evaluating Mitochondrial Subpopulation Dynamics in Stem Cells." Stem Cells Int **2017**: 7068567.

Xu, T., D. Close, W. Handagama, E. Marr, G. Sayler and S. Ripp (2016). "The Expanding Toolbox of In Vivo Bioluminescent Imaging." Front Oncol **6**: 150.

Zakharchenko, M. V., A. V. Zakharchenko, N. V. Khunderyakova, M. N. Tutukina, M. A. Simonova, A. A. Vasilieva, O. I. Romanova, N. I. Fedotcheva, E. G. Litvinova, E. I. Maevsky, V. P. Zinchenko, A. V. Berezhnov, I. G. Morgunov, A. A. Gulayev and M. N. Kondrashova (2013). "Burst of succinate dehydrogenase and alpha-ketoglutarate dehydrogenase activity in concert with the expression of genes coding for respiratory chain proteins underlies short-term beneficial physiological stress in mitochondria." Int J Biochem Cell Biol **45**(1): 190-200.

Zanotti, A. and G. F. Azzone (1980). "Safranine as membrane potential probe in rat liver mitochondria." Arch Biochem Biophys **201**(1): 255-265.

Zeleznikar, R. J., P. P. Dzeja and N. D. Goldberg (1995). "Adenylate kinase-catalyzed phosphoryl transfer couples ATP utilization with its generation by glycolysis in intact muscle." J Biol Chem **270**(13): 7311-7319.

Zeng, L., Y. H. Wang, C. X. Ai, J. L. Zheng, C. W. Wu and R. Cai (2016). "Effects of beta-glucan on ROS production and energy metabolism in yellow croaker (Pseudosciaena crocea) under acute hypoxic stress." Fish Physiol Biochem **42**(5): 1395-1405.

Zenteno-Savin, T., E. Clayton-Hernandez and R. Elsner (2002). "Diving seals: are they a model for coping with oxidative stress?" Comp Biochem Physiol C Toxicol Pharmacol **133**(4): 527-536.

Zhang, J., F. E. Frerman and J. J. Kim (2006). "Structure of electron transfer flavoprotein-ubiquinone oxidoreductase and electron transfer to the mitochondrial ubiquinone pool." Proc Natl Acad Sci U S A **103**(44): 16212-16217.

Zorov, D. B., M. Juhaszova and S. J. Sollott (2014). "Mitochondrial reactive oxygen species (ROS) and ROS-induced ROS release." Physiol Rev **94**(3): 909-950.

Zou, H., Y. Li, X. Liu and X. Wang (1999). "An APAF-1.cytochrome c multimeric complex is a functional apoptosome that activates procaspase-9." J Biol Chem **274**(17): 11549-11556.

Zuo, L., A. Shiah, W. J. Roberts, M. T. Chien, P. D. Wagner and M. C. Hogan (2013). "Low Po(2) conditions induce reactive oxygen species formation during contractions in single skeletal muscle fibers." Am J Physiol Regul Integr Comp Physiol **304**(11): R1009-1016.